An Experimental Study of Two-Stroke Cyclic Variation and a Prototype Component Design for Controlled Auto Ignition.

Juan Sebastian Vacas

Supervised by Malcolm McDonald and Dr. Owen Williams.

Submitted in partial fulfilment for the award of the degree of MRes Engineering.

University of Wales Trinity Saint David.

2025

Declaration Page

I declare that this thesis is entirely my own work and has not already been submitted in substance for any other or previous degree and is not concurrently being submitted for any other degree.

Juan Sebastian Vacas

Abstract

Given the current concern of global warming the automotive industry is under pressure to provide alternative powertrains to improve fuel efficiency and reduce the production of carbon dioxide and associated emissions.

2-stroke engines are known to provide considerable benefits in weight reduction and power density in comparison to their 4-stroke brethren. However, very poor cycle-to-cycle stability under low load and low RPM conditions has rendered them impossible to implement on a market wide basis because of the emissions problems inherent with poor cyclic stability.

In the early 1990s Honda Motor Corporation [60-67] introduced the concept of Controlled Auto Ignition to address the poor cyclic stability conditions but cost and complexity of the technology and an industry preference for 4-stroke engines has limited its take up.

This dissertation aims to improve the fundamental cycle-to-cycle understanding to help determine a practical way forward for the 2-stroke engine. The work will experimentally measure the cylinder pressure to a resolution of one crankshaft degree for hundreds of consecutive cycles on a contemporary 2-stroke engine under the sub optimal running conditions.

This will provide data with a depth and detail not currently available to the author in the academic literature.

In addition, the author will design and manufacture prototype exhaust restrictors and cast aluminium cylinder heads based on research, in particular that of Honda Motor Corporation.

The author believes that the enhanced high-resolution cycle-to-cycle analysis will provide an insight not currently available in the literature. It will help optimise the prototype exhaust restrictors and cylinder heads and better determine the engine design requirements to make a 2-stroke engine, with its inherent advantages, acceptable across the complete load and RPM range.

Nomenclature

AFR Air Fuel Ratio

AR Activated Radical

ATAC Active Thermo-Atmosphere Combustion

ATDC After Top Dead Centre

AVL Anstalt für Verbrennungskraftmaschinen List

BDC Bottom Dead Centre

BTDC Before Top Dead Centre

CA Crank Angle

CAD Computer Aided Design

CAI Controlled Auto Ignition

CC Cubic Centimetres

CMM Coordinate Measuring Machine

CO Carbon Monoxide

CO2 Carbon Dioxide

COV Coefficient of Variance

CT Computed Tomography

CVT Continually Variable Transmission

Delta P Change in Pressure

DFM Design for Manufacture

DICI Direct Injection Compression Ignition

DOE Design of Experiment

EGR Exhaust Gas Recirculation

EOC End of Combustion

EPO Exhaust Port Open

FEA Finite Element Analysis

GDI Gasoline Direct Injection

GM General Motors

GOM Gesellschaft für Optische Messtechnik

GTDI Gasoline Turbocharged Direct Injection

GTPE GT Performance Engineering

GW Grainger and Worrall

HC Hydrocarbons

HCAI Homogeneous Charge Auto Ignition

HCCI Homogenous Charge Compression Ignition

Honda Honda Motor Corporation

IMEP Indicated Mean Effective Pressure

JSAE Japanese Society of Automotive Engineers

KTM Kronreif Trunkenpolz Mattighofen

LPDI Low Pressure Direct Injection

MFB Mass Fraction Burned

mV Millivolts

NOx Nitrogen Oxide

OBD Onboard Diagnostics

P Pressure

PDI Pneumatic Direct Injection

Pmax Maximum Cylinder Pressure

PPM Parts Per Million

PSI Pounds per Square Inch

RPM Revolutions Per Minute

SAE Society of Automotive Engineers

SCAI Stratified Charge Auto Ignition

SI Spark Ignition

SOC Start of Combustion

STL Standard Tessellation Language

TDC Top Dead Centre

TFX TFX Engine Technology Canada

TH% Throttle Open Percentag

Acknowledgments

The whole project and my relative success in higher education at Swansea were not a solo effort and would not have been possible without the support and guidance of many people. Starting at the undergraduate level, Tim and Kerry provided great structure, while Abigail Summerfield, Kelvin, and Richard Sutton gave me confidence in my own ability to learn. Special thanks must also go to Owen Williams for creating the course that inspired me to pursue higher education, and for always being willing to help. Kerry, Alastair Clarke, and Peter Charlton provided invaluable feedback during the Viva, which greatly contributed to this rewrite.

Particular thanks must go to Malcolm McDonald and Claire Evans for their continued and unwavering support – both of whom are, for me, shining examples of professionalism, and of how to approach things with integrity and purpose. Beyond this project, they have left a positive and lasting impression on me.

Contents

D	eclaration Page	2
Α	bstract	3
N	omenclature	4
Α	cknowledgments	6
1	- Introduction	9
2	- Literature Review	. 12
	2.1 – Honda Motor Corporation (Honda)	. 12
	2.2 - Contemporary Research	. 17
	2.3 – COV of IMEP	. 18
	2.4 – Instrumentation and Data Collection	. 20
	2.5 – DOE and Testing	. 22
	2.6 – Summary	. 23
3	- Design	. 24
	3.1 - Inlet Design	. 24
	3.2 – Exhaust Design	. 25
	3.3 – Design of Cast Prototype Cylinder Head	. 27
	3.3.1 – Introduction	. 27
	3.3.2 – Appraisal of KTM Cylinder Head	. 27
	3.3.3 – Initial design	. 28
	3.4 – Modified KTM Cylinder Head for Initial Testing	. 33
	3.5 – Cylinder Pressure Transducer	. 34
	3.6 – Design for Manufacture Philosophy	. 36
4	- Testing	. 38
	4.1 – Design of Experiment - DOE	. 38
	4.2 – Practical Implementation of Test Variables	. 39
	4.3 – Test Facility Setup	. 40
	4.4 – Test Equipment and Calibration	. 41
	4.5 – Test Procedure	. 42
	4.5.1 – Bedding In	. 42
	4.5.2 – Testing	. 42
	5.0 – Results	. 43
	5.1 – Setup procedure	. 43
	5.2 – Test Results	. 46
	5.3 – Post Processing of Raw Data	. 47

6.	0 – Analysis	. 48
	6.1 – Coefficient of Variance (COV) of IMEP	. 48
	6.2 – Cycle-to-Cycle Analysis	. 49
	6.2.1 – 2500RPM Analysis	. 49
	6.2.1.1 – Region A	. 50
	6.2.1.2 – Region B	. 52
	6.2.1.3 – Region C	. 55
	6.2.1.4 – Region E	. 56
	6.2.1.5 – Transition into Region A	. 57
	6.2.1.6 – Determining Start of Combustion (SOC)	. 58
	6.2.1.7 – Regions D and F	. 59
	6.2.2 – 1600 RPM Analysis	. 60
	6.2.2.1 – Comparison with 2500RPM Data Set	. 63
	6.2.2.2 – Detailed 1600RPM IMEP Cycle-to-Cycle Analysis	. 64
	6.2.2.3 – Cycle-to-Cycle Pressure Per Degree Analysis	. 68
	6.2.2.4 – Anomalous Behaviour In the 5-Cycle Pattern	. 72
	6.2.2.4.1 – First Anomaly Type (IMEP Trace Anomaly)	. 72
	6.2.2.4.2 – Second Anomaly Type (Pressure Trace Anomaly)	. 75
	6.2.2.5 – Importance of Exhaust Port Opening (EPO) Activity and Correlation with Data Set at 2500 RPM	
	6.2.2.6 – Identifying Cycles with Combustion	. 82
	6.2.2.7 – Understanding of The Effect of Pressure at EPO	. 83
	6.2.2.8 - The "saw-tooth" IMEP Pattern and Cylinder Pressure Recovery at 1600RPM	. 84
	6.2.2.9 – Pattern Recognition	. 84
	6.3 – Summary of Analysis at 2500RPM and 1600RPM	. 85
	6.3.1 – 2500RPM	. 85
	6.3.2 – 1600RPM	. 85
	6.3.3 – Overall	. 85
7	– Conclusion	. 86
	7.1 – General	. 86
	7.2 – Background	. 86
	7.3 – Technical Conclusion	. 88
	7.4 – Implementation of Controlled Auto Ignition and the Next Research Steps	. 89
R	eference List	. 91
Δ	nnendix A - Measured Raw Data	102

1 - Introduction

Controlled Auto Ignition or CAI is a combustion process designed to optimise internal combustion by triggering spontaneous ignition of the fuel-air mixture without external spark or heat sources. Auto-ignition occurs when in-cylinder temperatures or pressures reach a critical threshold. Achieving CAI in 4-stroke and 2-stroke engines requires a method of increasing in-cylinder temperatures, usually by retaining exhaust gases, which raise the trapped charge's temperature and pressure. Many researchers introduce the concept of Homogeneous Charge Compression Ignition (HCCI), which can also be considered a form of CAI.[32]

CAI has been a subject of interest to automotive manufacturers for the past few decades as it allows rapid combustion of lean mixtures leading to increased engine efficiency and a considerable reduction in NOx and particulate emissions. [139]. Indeed, it is the basis of the current generation of F1 engines with thermal efficiencies reportedly exceeding 50%. [112]

In 4-stroke engines, CAI is often implemented through valve timing, allowing modified opening of exhaust and intake valves, or by using exhaust gas recirculation (EGR) systems. Both methods increase the internal cylinder temperature by retaining hot exhaust gases. However, modified valve timing comes with limitations, such as negative impacts on scavenging and flow dynamics, which affect engine performance. [78]

In 2-stroke engines, CAI can be more easily achieved due to inherent behavioural characteristics and volatility in the gas exchange processes. The timing and composition of the charge that enters and is trapped in the combustion chamber in a 2-stroke engine is largely governed by port timings and resonance chambers. Intake and exhaust ports are cut into the cylinder liner, their opening and closing being governed by the movement of the piston in the cylinder liner. There will be certain points of the engine's operation where the intake and exhaust ports are open at the same time. The engine is a collection of resonance chambers, their tuning determining when and how intake and exhaust enters the combustion chamber. The fact that a 2-stroke engine fires every cycle means that residual gases are naturally hotter giving an inherent advantage over 4-stroke engines for implementation of CAI.

These inherent characteristics can increase in-cylinder temperatures more readily than in 4-stroke engines. However, 2-stroke engines have historically been sidelined due to emissions issues, despite their advantages in power-to-weight ratio and simplicity. [82]

The author's interest in 2-stroke engines and alternative combustion methods originated during undergraduate studies, when a thesis was carried out focusing on 2-stroke combustion, simulations and the feasibility of achieving Controlled Auto Ignition (CAI). This work was based on 300-cycle averaged data over an RPM range of 2000-10000, provided by KTM of Austria. A two-zone burnt combustion model developed in Excel facilitated the analysis of key combustion characteristics, including Start of Combustion (SOC), End of Combustion (EOC), polytropic indices, Mass Fraction Burned (MFB), Wiebe constants, pressure differentials (Delta P), and temperatures. This model enabled cycle-to-cycle

graphical representations, providing insight into combustion behaviours under various conditions. [128,51]

As part of the undergraduate study a 2D engine simulation model, constructed using physical parts and manufacturer-supplied data (e.g., ignition timing, fuel and air flow), was validated against supplied combustion data. Simulated exhaust throttling predicted residual gas percentages, which were then inputted into the Excel model to determine whether temperatures necessary for auto-ignition could be achieved. While results indicated that CAI was possible, they were not conclusive. [128]

Current literature reveals a lack of information in the exact nature of the pressure changes during CAI combustion and their relationship to cyclic variability. These shortfalls in understanding form a key part of the motivation for this project. The literature looking at combustion analysis in 2-stroke engines does show some analysis of pressure profiles but often these are pressure profiles created from averaged data (large samples) or a collection of non-consecutive cycles. There is very little literature that can be found looking at consecutive cycle-to-cycle behavioural patterns or showing a large number of cycles in any resolution to determine whether there is any deterministic pattern in the instability. The literature review will demonstrate the information that is available to date. [10, 68, 116.118, 141-146]

Given the lack of detailed cycle-to-cycle variation found in the literature the aim of this project is to investigate cyclic variability in a contemporary 2-stroke engine under low RPM and low load conditions with the aim of achieving CAI. 2-stroke engines, while efficient at high RPM and full load, suffer from poor emissions and performance at low RPM and low load, limiting their viability for automotive production. [31-33]

It is important to quantify the extent of cyclic variability and explore methods for mitigating it through CAI. By stabilising combustion at low load, the goal is to improve emissions and fuel efficiency, potentially reviving 2-stroke engines as a feasible option for production. Current 2-stroke engines can typically exhibit a Coefficient of Variance (COV) of IMEP of up to 25% at low load, low RPM conditions, whereas a current 4-stroke engine will require a COV of IMEP in the region of 3-5% under similar low load, low RPM conditions to meet regulatory emissions standards. [10]

The project methodology was to carry out practical testing using a 250cc Husqvarna TE250i (incorporating a KTM engine) specifically purchased by the author for the study and mounted on the University's chassis dynamometer. The author also purchased a complete pressure data and analysis measuring system to allow dependability and self-sufficiency throughout all the testing. This approach allowed for real-time, cycle-to-cycle measurement of combustion pressure data. In order to fit the pressure transducer, the standard cylinder head needed to be modified, and the author secured the help of GT Performance Engineering (GTPE) in Plymouth for this work. [2]

Whilst the ultimate goal of the project was to understand how to implement CAI in the KTM engine, this study very much focused on achieving a practical understanding of the cyclic variation in the KTM engine in the operating region where CAI would be desirable.

In anticipation that CAI might actually be able to be implemented on the KTM engine in the timescale of the project, the author designed a cylinder head based on an extensive literature study of a design successfully introduced by Honda Motor Corporation (Honda) in the 1990s [12-16, 52, 60-67]. The cylinder head was designed as a casting with sufficient metal stock to allow final machining to provide variations across several combustion chamber characteristics, such as compression ratio, combustion chamber volume/shape and squish. These characteristics would be better determined following the results of the cyclic variation testing. The author secured the assistance of specialist casting company Grainger and Worrall (GW) and by necessity the author had to start the design process at the beginning of the project to provide GW with completed designs for the rough stock head to meet their internal time scales to enable them to provide castings to the author within the project timescale. The author's aim was to carry out final machining subsequent to the analysis of the cycle-to-cycle data when a better understanding of the appropriate combustion characteristics could be determined.

In addition, the author also designed a range of exhaust restrictors, exhaust restriction being known from the literature to assist the implementation of CAI by trapping hot residual gases in the combustion chamber [12-16] and it was particularly important to understand how these affected the cycle-to-cycle variation. The manufacture of these restrictors was planned to be carried out in house at the University and their machining was not subject to the same time constraints as required by the foundry for the cylinder heads.

From the outset it was intended that this project should be practical, to be informed by literature and to establish through data collection a better understanding of cyclic variation under low load, low RPM conditions to enhance the existing literature and thereby give a better understanding of how to implement CAI.

As an additional comment, the literature survey will demonstrate that Honda entered limited production in the late 1990s with two commercial models and met the then emissions standards. However, the technology proved too difficult to implement for later generations of emissions standards and achieve market acceptance given their additional noise and driveability characteristics. In fact, there was a general industry wide move to 4-stroke engines at the start of the 21st century. The author's intention was that by achieving a better fundamental understanding further avenues of study might be identified such that future implementation of 2-stroke engines incorporating CAI could become practical.

2 - Literature Review

The author has divided the literature survey into several distinct study areas.

2.1 – Honda Motor Corporation (Honda)

This first section is a study of how Honda introduced a working CAI 2-stroke motorcycle into limited production in the 1990s. The study was of particular importance in guiding the author towards a choice of components to be designed (cylinder head and exhaust restrictors). It is very important to embrace design aspects that have previously shown success in order to form a basis of understanding and further advance implementation. Honda has carried out significant practical research into 2-stroke CAI and their papers will be explained in some depth in the review. These papers have also been particularly motivating to the author and influenced his desire to carry out further research in this field.

[12] - Asai, M., & Ishibashi, Y. (1996 International Congress & Exposition). *Improving the Exhaust Emissions of Two-Stroke Engines by Applying the Activated Radical Combustion*. Detroit: SAE.

This paper show the practical application of Active Radical Combustion (AR Combustion) to improve emissions, fuel consumption and noise. This approach has been applied to several different engines, varying in capacity and use cases. HC emissions were reduced by up to 60%. Specific attention is paid to the commercialisation of a 250cc 2-stroke engine with an exhaust valve.

[13] - Asai, M., Ishibashi, Y., Isomura, S., & Kudo, O. (1993). Japan Patent No. EP 0606095 A1

This patent shows the implmentation of an exhaust valve where the focus appears to be on a design that minimises disruption of the physical continuity and flow characteristics of the exhaust port/passageway.

[14] - Asai, M., Ishibashi, Y., Isomura, S., Kudo, O., & Nishida, K. (1993). *Japan Patent No. US* 5697332 A

This patent shows the particulars of the design of an exhaust valve for AR combustion; specifically the patent shows an exhaust valve produced from a metal pressing, as used on the Dakar race bike.

[15] - Asai, M., Ishibashi, Y., Isomura, S., Nishida, K., Noritake, H., & Takubo, M. (1996). *Japan Patent No. EP 0831214 B1*.

This patent shows the implementation of a novel pneumatic direct injection system in combination with an exhaust valve to implement CAI/AR combustion whilst avoiding the short circuting of fuel.

[16] - Asai, M., Kurosaki, T., & Okada, K. (1995). *Analysis on Fuel Economy Improvement and Exhaust Emission Reduction in a Two-Stroke Engine by Using an exhaust Valve*. Saitama: Honda R&D Co., Ltd.

The study investigates the use of an exhaust valve to improve fuel economy and reduce emissions in 2-stroke engines through the application of Activated Radical (AR) combustion. This paper shows that by maintaining the original advantages of 2-stroke engines, such as high specific power output, the AR combustion system significantly improved fuel consumption and hydrocarbon emissions in bench experiments. It is shown that when tested in a motorcycle during the Dakar rally, the engine demonstrated superior fuel economy compared to 4-stroke models, along with improved driveability and durability. The results suggest strong potential for practical application of AR combustion in 2-stroke engines.

[52] - Honda. (1997). *Press Information FACT BOOK*. Retrieved 02 04, 2018, from http://www.honda.co.jp/factbook/motor/CRM250AR/199701/crm97-005.html

This press release from Honda discusses the technical changes made to the cylinder head for AR combustion in their application and for release of this technology in a production model. Graphics are shown of the combustion chamber shape optimised for AR combustion vs a previous generation cylinder head of the SI engine from which the AR engine was derived. The press release also discusses the design of the exhaust valve, and the important characteristics sought.

[60] - Ishibashi, Y. (2000). Basic Understanding of Activated Radical Combustion and Its Two-Stroke Engine Application and Benefits. *International Spring Fuels & Lubricants Meeting & Exposition Paris, France*, 1-13.

This is quite an extensive summary as this was a key paper in the author's reading and understanding of the AR concept.

The research investigates the auto-ignition phenomenon in internal combustion engines, with a primary focus on the relationship between in-cylinder gas temperature and the onset of auto-ignition. A key finding is that the gas temperature at the end of the compression stroke, referred to as the "auto-ignition temperature," is crucial for initiating auto-ignition. In particular, the study explores the potential of Activated Radical (AR) combustion in optimising auto-ignition, with exhaust valve regulation playing a critical role in maintaining this auto-ignition temperature. This control mechanism is particularly promising for 2-stroke engines, which can leverage AR combustion to improve combustion stability and efficiency.

The paper shows that 2-stroke engines, with their distinct gas exchange characteristics, are particularly well-suited for AR combustion.

This study identifies exhaust valve control as a key mechanism for managing gas exchange and achieving optimal conditions for stable combustion in 2-stroke engines.

This study highlights that maintaining a stable auto-ignition temperature around 1000K is essential for achieving consistent combustion timing, especially in 2-stroke engines.

The research also explores the impact of air-fuel ratio (AFR) on auto-ignition, identifying an optimal AFR of 14.7 for AR combustion. Deviations from this ratio reduce residual gas temperature and delay auto-ignition timing.

The paper shows that AR combustion offers significant benefits for fuel efficiency and emission reductions, especially in 2-stroke engine applications. By controlling the large amount of residual gas, which typically causes unstable combustion, AR combustion stabilises combustion, leading to improved fuel economy. The study suggests that the successful control of AR combustion lies in the management of in-cylinder gas temperature at the end of the compression stroke, which must reach approximately 1000K for effective auto-ignition. This temperature can be regulated through exhaust valve control and other gas exchange processes.

In conclusion, the paper demonstrates that AR combustion holds significant promise for improving the performance of internal combustion engines, particularly 2-stroke engines.

[61] - Ishibashi, Y., & Asai, M. (1998). A Low Pressure Pneumatic Direct Injection Two-Stroke Engine by Activated Radical Combustion Concept. Detroit: SAE.

The paper discusses how to improve emissions in 2-stroke engines by examining the concept of a stratified scavenging homogeneous charge engine that employs Activated Radical (AR) combustion. This concept was demonstrated in an experimental motorcycle engine equipped with a low-pressure pneumatic direct injection system and an exhaust valve. The study successfully implemented a pump-less pneumatic injection system, highlighting its feasibility for practical vehicle applications. The pneumatic system took advantage of the inherent 2-stroke engine architecture, a rotary valve adjoined to the cylinder being charged via in-cylinder pressure. Timing of this valve was controlled via crank rotation.

Emissions testing showed that hydrocarbon (HC) emissions were significantly reduced, approaching levels typical of 4-stroke engines. Additionally, the findings demonstrated the advantages of 2-stroke engines, such as lower nitrogen oxide (NOx) and carbon monoxide (CO) emissions.

[62] Ishibashi, Y., & Morikawa, H. (2010). *A Macroscopic Understanding of the Controlled Auto-Ignition for Vehicle Engines*. Saitama: Honda R&D Co Ltd.

This paper discusses investigation into the understanding of the application of CAI in 4-stroke engines. Conceptual approaches and inherent similarities with the 2-stroke AR concept are demonstrated. Exhaust gas dilution and control of compression temperatures are shown to be similar between both 2-stroke and 4-stroke engines.

[63] - Ishibashi, Y., & Nakano, Y. (1993). Japan Patent No. US 5701851 A

This patent shows a more precise system for controlling coolant flow and cylinder head temperature.

[64] - Ishibashi, Y., & Sakuyama, H. (2004 Fuels & Lubricants Meeting & Exhibition). An Application Study of the Pneumatic Direct Injection Activated Radical Combustion Two-Stroke Engine to Scooter. Toulouse: SAE.

This paper investigates the potential of combining auto-ignition combustion with engine downsizing as a means to reduce CO2 and NOx emissions. Interestingly it demonstrates how to achieve a 70% improvement in fuel economy compared to a conventional 4-stroke engine, while meeting the then Euro 3 emission standards with only the need for a small catalyst. It proposes that 2-stroke engines, due to their operational characteristics, offer a more viable platform for exploring the combined benefits of downsizing and auto-ignition combustion.

[65] - Ishibashi, Y., Asai, M., & Nishida, K. (1997). *An Experimental Study of Stratified Scavenging Activated Radical Combustion Engine*. Saitama: Honda R&D Co., Ltd.

This paper explores the development of a 2-stroke engine utilising a low-pressure pneumatic direct injection system to solve the problems of irregular combustion and fuel shortcutting. It shows that Activated Radical (AR) combustion effectively cures irregular combustion at light loads. This method offers a simpler and more efficient solution by combining stratified scavenging, homogeneous charge, and AR combustion.

[67] - Ishibashi, Y., Nishida, K., & Asai, M. (2001). Activated Radical Combustion in a High-Speed High Power Pneumatic Direct Injection Two-Stroke Engine. In P. Duret (Ed.), *A New Generation of Engine Combustion Processes For The Future?* (pp. 141-152). Rueil-Malmaison: Editions TECHNIP.

This paper investigates the application of Activated Radical (AR) combustion in a high-speed, high-power pneumatic direct injection (PDI) engine, achieving a specific power output of 180 kW/L at 11,000 rpm. The study analyses the impact of various operating conditions, such as load, scavenging efficiency, and engine speed, on the auto-ignition process. It was shown that scavenging efficiency plays a critical role, as increased air flow delayed auto-ignition but improved combustion efficiency.

[94] - Morikawa, H., & Ishibashi, Y. (2007 World Congress). An Experimental Approach to the Controlled Auto-Ignition. Detroit: SAE.

This paper investigates the control of heat release in auto-ignition combustion, specifically focusing on Controlled Auto-Ignition (CAI) in 4-stroke gasoline engines.

It highlights that despite its promise, auto-ignition has faced challenges in practical automotive applications due to the complexity of controlling the combustion process and expanding the operational zone. The paper identifies three major challenges of CAI: expanding the operational zone, developing effective combustion control methods, and designing a control mechanism that is cost-effective for vehicle engines.

[100] - Nishida, K., Kimijima, T., Sakuyama, H., & Murakami, Y. (2007). Enlargement of Auto-Ignition Regions by Applying a Stratified Charge Concept. Nigata: JSAE.

This paper explores the stratification of heat concentration in the cylinder head, making changes to the design such that there is a suitable heat concentration that can act as an ignition source when targeted by an in-cylinder direct injection event, thus triggering CAI. The study demonstrates that Stratified Charge Auto Ignition (SCAI) and heat concentration control successfully extends the auto-ignition range, reducing hydrocarbon emissions by 20% while maintaining fuel consumption and NOx emissions at levels comparable to Homogeneous Charge Auto-Ignition (HCAI).

[101] - Nishida, K., Sakuyama, H., & Kimijima, T. (2005). *Japan Patent No. US 7685989 B2*

The patent outlines a 2-stroke engine that optimises combustion control across various operating conditions using a combination of spark ignition and CAI. The engine features a controller that manages both spark timing and exhaust port restriction. At higher loads, the controller activates spark ignition, while at lower loads, it adjusts the exhaust port to regulate in-cylinder residual gas content and enable CAI. In the low load and low RPM conditions, the engine aims to create a stratified mixture, with the fuel air mixture in the centre of the combustion chamber and with burned gases towards the outside.

[136] - Yamazaki, R., Kurosaki, T., Tsushima, Y., Noda, K., & Ishibashi, Y. (1993). *Japan Patent No. US 5507263 A.*

The patent describes a combustion controller for a spark-ignition, 2-stroke engine that adjusts the exhaust port restriction and ignition timing based on engine speed and throttle position, while including some mechanisms to apparently detect abnormal combustion to optimise the CAI timing to try to ensure stable performance under low-load conditions.

2.2 - Contemporary Research

126 - Turner, J., Blundell, D., Pearson, R., Patel, R., Larkman, D., Burke, P., . . . Kee, R. (2010). *Project Omnivore: A Variable Compression Ratio ATAC 2-Stroke Engine for Ultra-Wide-Range HCCI Operation on a Variety of Fuels.* Hethel: Lotus Enginnering.

This paper explains that a 2-stroke engine is naturally suited for CAI operation because there is less time for heat loss between firing cycles than for a 4-stroke. This means that residual gases in the cylinder are naturally hotter and that the poor scavenging characteristics associated with a 2-stroke engine at low load, low RPM naturally leave a significant amount of hot residual gas in the cylinder. The paper shows that with a compression ratio up to 40:1 (which is not possible in a 4-stroke because of the poppet valves) and a trapping valve to control the amount of trapped residual gases a stable combustion can be achieved under CAI conditions achieving a COV approaching 1-2% of an ideal 4-stroke and because of lean operating conditions achieve NOx outputs in single digit PPM. At these high compression ratios engine efficiencies of over 50% can also be achieved. This is a landmark paper showing the potential of 2-stroke CAI engines in the future.

[149] - Design of a 4-Cylinder GTDI Engine with Part-Load HCCI Capability. Wheeler, J., Polvina, D., SAE 2013-01-0287

This paper shows research carried out by AVL in conjunction with Bosch based on redesigning a GM I4 2.0 Turbo GDI engine. The design changes included a modified cylinder head to incorporate rapid acting variable valve actuation, a modified combustion chamber shape with a smaller 10mm spark plug aimed to be at the center of combustion and angled to be in close proximity to the GDI injector. Additional modifications included a new piston with revised profile and a higher compression ratio of 11.5:1 and the introduction of a supercharger to work in conjunction with a turbo charger. The facility to add cooled EGR back into the intake system was also included.

The combination of supercharger and turbocharger allowed control of the air temperature entering the combustion chamber which was able to be high enough to allow HCCI operation under part load whilst the cooled EGR allowed conventional SI combustion under full load. This is an approach to CAI operation in a 4-stroke engine without the use of a pre-chamber.

[150] - A Review of Pre-Chamber Initiated Jet Ignition Combustion Systems. Toulson, E., P. Attard, W. SAE 2010-01-2263

This paper is a review of pre-chamber design used historically in the cylinder head to improve combustion characteristics and efficiency and which has led to the current use of a pre-chamber by Mahle Powertrain and other researchers as a method to implment CAI. The principle is to have a small volume pre-chamber (around 5% of total TDC chamber volume) at a stochiometric mixture and containing the spark plug to initiate combustion. The pre-

chamber is connected to the main chamber through a number of small holes which allow a series of plasma jets to enter the main chamber and act as multiple ignition sources to allow very rapid combustion of very lean mixtures. The rapid combustion of lean mixtures leads to high engine efficiency.

[148] - Gasoline HCCI/CAI on a Four-Cylinder Test Bench and Vehicle Engine - Results and Conclusions for the Next Investigation Steps. Gottschalk, W., Magnor, O., Jakobs, J. SAE 2010-01-1488.

This paper shows the approach of Volkswagen AG to implement CAI using a combination of an electrically driven compressor, an active valve control system and EGR to control temperatures to achieve CAI/HCCI under part load operating conditions.

[147] - Concept and Implementation of a Robust HCCI Engine Controller. Kang, J., Chen, J., Chang, M. SAE 2009-01-1131

This is a paper by General Motors, implementing HCCI/CAI using cam phasing to control EGR and emphasizes the complexity of attempting to implement HCCI/CAI in a 4-stroke engine and strategies for the control of transitional periods in between CAI and normal operational modes.

2.3 - COV of IMEP

[10] – Antonio Mariani, F. F. (2013). The Effects of a Radio Frequency Ignition System on the Efficiency and the Exhaust Emissions of a Spark-Ignition Engine. *SAE*.

This paper indicates how a COV of IMEP shouldn't exceed 5% in a 4-stroke engine to achieve acceptable emissions control.

[116] - Improving Thermal Efficiency of Internal Combustion Engines: Recent Progress and Remaining Challenges.

This paper shows research on spark assisted controlled auto ignition in a 4-stroke engine and is aiming to achieve a COV of IMEP of less than 3%.

[118] – Richard Samson, A.-G. M. (2023). Effects of the Combustion Enhancer Containing Alkyl Nitrate (CEN) to Methanol in a Direct-Injection Compression Ignition (DICI) Engine. *SAE*.

This paper shows that for a 4-stroke diesel engine a COV of IMEP of less than 5% is required.

[141] - Combustion Analysis with Residual Gas as a Design Parameter for Two-Stroke Engines 2018-32-0045

This paper demonstrates that as residual gas fraction rises on a 2-stroke engine (which occurs under low load, low RPM conditions) the COV can rise rapidly above 5%.

[68] - Ishibe, N., & Ohira, T. (1995). *Combustion Analysis and Its Optimization in Two-Stroke Engines*. Hokkaido: Suzuki Motor Corp.

This study shows the effect on cylinder pressure on a 2-stroke engine operating at 3000RPM and going rapidly from a low load to a higher load condition but is above the RPM condition of the author's area of study and does not show the cyclic variation and high COV problems exhibited at the unstable lower RPM conditions. The paper showed a limited number of consecutive cycles with poor resolution.

[142] - Studies on the Cyclic Variations of Single Cylinder Two-Stroke Engines - Cycle Analysis. Lu, J., Wang, C. SAE 950225

This paper is a comprehensive simulation analysis of cyclic variation in the unstable low RPM, low load operating conditions. It describes how the instability can be divided into three distinct modes, the first being normal combustion, the second being retarded combustion and the third being a misfire. It suggests that whilst the instability is seemingly random, it may actually have a deterministic cause. The simulations show clear emissions increases in the unstable region but lack any experimental data to support their findings.

[143] - A Study of Irregular Combustion in 2-Stroke Cycle Gasoline Engines. Tsuchiya, K., Nagai, Y., Gotoh, T. SAE 830091

This paper is a study by Yamaha Motor Corporation (Yamaha) of cyclic variation at low load and at 3000RPM. Whilst not the author's lower RPM range it does show cyclic variation and a maximum of 5 consecutive cycles in per degree high resolution data points and a total of hundred consecutive cycles. However, it does not show hundreds of cycles in high resolution to determine whether the random instability is indeed deterministic and does not show how unstable regions can recover into stability or vice versa. The engine used is non-standard and has had its exhaust port timing retarded for the purpose of this study and may not be representative of a current production engine.

[144] - Experimental Investigations of Two-Stroke SI Combustion with Simultaneous Cycle-Based Fuel Consumption Measurements. Beck, K., Sarikoc, F., Spicher, U. SAE 2010-32-0061.

This paper predominantly shows an investigation into measuring cycle-to-cycle fuel consumption at low load low RPM operating conditions. It demonstrates the difficulty of such measurements when the fuel flow itself is very low. It does show 6 consecutive cycles of cylinder pressure in some resolution but lacks the high-resolution display of hundreds of cycles to understand how the instabilities can vary over a period of time.

[145] – Intermittent Injection for a Two-Stroke Direct Injection Engine. Balduzzi, F., Romani, L., Bosi, L. SAE 2019-32-0524

This paper explores the impact of an intermittent injection strategy on 2-stroke engine performance at low-load conditions, where cycle-to-cycle variation often leads to high fuel consumption and emissions. The study uses a low-pressure direct injection (LPDI) system to skip fuel injection in selected cycles, allowing only fresh air scavenging and reducing the residual gas ratio. By intermittently supplying fuel, combustion efficiency improves, misfiring is reduced, and unburnt hydrocarbon emissions are lowered. The paper is interesting in that it identifies the low load low rpm instability and proposes a method to improve it. Whilst it shows 100 consecutive cycles of IMEP, it does not show consecutive cycles of cylinder pressure and lacks the detail to understand from the literature how the cycles actually vary from one to the other and how they go through the recovery phase from very unstable regions. The author believes that high resolution consecutive cycle-to-cycle behaviour is needed to better understand the mechanisms at these low stability operating conditions.

[146] - Technologies to Achieve Future Emission Legislations with Two Stroke Motorcycles. Oswald, R., Kirchberger, R., Krimplstatter, S. SAE 2018-32-0042.

This paper shows the difficulties in getting a 2-stroke engine to meet Euro 5 and later emissions standards because of the very poor scavenging characteristics at low load, low RPM conditions and particularly at cold start. It proposes a method of direct injection to try to improve the poor emissions under these conditions. Whilst the paper does not discuss cyclic variation the poor scavenging conditions are undoubtedly a significant part of the reason for the high cyclic variation instability under these conditions.

2.4 – Instrumentation and Data Collection

[6] - A.Randolph. (1990). *Cylinder-Pressure-Transducer Mounting Techniques to Maximize Data Accuracy.* Detroit: SAE 900171.

This paper demonstrates that cylinder-pressure per degree is acquired using piezoelectric transducers due to their high-frequency response and small size. It shows that these transducers are susceptible to thermal shock, which influence the accuracy of the data. It shows that water cooling and proper transducer mounting are very important to control data accuracy. It shows that remote mounting can give significant advantages over flush mounting in the cylinder head.

[140] - In-Cylinder Fiber-Optic Pressure Sensors for Monitoring and Control of Diesel Engines 981913

This paper discusses the development and performance of the Optrand Inc (Michigan) high-temperature, miniature fibre-optic pressure sensor, designed for advanced diesel engine control and monitoring. The paper shows that the sensor can be integrated with fuel injectors or glow plugs enabling real time cylinder pressure measurement. The paper shows a significant advantage over piezoelectric sensors in the ability to be far less influenced by thermal shock.

[47] - H.-J. Kress, J. M. (1995). *Integrated Silicon Pressure Sensor for Automotive Application with Electronic Trimming.* Detroit: SAE 950533.

This paper shows a silicon chip concept that can be integrated inside the pressure sensor to provide signal conditioning.

[121] - T. Poorman, L. X. (1997). *Ignition System-Embedded Fiber-Optic Combustion Pressure Sensor for Automotive Engine Control and Monitoring,*. SAE 970853.

This paper demonstrates that the Optrand sensor can be successfully incorporated in the spark plug/coil pack on a working engine and resists thermal drift to provide data accuracy comparable with a professionally installed laboratory grade piezoelectric sensor.

[69] - Ivansson, N. (2003). *Estimation of the Residual Gas Fraction in an HCCI-engine using Cylinder Pressure*. Linköping: Linköping University.

This paper demonstrates the use of a signal pressure transducer to estimate the residual gas fraction by using the ideal gas law and a separate measurement of temperature. It simply demonstrates the importance of being able to measure cylinder pressure and validate its use as an essential part of engine development.

[84] - Lavy, J., Angelberger, C., Guibert, P., & Mokhtari, S. (2001). Towards a Better Understanding of Controlled Auto-Ignition (CAITM) Combustion Process from 2-Stroke Engine Results Analyses. Pisa: SAE.

[87] - Manente, V., Tunestal, P., & Johansson, B. (2008 Small Engine Technology Conference). A Novel Model for Computing the Trapping Efficiency and Residual Gas Fraction Validated with an Innovative Technique for Measuring the Trapping Efficiency. Milwaukee: SAE.

This paper demonstrates the application of a cylinder pressure transducer in a 2-stroke engine to measure the residual gas fraction by using pressure in combination with inlet and exhaust port gas temperature measurements.

2.5 - DOE and Testing

[151] – Engine Testing: The Design, Building, Modification and Use of Powertrain Test Facilities Hardcover – 4 Dec. 2012 - A. J. Martyr, M.A. Plint

The book forms a baseline for how to carry out high quality and repeatable engine testing. It covers the need to control accurately aspects such as engine and environmental test chamber temperature, the use of correct measuring sensors and their calibration and how to condition the engine prior to testing to achieve repeatable results.

[152] – The Design of Experiments – 1 April 1972 – Ronald A. Fisher

Ronald Fisher is considered to be the father of design of experiment and his first work was published in 1935. It focuses on the need to rationalise the number of factors involved in a test given that there is not an infinite amount of time for testing. It is important to recognise the important factors involved and to reduce the number of variable changes to manageable steps.

[153] - Taguchi Methods: Design of Experiments (TAGUCHI METHODS SERIES) – 1 Nov. 1993 - Genichi Taguchi, Yoshiko Yokoyama

Based on the work by Fisher, the design and analysis of experiments was further enhanced using statistical methods to reduce the number of tests with multiple variables from a factorial number to a much more realistic number which nevertheless can provide meaningful conclusions. Emphasis is put on establishing a suitable signal to noise ratio to achieve reliable analysis.

2.6 – Summary

The papers of section 2.1 in particular have provided inspiration and background to the author in helping determine the initial designs for prototype cylinder heads and exhaust restrictors for use in the KTM engine.

Contemporary research papers included in section 2.2 have provided additional insight but also reinforced the complexity of practically implementing CAI in a modern 2-stroke engine. However, they illustrate the continued automotive interest to develop a practical engine with the technical advantages which CAI operation can provide under low load, low RPM conditions.

The papers highlighted in section 2.3 demonstrate the lack of in-depth consecutive cycle analysis available in the academic literature when studying a 2-stroke engine under low load and low RPM sub optimal operating conditions.

To the author such a lack of available detailed consecutive cycle information is a major disadvantage when contemplating the design and implementation of CAI to counter the real disadvantage of 2-stroke engines for general automotive application.

This lack of in-depth consecutive cycle behaviour was a fundamental motivation for the author to address in an experimentally driven practical research project using a currently available KTM motorcycle engine.

The author believes that such measured and published data would provide benefit to both the author and the wider research community and form a platform of data for ongoing analysis not possible from the current literature.

The papers of section 2.4 and 2.5 provided the author with significant information on the instrumentation required for the project, the test procedures and an efficient method to carry out the testing.

3 - Design

3.1 - Inlet Design

Following on from the large body of work conducted by Honda [12-16, 52, 60-65, 67, 94, 100-101 & 136], it can be stated that to achieve CAI operation the aim is to increase the amount of residual gas contained within the cylinder. A greater quantity of residual gas in the cylinder results in a higher average temperature. It has been shown that in practice an inhomogeneous distribution of temperature is preferable to a homogeneous distribution of temperature in the cylinder to create hotspots/ignition kernels to initiate combustion [32]. The main mechanisms for increasing the amount of residual gas retained within the engine is to throttle the engine either via the inlet or the exhaust. Throttling via the intake is more difficult and involves making significant changes to the inlet in terms of both diameter restriction and restriction via the modulation of passage lengths. Adaptations such as these are harder to make, as the inlet tract in the chosen engine is incorporated into both the crankcase and the cylinder block, both of which would be unfeasible to redesign or modify considering the financial and time-based limitations of this project. Figure 1 shows the inlet tract of the project engine (reed valve assembly, crank case, and cylinder).

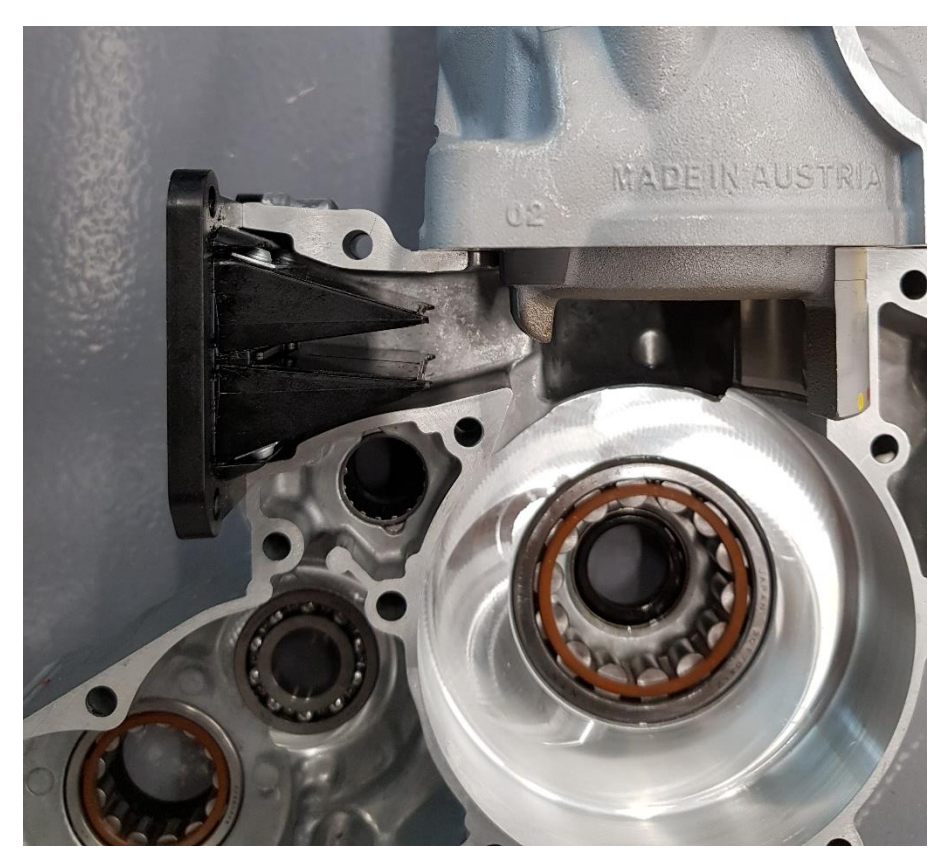


Figure 1 - Engine Inlet Tract (split/half crankcase)

3.2 - Exhaust Design

With the decision made to avoid modifying the inlet tract, the focus was put on exhaust design. Honda had showed in commercial and experimental applications that restricting or throttling the exhaust port was effective in implementing CAI [60]. The restricting was achieved in two different ways, either by a butterfly design or by a trapping valve as close to the cylinder as possible. Both methods were dynamic in their operation, as necessitated by the varying RPM and load conditions. Honda's first commercial application of CAI was in a 125cc scooter with a CVT transmission and used the butterfly valve.

The second application demonstrated by Honda was one geared more towards performance and transient dexterity. The application was a commercialised 250cc road legal enduro bike. The vehicle incorporated a trapping valve, which could both restrict and change the timing of the exhaust port opening according to dynamic situations and provide a large range of operation and a tighter fit than a traditional trapping valve. In comparison to a traditional exhaust valve which typically can only restrict the exhaust by less than 50%, the Honda trapping valve was capable of a much greater restriction.

Honda made a specific effort to sculpt the exhaust valve to fit as close as possible to the curvature of the piston and cylinder, even going as far as to produce a lost wax casting in stainless steel and precisely machine the sealing face. This precision was necessary to achieve a sufficiently tight seal to enable increased control over both the trapping of exhaust gases and the effective compression ratio to better support CAI. A very similar design was later adopted in the Lotus Omnivore engine. [126]

The engine being used in the author's project was a modern high performance 2-stroke and is quite similar to Honda's 250cc commercial engine discussed in the second paragraph but unfortunately contained a more traditional trapping valve lacking the ability to accurately control trapped gases and effective compression ratio. For this reason and following a review of the literature it was decided that a static exhaust restrictor would be fit for purpose (providing a simple means of throttling the exhaust and increasing residual gas content). Examples of the exhaust restrictors designed by the author and manufactured at the University are shown in Figures 2 and 3. Several exhaust restrictors of different areas were manufactured, and the standard exhaust was modified so that they could be installed with ease. The standard exhaust had two O-ring grooves, one of which was ground away to allow the restrictors to be fitted without effecting exhaust position. Care was taken to ensure that the exhaust restrictors were angled symmetrically to ensure minimal disturbance of the exhaust gases.



Figure 2 - Exhaust Port Restrictor Adjacent to Modified Exhaust



Figure 3 - Exhaust Port Restrictor Inserted in Modified Exhaust

3.3 – Design of Cast Prototype Cylinder Head

3.3.1 - Introduction

Following the work completed by Honda [12-16, 52, 60-65, 67, 94, 100-101 & 136] the important design elements of the cylinder head to achieve CAI include squish (angle, area, clearance), combustion chamber and spark plug location. The combustion chamber design itself is particularly important and may contain non symmetrical squish bands and an offset chamber in contrast to a traditional 2-stroke cylinder head design.

Having secured the cooperation of Grainger and Worrall the author's design aim was to create ten prototype castings which would have sufficient rough stock to allow final machining to achieve many of Honda's combustion chamber findings and also to reflect further understanding obtained as a result of initial testing using the standard KTM head. The decision to manufacture only ten rough stock heads was influenced by the practical consideration that any more than ten heads would be financially too burdensome for the project and from Design of Experiment (DOE) studies by the author indicating that there would be enough rough stock on each head to allow a sufficient range of final machining to achieve the project aims. [152, 153]

3.3.2 - Appraisal of KTM Cylinder Head

The first step in the design process was to complete a thorough appraisal of the standard KTM cylinder head. Appraising the standard cylinder head would help define important features such as hole spacings, heights and other core features and properties as it was essential that any prototype part be a direct replacement for the KTM head. Because it was a practical project, the appraisal of features such as combustion chamber wall thickness was very important to ensure structural integrity when used in the running engine. The author was able to personally use the facilities of Grainger and Worrall to comprehensively appraise the physical dimensions of the head through both tactile (CMM) and non-tactile (CT scan) measurement techniques. The CT scan gave a great view of global relationships and internal features, whilst the CMM measurements provided final geometric accuracy to allow the design process to go ahead. Figure 4 shows the cut away image of the CT scan and Figure 5 shows the CMM measurements in process.

A 3D CT scan is expensive and slow as it operates in a series of 2D slices. The author had to choose a resolution step between slices of 0.5mm in order to achieve sufficient internal geometric accuracy needed to properly represent the KTM head. Useful to the author was his previous experience of operating and collecting data from the CT scanner. The huge advantage of the CT scan is that it enables internal examination without the need to physically dissect the head.

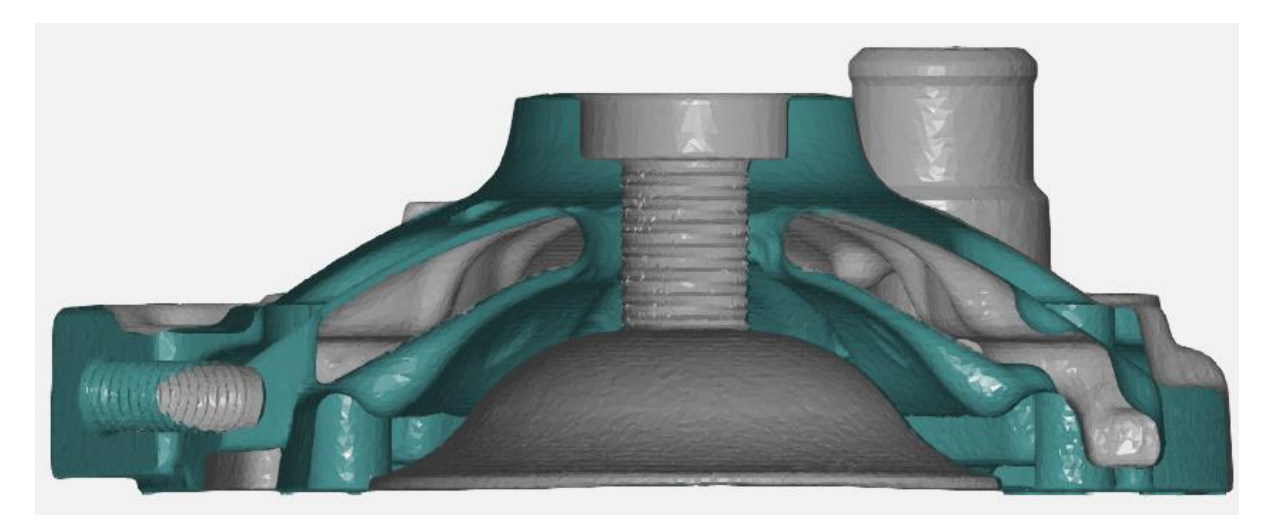


Figure 4 - CT Scan of Original KTM Cylinder Head (cross sectional view)

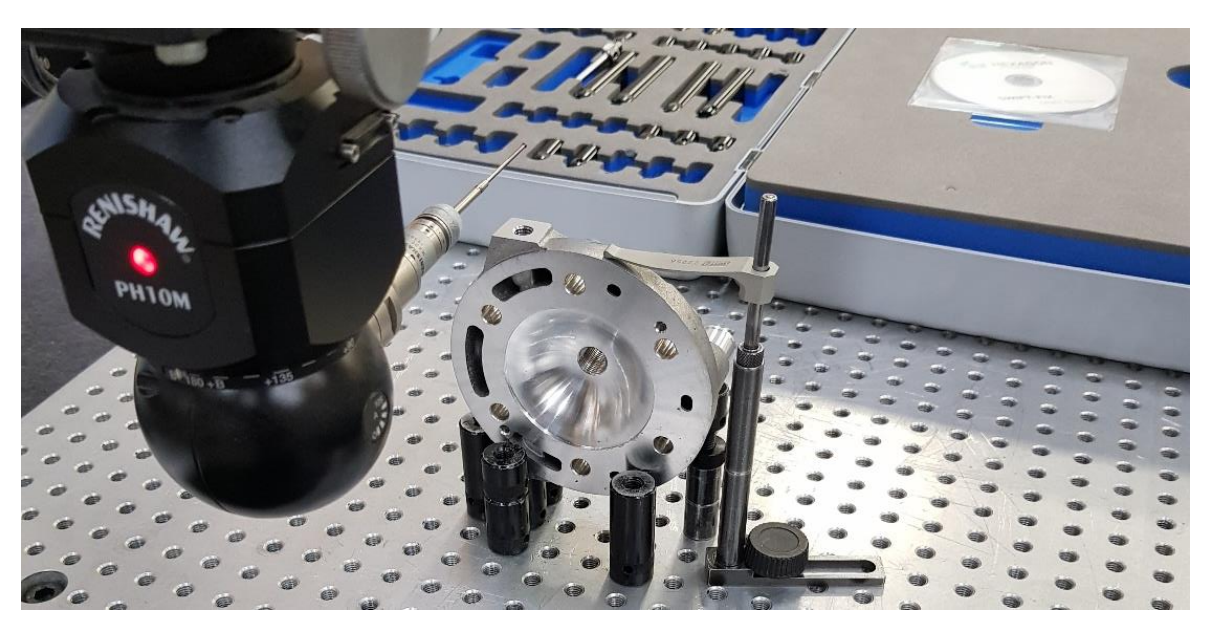


Figure 5 - Tactile Measurement of Critical Features

3.3.3 - Initial design

Following the thorough dimensional appraisal of the KTM head and the review of Honda's design process it was clear that quite drastic design changes would be needed. The author needed to change aspects such as combustion chamber shape, squish area, squish clearance, squish angle and compression ratio whilst realising that all these features interact and affect each other. The author believed that the ten rough stock prototype castings would allow sufficient variations to allow a broad study of the above design aspects. Informed by DOE literature [152, 153] the author designed five core variations, all five variations sharing the same starting squish clearance of 1.8mm and squish angle but differed in compression ratio

by varying the size of the central spherical combustion chamber, which in turn affected the area of the squish band. The author chose a spherical combustion chamber similar to Honda on the basis that it had the least surface to volume ratio and can minimise heat losses out of the chamber. The author also recognised the need to retain the standard KTM wall thicknesses whilst implementing the above chamber redesigns in order to retain structural and working reliability.

In addition to modifying the combustion process it was also essential to include measuring sensors in the cylinder head design. Absolutely vital was the inclusion of an in-cylinder pressure transducer and, in addition, sensors to measure the temperature of the combustion chamber and squish band. Understanding temperatures is important when separately analysing heat transfer from the squish band and from the cylinder volume and the author wanted his practical work to provide data for ongoing theoretical analysis by interested parties.

As an example of calculations behind the design process, Figure 6 shows the effect on squish velocities of the five core designs through skimming and reduction of squish clearance.

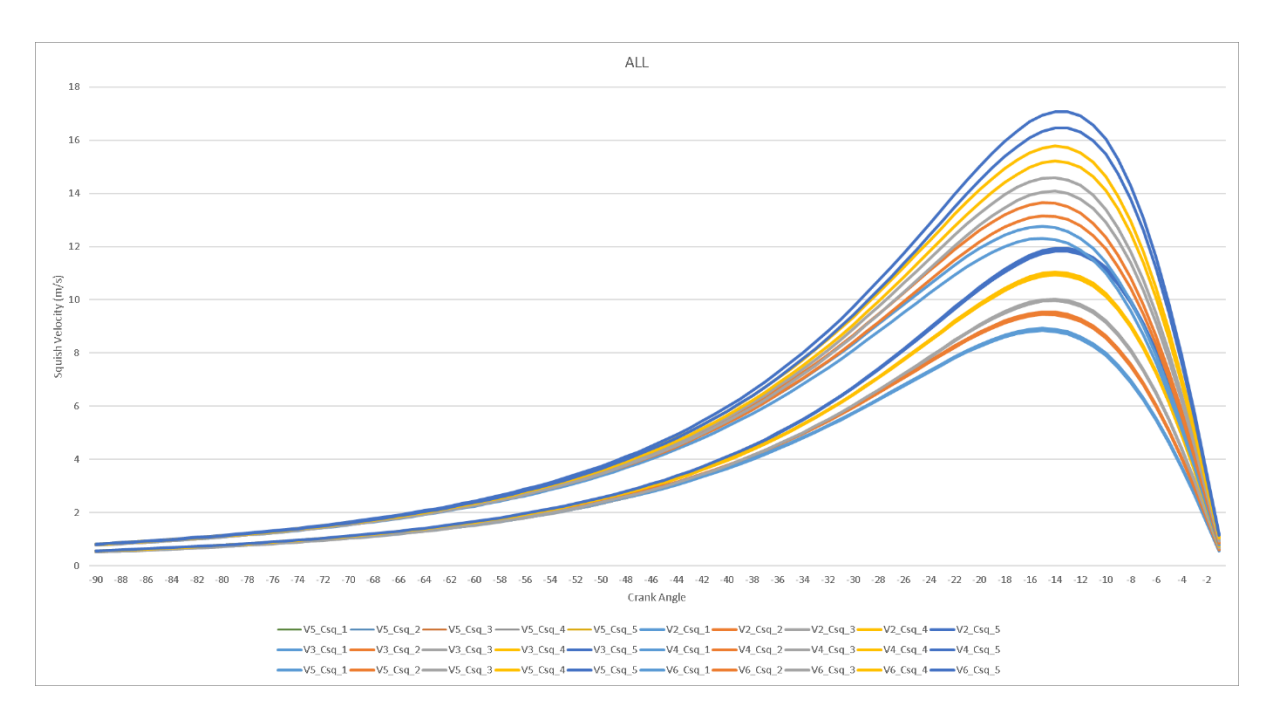


Figure 6 - Squish Calculation Variants

The main combustion chamber volume has different demands to the squish volume and its significantly larger volume needs to retain as much heat as possible. Whilst researchers have shown the advantages of inhomogeneity in the combustion chamber [96,100], simulation of such characteristics was beyond the scope of the project and the author's initial design was to replicate the features of the Honda cylinder head. [63]

In an ideal design world, a combination of FEA and practical testing would take place in an iterative design process. In this case, as a practical project temperature sensors incorporated in the cylinder head would provide measurements to allow analysis for any required re-design.

Two temperature sensors using bolt thermocouples were positioned in the cylinder head as can be seen by two adjacent holes at the 7 o'clock position in the CAD diagram in Figure 7. The bolt thermocouples incorporate a thermocouple embedded in an M8 bolt in which the end face of the bolt is the sensing surface. Figure 8 shows a bolt thermocouple. The holes in the cylinder head are threaded such that the bolt sensor end faces touch on machined pads near the surface of the main combustion volume and the squish band.

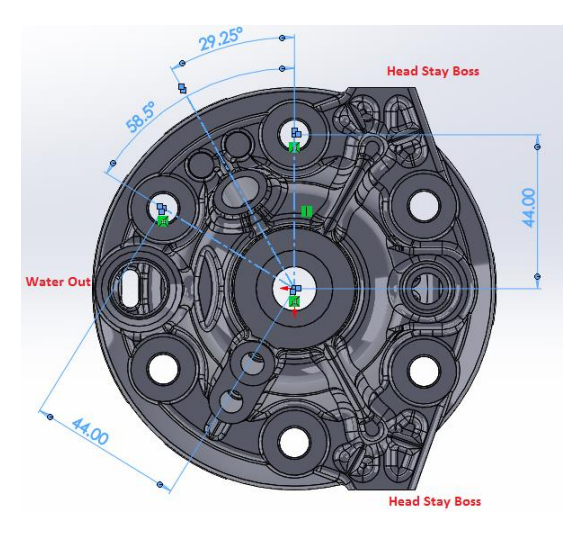




Figure 7 - CAD Design

Figure 8 - M8 Bolt Thermocouple (TCDIRECT, 2019)

In the design of a cylinder head the water jacket must be configured to take into account the different cooling requirements of the main volume, the squish band and the spark plug. The requirements all interact with each other and whilst the main volume combustion gas needs to retain its heat energy it is important that the squish band and spark plug don't get too hot. The bolt thermocouples will allow the author to understand the temperatures of the main volume and squish band but are not appropriate to measure the temperature of the spark plug. To measure the temperature of the spark plug the author planned to fit a washer type thermocouple beneath the spark plug. Bolt thermocouples were not suitable in this case as the waterflow near the plug is already limited and it is important not to further compromise the flow with a bolt obstruction.

The spark plug, which is central in the main combustion chamber, would ideally require a higher rate of cooling as its combination of ceramic and steel naturally reduces its capacity for heat transfer. It is important that the spark plug is kept cool to avoid any unnecessary preignition.

The need for different cooling requirements for the main volume, squish band and spark plug illustrate the complexity when designing a cylinder head and its cooling jackets.

Whilst the project aim was to create a cylinder design capable of implementing CAI, it must be remembered that CAI operation is targeted for low RPM, part load conditions to improve

cyclic variation and coefficient of variance of IMEP. However, the engine must also operate as a normal spark ignition (SI) engine under full load conditions where CAI is not permissible due to a lack of residual gas and any cooling system must consider both CAI and SI requirements. In recognition that under CAI operation the engine may need to be kept hotter, Honda introduced a CAI mapping strategy to reflect the different needs using water temperature sensors, RPM and throttle position measurements. Cognisant of the above the new design had to maintain a normal cooling jacket to allow both CAI and SI operation and to stay as close as possible to the KTM design in terms of water jacket and general form. In combination with this requirement a literature informed combustion chamber shape was implemented such that the shape could be varied in size to allow for different combustion chamber volumes, squish areas, compression ratios. Because each different machined variation is made from one casting design it will mean that there would be a variety of combustion chamber wall thicknesses, though the thickness of the squish band will stay consistent through all variations. The author feels that with such a significant number of variations possible, it would be unwise to diverge further from conventional design as too many changes are more likely to jeopardise meaningful interpretations.

The intention is that the above variations would provide useful data to inform future design and control strategies. Although future designs might have to stay aligned with conventional approaches for an engine that operates in both CAI and SI modes, it was hoped the data would provide insight into what could be changed in more extreme scenarios such as dedicated CAI engines under all operation conditions.

Having developed the design concept, the next step was to create a parametric design and rapid prototyped 3D model of the head. 3D models help enormously in achieving a greater global appreciation of the practical design issues.

In addition to ensuring that the design meets all geometric and functional targets, the 3D model also assists greatly with the design for manufacture (DFM) process given that the design was to be implemented as a casting in which metal flow and solidification characteristics need to be considered.

With a combination of CT scan and CMM data, a first design model was produced to be as close as possible to the original KTM design. Given that the original KTM head had been designed using a CAD package the above measured data was used to re-create a CAD model similar to that of KTM. Although not knowing what CAD package was used by KTM most CAD packages have very similar functions. Given a lack of feature recognition software, it was a task of splitting the scan and tactile measurement data into identifiable parametric features (a central dome, prism shapes) to establish how the features are dimensionally related to each other and which software tool had been used to construct each feature.

Once the CAD model was completed it was converted into an STL file and then imported into geometric inspection software (GOM). The STL files of both the scanned CT data and created CAD model were overlayed and from this a colour map of any deviation was produced to confirm that the CAD model fulfilled the basic accuracy requirements.

Figure 9 shows the initial CAD design created from the scanned and measured data. At this stage the design is the standard, mass produced part and contains a provisional placement for a cylinder pressure transducer. It is to be noted that at this initial stage the CAD design lacks the facility for temperature sensors shown in the finalised version in Figure 7.

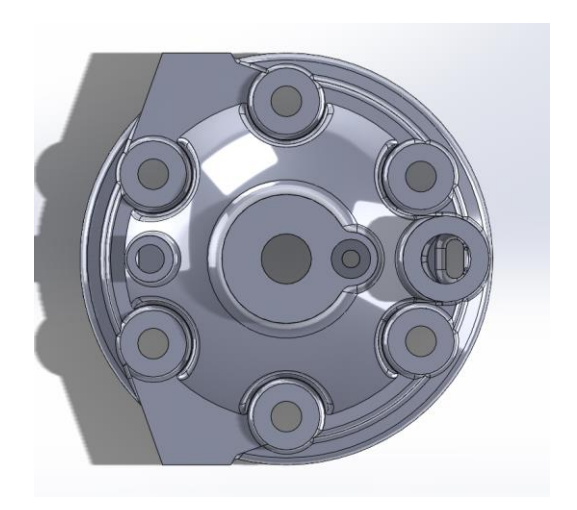


Figure 9 - Initial Design Layout Incorporating Provisional Placement of Pressure Transducer

Figure 10 shows a different view of the initial CAD design whilst Figure 11 shows a cross-sectional view showing the pressure transducer placement next to the spark plug.

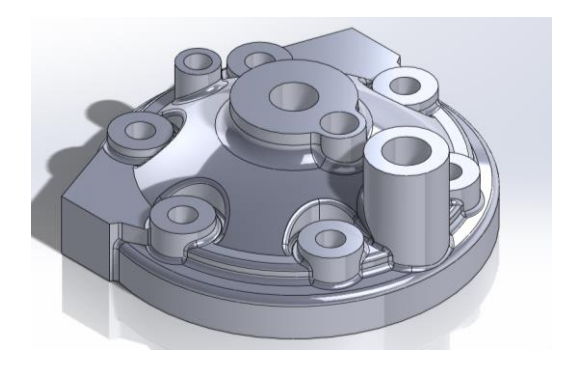


Figure 10 - Initial Design Layout

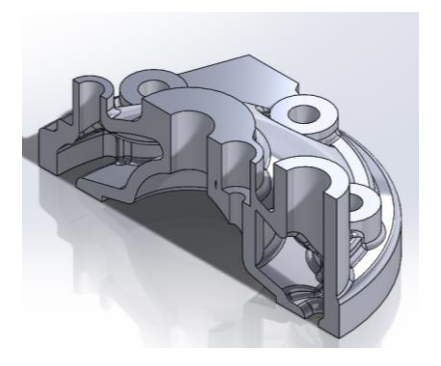


Figure 11 - Cross-Section

However, the initial design incorporating the location of the cylinder pressure transducer next to the spark plug subsequently proved to be problematic from two perspectives; firstly, the passageway was not normal to the combustion chamber surface and secondly putting the transducer so close to the spark plug would mean significantly reduced coolant flow in this area.

The final design shown in Figure 7 shows the cylinder pressure location correctly positioned to reflect the above considerations and illustrates why it is so important to consider basic placement of components from the outset to avoid further compromises down the line.

3.4 - Modified KTM Cylinder Head for Initial Testing

In terms of the initial engine testing the standard KTM cylinder head needed to be modified to incorporate measuring sensors. For machining work the author had secured the cooperation of GT Performance Engineering (GTPE) in Plymouth. It was realised that using the standard head it would not be practical to incorporate bolt thermocouples because of cooling and structural integrity, so effort was concentrated on fitting an essential in-cylinder pressure transducer to provide crank angle degree pressure measurements to establish cyclic variation combustion characteristics of the standard production engine.

Initially it was thought that a welded insert incorporating the pressure transducer could be fitted into the outer part of the head. However, given the double skinned nature of the head, suitable water coolant sealing and subsequent removal of the insert would have been impossible. The second option was to machine away more of the outer part of the head to allow welding of an insert directly to the combustion chamber wall, but this would have created unacceptable heat distortion of the chamber and head structure.

The final solution was to install the insert without welding by drilling through the outer skin and machining a flat on the outer surface of the combustion chamber. The hole in the outer skin would then be threaded to allow a screw-in insert containing the pressure sensor. The insert itself would seal on the machined flat on the outer surface of the combustion chamber using an O-ring groove machined on the insert's inner face. The insert was drilled internally to allow fitting of the pressure sensor and a suitable diameter hole drilled through into the combustion chamber itself. This solution was very much a practical one to minimise any compromise to the integrity of the standard head. Figure 12 shows the machined flat with a small drilling through to the combustion chamber to allow cylinder pressure measurement. Figure 13 shows the drilling process for the narrow passageway to the combustion chamber.







Figure 13 - Drilling of Pressure Passageway (GTPE, 2019)

Figure 14 shows the insert next to the modified head whilst Figure 15 shows the machined insert with O-ring placed in the O-ring groove on sealing face.







Figure 15 - Machined Insert and O-ring (GTPE, 2019)

3.5 – Cylinder Pressure Transducer

In addition to physically appraising the cylinder head design, one of the most important design considerations was which sensor would be used to measure in-cylinder pressure. The industry standard of sensor for the monitoring of in-cylinder combustion pressure is the piezoelectric sensor, the most prominent producer of these sensors being Kistler Instruments LTD. The basic premise of these sensors is that they contain a piezoelectric material which allows a charge to be generated that can be measured as a voltage proportional to the pressure. To be able to measure this, a charge amplifier is needed to convert the charge into a voltage. From very early on the author realised that piezoelectric pressure sensors were not an option, simply due to price (one sensor alone could cost several thousand pounds Sterling). (Kistler, 2019).

Their literature indicated that whilst this type of sensor did not have the same level of accuracy as the piezoelectric type indicative results were nevertheless promising that it would be sufficient for this project. Ultimately the type of sensor used was highly constrained by the project's financial limitations, but the fibreoptic sensors did have some inherent advantages which included size (available as small as 3mm diameter), the lack of need for water cooling and being resistant to electromagnetic interference. The pressure sensors and combustion logging equipment were purchased from TFX Engine Technology in Canada [154]. The project requirements were discussed with TFX from which the appropriate sensors were specified

along with installation advice. The advice for installation had a significant bearing on the design of the prototype cylinder head and the machined KTM head. When connecting to the combustion chamber the pressure sensor had to have a pilot passage of specified diameter of 0.75mm and ideally a specified length of 3.75mm although the latter was not possible in the KTM head but was still considered acceptable. This passageway served two functions; it would naturally act as a flame quenching device, protecting the pressure sensor diaphragm from heat and flame damage and as a damping device to filter out noise and undesirable pressure oscillations [1]. As well as having quite specific dimensions, the instructions also placed importance on the orientation of this passageway, the passageway needing to be normal to the combustion chamber surface. To achieve this the author provided GTPE with a cross-sectional drawing of the cylinder head, specifying the placement of the passageway as shown schematically in Figure 16 whilst Figure 17 shows the drilled pressure pilot hole in the combustion chamber.

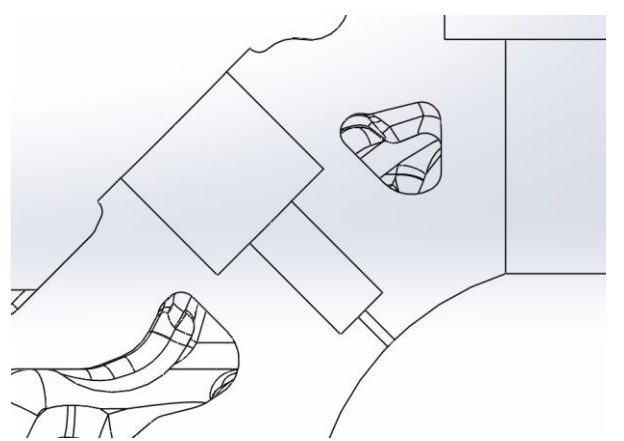




Figure 16 - Passageway Placement for Pressure Sensor

Figure 17 - Pressure Pilot Hole in Combustion Chamber

Figures 18 and 19 show the pressure sensor installed in the insert and the combined pressure sensor and insert installed in the cylinder head.



Figure 18 - Pressure Sensor in Insert



Figure 19 - Pressure Sensor and Insert in Head

3.6 – Design for Manufacture Philosophy

The initial digital design process was an iterative one starting with a basic mapping out of the elements in terms of their composition and placement. It is also very important to bring digital designs to the physical world at an early stage. The latter can provide a far better perspective for the designer. In the case of the KTM engine the author had access to the actual bike but not the bike's CAD drawing, so creating rapid prototyped cylinder heads and components allowed simple confirmation that the designed parts would fit the real bike correctly.

3D prototype parts allow a designer to use sensory measurements such as touch and can identify, for instance, stress concentrations which were not apparent from a blended radius in a CAD model. The migration from a CAD model to a physical part can often bring up unexpected consequences which only become apparent on the physical object and the use of 3D modelling is considered by the author to be an essential part of successful design.

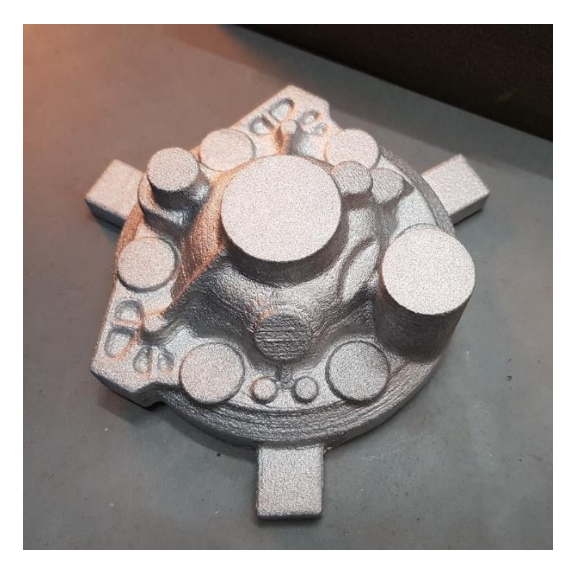
The creation of 3D physical models also brings some very practical advantages with other stakeholders in the design and manufacturing process.

To illustrate this, the 3D models formed an essential tool in discussions with Grainger and Worrall and GTPE to allow them to accurately appraise the design validity and provide feedback as to what was possible to achieve during the respective manufacturing processes. CAD models are often insufficient by themselves when seeking the cooperation of practical manufacturing companies.

At GTPE, time was saved as the need for technical drawings was avoided by having in-person discussions using the rapid prototyped part to give context and appreciation of the project requirements and prevent any machining mistakes in this one-off modified KTM cylinder head.

In the case of Grainger and Worrall, the 3D part allowed their casting engineers to identify that the "chill" designed by the author to enable correct cooling of the thicker walled combustion chamber would not work. The author had designed the "chill" to match the curvature of the combustion chamber, but GW instantly explained that this would not be economically possible due to it requiring a custom made "chill". Instead, the author redesigned the combustion chamber profile to suit a standard "chill".

A second example at Grainger and Worrall centered around the machining tabs the author had initially designed into the casting. The 3D part allowed the GW machinists to quickly recommend the use of three basic tabs which would meet all the technical requirements but would be much more economical to cast.





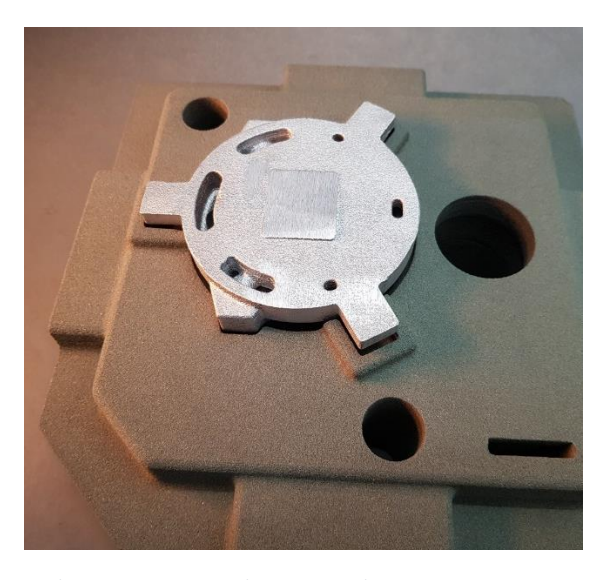


Figure 21 - Cast Cylinder Head in Sand Mold

Figures 20 and 21 show the as cast manufactured part by GW, in isolation and then placed in its sand mold for illustration. Out of interest, Figures 22 and 23 show the standard "chill" used by GW and its impression left in the cast part.





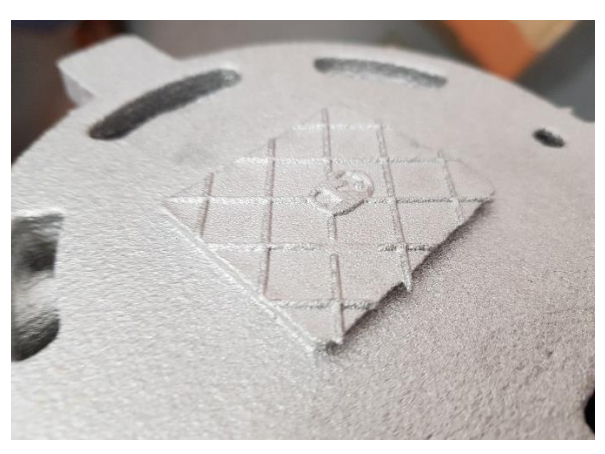


Figure 22 - Standard "Chill" (Grainger & Worrall, 2019) Figure 23 - "Chill" mark in Casting (Grainger & Worrall, 2019)

To summarise, the use of 3D models helps both the designer to fully appraise a design and allows very practical interactive discussions with manufacturing partners.

4 - Testing

4.1 – Design of Experiment - DOE

Considerable time had to be spent developing the test procedure. A literature survey studying experimental engine test work [150] was used to help guide the author in that engine testing can be prone to failures and that dynamometer test time at the University would also be limited because of other activities using the facility. It was essential to focus on the operating conditions most likely to gain improvement from CAI operation and to establish a realistic and finite set of operating steps to properly cover the areas of interest.

Having conducted a review of literature concerning 2-stroke cyclic variation, [142, 143] the author had a clear idea of the operating conditions under which the engine would be operating at its worst with high cycle-to-cycle variation. Literature had identified the problematic operating conditions to be at low RPM and at low load under which conditions the COV of IMEP deteriorates significantly. It was not clear from the literature how the COV of IMEP actually changes as a function of load and RPM. Such high values of COV of IMEP are a result of large cycle-to-cycle variation and explain why exhaust emissions control is so difficult under these conditions. [68]

The work by Honda [12-16, 52, 60-65, 67, 94, 100-101, 136] shows that it is under these same conditions that CAI operation can provide significant improvement and that it is under these conditions with high amounts of residual gas that CAI operation is most likely to be successfully implemented.

Although initially the KTM engine under test was not going to be modified and would be running as a conventional SI engine, none the less, devising a test plan centered around these operating conditions would be of great benefit to establish a thorough understanding of cycle-to-cycle behaviour in a contemporary KTM engine. The recording of multiple consecutive successive cycles of cylinder pressure per crank angle degree would provide data which the author has been unable to find in literature. It would provide the basis for new and detailed academic analysis. Given the dynamometer time constraints and the ever-possible risk of engine or sensor failure, DOE techniques were implemented to reduce the test load and RPM conditions to a finite number of steps which would cover the unstable region of 2-stroke operation. [152,153]

Variables would be load and RPM and a realistic set of parameters needed to be established under varying degrees of exhaust restriction. The exhaust restrictors were designed to restrict cross sectional area in 10% steps from no restriction to 90% restriction through calculations carried out in Excel linked to models in Solidworks.

The test plan was to start at 0% restriction to provide baseline data for a standard unmodified KTM engine. This was considered an essential starting point and would provide consecutive cycle-to-cycle cylinder pressure data not found in the literature. Analysis suggested that finer

restriction than 10% would simply be too time consuming and not provide a wide enough initial view whereas coarser steps would likely change the gas dynamics too much to understand the subtlety of how increasing quantities of residual trapped gas changed the combustion process. It is a balance of having steps sufficiently broad such that results are not negated by noise in the data collection and engine operating conditions but not too broad that transitional details are lost.

4.2 – Practical Implementation of Test Variables

To practically achieve an indicative measurement of load a throttle position sensor was used. Its opening angle could be accurately measured electronically and would allow repeatable back-to-back testing. Throttle opening was set manually according to measured voltage. During engine testing ideally the voltage would provide automatic markers to the recorded data but in this case that was not readily practical. However, the author appreciated that the 10% throttle open increments would provide sufficiently significant changes in recorded peak cylinder pressure that on continuous engine running it would be obvious from data when the steps occurred.

Continuous running was considered essential once data collection started to maintain stable and consistent engine operating conditions such as engine and environmental temperatures.

RPM would be monitored via a pick-up clamp placed around the spark plug coil wire, this signal to be fed to the chassis dynamometer control system for the purpose of speed control. The data logging system would be readily able to monitor RPM via the crank pick-up sensor and changes in RPM during continuous engine running would be easily identifiable.

In practice, adjusting the exhaust restriction percentage would require a certain amount of downtime (circa 2 hrs) as the bike, engine and exhaust would need to cool for safety, although the exhaust change itself would be relatively simple. Table 1 shows the designated RPM and throttle opening percentages for 0% exhaust restriction, the same parameter set would apply to additional percentages of exhaust restriction.

Exhaust port restriction = 0%											
RPM	Throttle (TH%)										
Idle*	0%**	20%	30%	40%	50%	60%	70%	80%	90%	100%	
2000	0%**	20%	30%	40%	50%	60%	70%	80%	90%	100%	
2500	0%**	20%	30%	40%	50%	60%	70%	80%	90%	100%	
3000	0%**	20%	30%	40%	50%	60%	70%	80%	90%	100%	
3500	0%**	20%	30%	40%	50%	60%	70%	80%	90%	100%	
4000	0%**	20%	30%	40%	50 %	60%	70%	80%	90%	100%	
4500	0%**	20%	30%	40%	50%	60%	70%	80%	90%	100%	

Table 1 – Test Run Schedule

4.3 – Test Facility Setup

The decision was made to use the University chassis dynamometer for testing as the time involved in setting up the engine dynamometer would have been too long and the amount of work too extensive. The first step was the mounting of the motorcycle safely to the chassis dynamometer. This was a simple task that involved a largely standard routine whereby the motorcycle was held by its front wheel in a wheel chock and the wheel chock was adjusted so that the rear wheel sat centrally between the rear rollers. Ratchet straps were used to ensure safety and that the driven rear wheel had sufficient load on the rollers. An important practical consideration for the chassis dynamometer was that the motorcycle needed to have its rear tyre changed because, as standard, it came with an off-road tyre. Such a tyre would lack grip on the rollers and would skip. The tyre was changed to a traditional smooth road pattern and in this instance a part worn tyre was used for economy as ultimate performance would not be needed at part load. Figure 24 shows the bike on the chassis dynamometer. This setup provided a realistic solution to obtain data from the running KTM engine as a function of RPM and load. Reference [150] indicates the importance of controlling engine and test environmental conditions such as temperature and atmospheric pressure. In this case, whilst the author could pre-condition the engine by a period of running to ensure data collection would start at repeatable engine temperatures, the test cell facility itself lacked the ability to control its temperature and pressure. These would be recorded and can allow compensatory calculations for power and torque but would be somewhat problematic when studying cycleto-cycle variation. The author recognised this weakness and whilst already aiming to start data collection at fixed engine temperatures a standard baseline test at fixed RPM and load and at a fixed exhaust restriction of 0% would be carried out prior to any testing to determine whether the measured cycle-to-cycle variations were sufficiently consistent in character to previous testing that worthwhile data could be collected. This was considered the best route to continue with the academic project given the facility limitations and as shown in the later analysis, valuable and consistent data was achieved to allow satisfactory conclusions to be drawn.

Exhaust extraction was implemented using the facility's fan assisted extraction system as shown in Figure 24. Carbon Monoxide monitoring was continually carried out in the cell and at all times all health and safety regulations were followed to ensure no risk to the test personnel.



Figure 24 – Bike on Chassis Dynamometer

4.4 – Test Equipment and Calibration

A practical approach to monitoring the engine temperature proved to be the use of the bike's On-Board Diagnostics (OBD) system to monitor coolant temperature. The measurement of cylinder pressure involved the use of the Optrand cylinder pressure transducer described in section 3.5. In discussions with TFX engine Technology in Canada [154] the author underwent both a calibration procedure and the determination of TDC.

For calibration a separate software module was used to check that static voltages of the pressure transducer and pickup were within guidelines specified by TFX. This was carried out with the engine off but with the system powered up. The software module provided by TFX included a screen with several readouts relating to channel voltages to ensure that the sensor output was within the limits provided by TFX. This provided the author with confidence that the pressure readings would be correct.

For crank angle and TDC determination a specific coast down test was conducted as per TFX guidance. This test involved running the engine up to a steady medium load and RPM and then the throttle would be held open fully whilst simultaneously cutting the ignition and recording the coast down event. The TFX data logger recorded two channels for this event,

channel one was a feed taken directly from a Hall sensor adjacent to the flywheel which had a missing tooth, and which gave RPM and positional data and channel two was the Optrand pressure transducer. The data that was recorded in this event was sent to TFX and in return they specified an offset value to be inputted into the software. The offset is the angle between the missing tooth on the flywheel point and the true thermodynamic TDC measured from the cylinder pressure coast down test. The thermodynamic TDC as measured is typically very close to the true mechanical TDC and is sufficient for the project requirements. [6]

4.5 - Test Procedure

4.5.1 - Bedding In

The motorcycle was brand new and the author needed to carry out a bedding in procedure prior to any real data collection. As a competition bike only a limited running in would be needed but it was important to put the bike through a number of heat cycles initially.

The procedure used consisted of first bringing the bike up to temperature, selecting 4th gear and then opening the throttle to take the engine up to maximum RPM. This was completed several times putting the engine through a series of heat cycles. This had the benefit of both bedding in the engine and obtaining a power curve which allowed the author to determine that the project engine was within KTM specifications and thus suitable for test.

4.5.2 - Testing

Having successfully calibrated the sensors described in section 4.4, prior to any data collection the engine was brought up to a stable temperature. Test cell ambient temperature and pressure were recorded. A baseline test at 2000 RPM and 0% throttle position was always carried out to establish quality of data and repeatability with other test runs.

At each RPM and throttle test point (including baseline tests) the engine would be run for sufficient time to allow a data sample of circa 500+ plus cycles. This was considered a sufficient sample size for data analysis and in line with sample sizes commonly used in industry [79], whilst also being manageable in respect of the storage and processing limitations of the test equipment.

5.0 – Results

5.1 – Setup procedure

To ensure the accuracy of the data recorded the author worked in conjunction with TFX [154] and carried out the initial coast down procedure as described in chapter 4.

A setup file is required to run the data logger and view captured data. It contains various engine parameters and values that help establish the scale, positioning and form of the raw data captured as well as basic engine parameters.

The file is important to allow calculations such as cylinder volume versus crank angle, to accurately determine the amplitude of the recorded cylinder pressure and to obtain accurate crank angle determination in degrees.

The coast down test allows the determination of the thermodynamic top dead centre position (TDC) essential for subsequent cycle-to-cycle analysis.

Raw data was recorded and sent to TFX upon which they were able to provide the author with a modified gain parameter for the cylinder pressure amplitude and a corrected crank angle offset to be used in all subsequent testing.

Figure 25 shows a screen shot of the uncorrected setup. Following on from TFX's review, TDC offset, and sensor gain were changed to 156 degrees and 0.790 mV/psi.



Figure 25 - Initial Setup File

Important to note is that the pressure amplitude in the recorded raw data is in PSI which was subsequently corrected to Bar by the author during post processing.

Figure 26 shows the corrected raw data collected during the coast down test. In the upper graph the white trace shows RPM with the ignition being cut and throttle opened wide open at circa 9250RPM. The turquoise trace shows cycle-to-cycle peak pressure whilst the X-axis shows the number of cycles. The pink trace shows the moving average of the peak recorded pressure per cycle.

In the lower graph of figure 26, the turquoise trace shows the angle of peak pressure relative to TDC. Positive angles show peak pressure occurring after TDC. The pink trace is a moving average of the peak pressure position on each cycle. The X-axis is the cycle number.

Whilst the RPM trace shows how the bike was brought up to speed slightly unsteadily through several gears on the chassis dynamometer, once the ignition was cut and throttle opened it had a smooth coast down deceleration on the rollers.

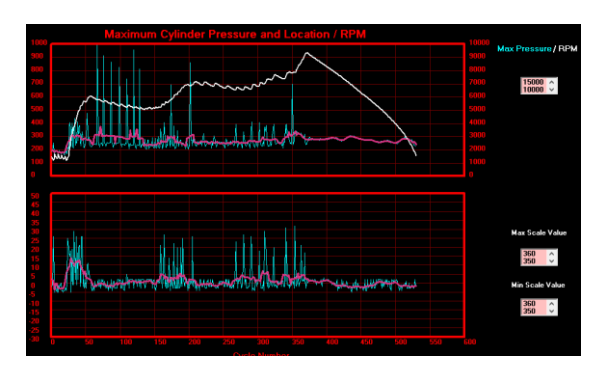


Figure 26 - Initial Cost Down Run (Corrected)

When analysing the location of peak pressure relative to TDC during the coast down it can be seen to be generally around 0 degrees (TDC) though there does appear to be a level of unexplained variation, possibly due to some residual combustion activity. However, further detailed analysis in chapter 6 confirms that the location of TDC proved quite satisfactory for the cycle-to-cycle investigation.

Figures 27 to 30 show several examples of coast down tests carried out during initial testing confirming the correct determination of TDC and giving confidence to the repeatability of the test procedure and data acquisition.

Additional coast down test results are shown in appendix A for completeness and further possible analysis in potential future work.

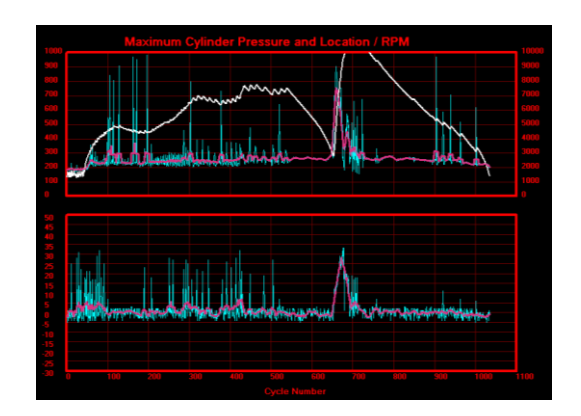


Figure 27 – Coast Down Test Example

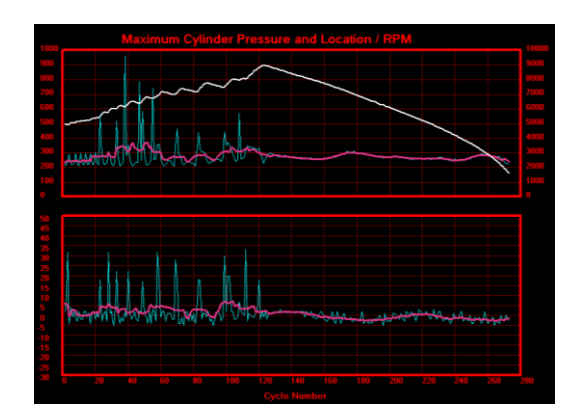


Figure 29 - Coast Down Test Example

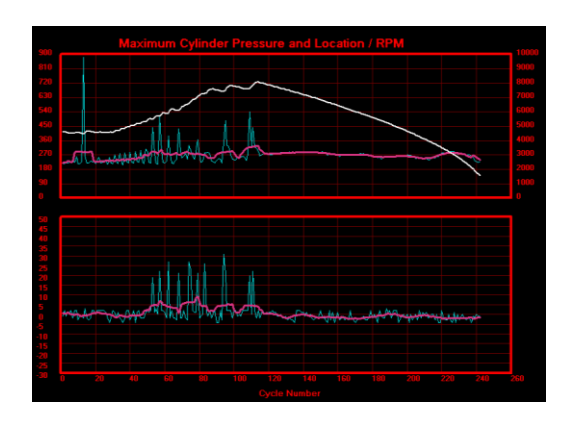


Figure 28 - Coast Down Test Example

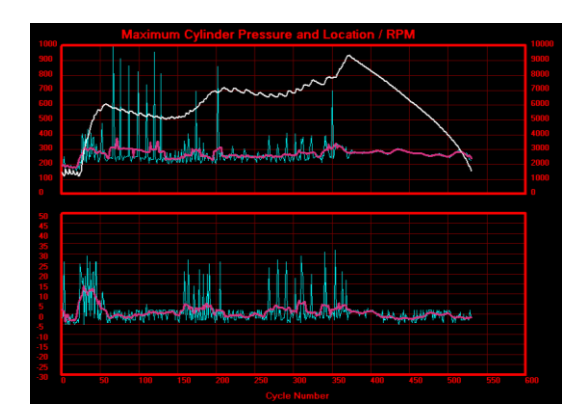


Figure 30 - Coast Down Test Example

5.2 - Test Results

Following the set-up procedure and initial trial results in section 5.1, a number of tests logging continuous cycles were carried out over a 3-week test period. The axes and colour annotation of the graphs are as defined in section 5.1

Figures 31-37 show successfully recorded data up to 6000 cycles per run. Figure 31 in particular shows a sample of the setup procedure in establishing stable RPM control on the chassis dynamometer. Establishing stable control of RPM and throttle opening position formed a significant part of the setup procedure to achieve stable repeatable results.

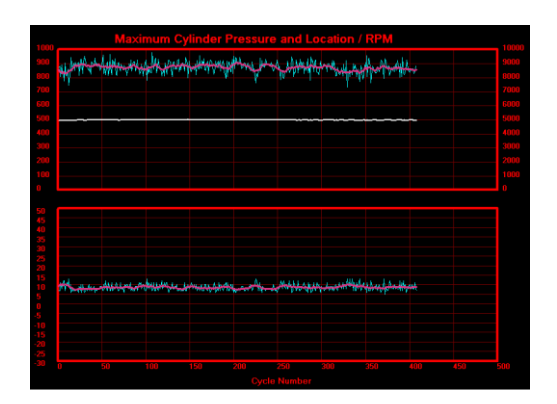


Figure 31 - Test Run Determining RPM Stability Control

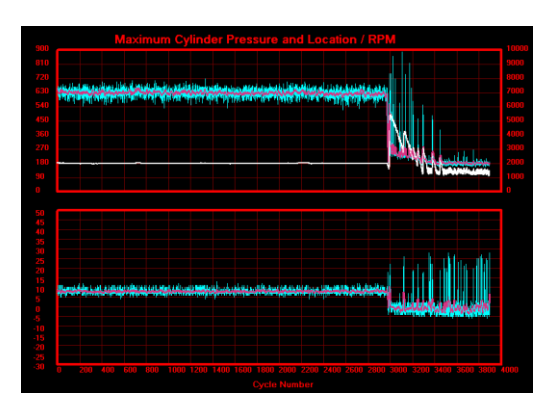


Figure 33 - Test Run 2000RPM Stability Control Test

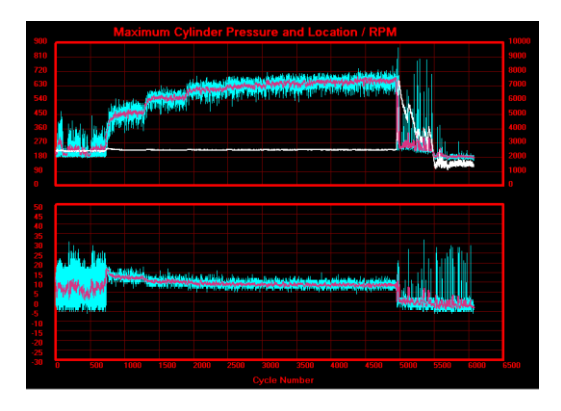


Figure 35 - Test Run 2500RPM

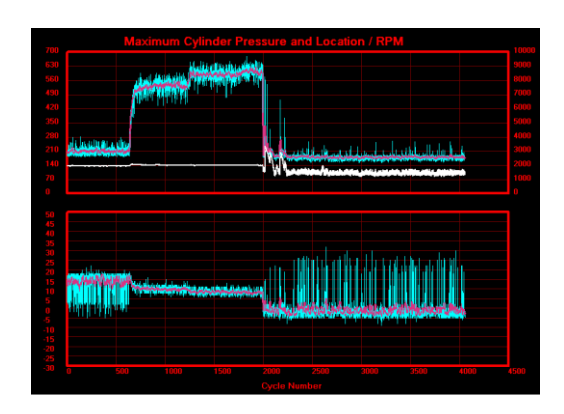


Figure 32 - Test Run 2000RPM and Idle

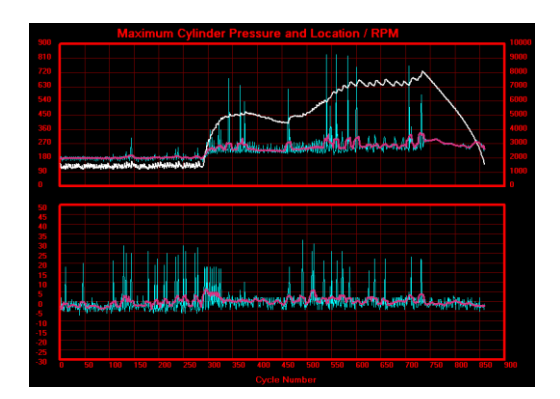


Figure 34 - 1600RPM Idle Test

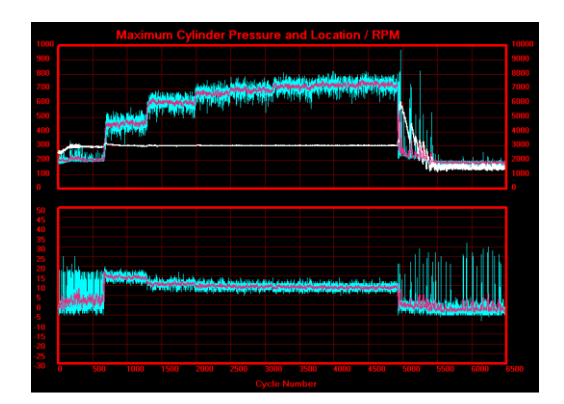


Figure 36 - Test Run 3000RPM

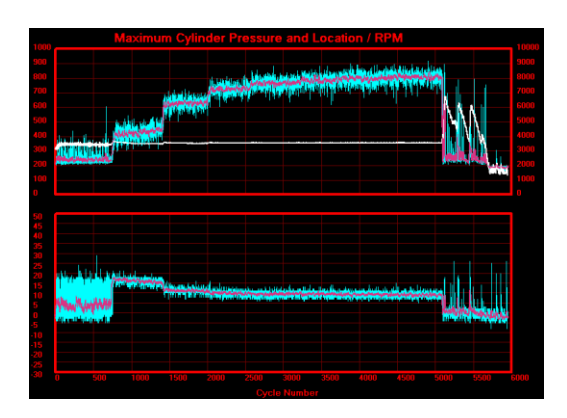


Figure 37 - Test Run 3500RPM

Figures 34 and 35 form the basis of the analytical work carried out in chapter 6. For each run and corresponding to engine speed, sample sizes for each throttle position were targeted at around 500 cycles by working out the corresponding time needed for their capture and then holding at the given throttle position for this amount of time. In between each throttle position there would be a short period of transient behaviour which is visible in the recorded data. Although figures 34 and 35 were chosen for analysis, the control implemented and quality of the data gives confidence that there is consistency between all the test runs showing very similar trends. Choosing figures 34 and 35 was thought to give a very meaningful first insight into the unstable characteristics of the 2-stroke engine from idling in figure 34 to a number of throttle openings at 2500RPM in figure 35.

The whole data set however, may allow significant additional analysis in the future beyond the scope of this project to develop further understanding of 2-stroke phenomena given the large number of cycles recorded.

The results themselves are very encouraging showing the repeatable quality of the recorded data, accuracy of TDC determination and pressure amplitude.

5.3 – Post Processing of Raw Data

During the continuous cycle test runs, cylinder pressure has been measured every degree and given the large number of data points collected per run (circa 2x10^6), a specific software routine was written to break the data down into manageable sections that could be worked with in Excel. The data was broken down corresponding to changes in throttle position. When the data was extracted from the logger software its output was in the form of a single column of data points which was too big for Excel to import without clipping. The software routine broke down each data set into 500 cycle sample sets corresponding to the sample set size used for each throttle position. Any overlap occurring between each sample set could be manually corrected with ease.

6.0 - Analysis

6.1 – Coefficient of Variance (COV) of IMEP

Given the understanding that 2-stroke engines exhibit worsened stability and COV of IMEP at low RPM and low load conditions it is interesting to quantify this phenomenon for the KTM engine.

The test run at 2500RPM shown in figure 35 is used to calculate the COV of IMEP at throttle openings from 0% to 40%.

Figure 38 shows the calculated results. The engine exhibits a COV of IMEP of 24.2% at 0% throttle improving progressively to 5.1% at 40% throttle opening.

A value of 24.2% at 0% throttle shows clearly the poor cycle-to-cycle stability exhibited by the KTM engine under this operating condition.

The higher load value of 5.1% would be considered just above the upper limit of the accepted range for stable operation. [10]

Figure 38 clearly demonstrates the problems running a 2-stroke engine at low load and low RPM conditions.

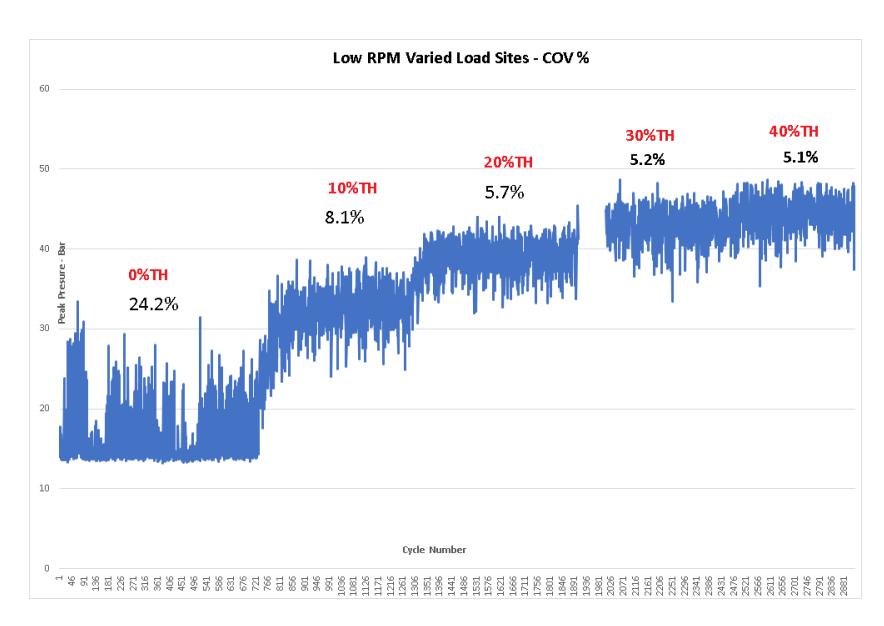


Figure 38 – Cycle-to-Cycle Peak Pressure Amplitude and COV of IMEP 2500RPM

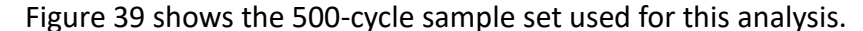
For figure 38 red is throttle opening percentage and black is COV of IMEP percentage.

6.2 - Cycle-to-Cycle Analysis

Figures 34 and 35 were chosen to carry out cycle-to-cycle analysis at engine speeds of 1600RPM and 2500RPM respectively.

In each case a circa 500 cycle sample set was chosen at the 0% throttle opening position. This region can be easily visually identified looking at the plot of the cycle-to-cycle peak pressure amplitudes. Care was taken to avoid choosing samples from the transitional regions at the start and the end of the 0% throttle run.

6.2.1 - 2500RPM Analysis



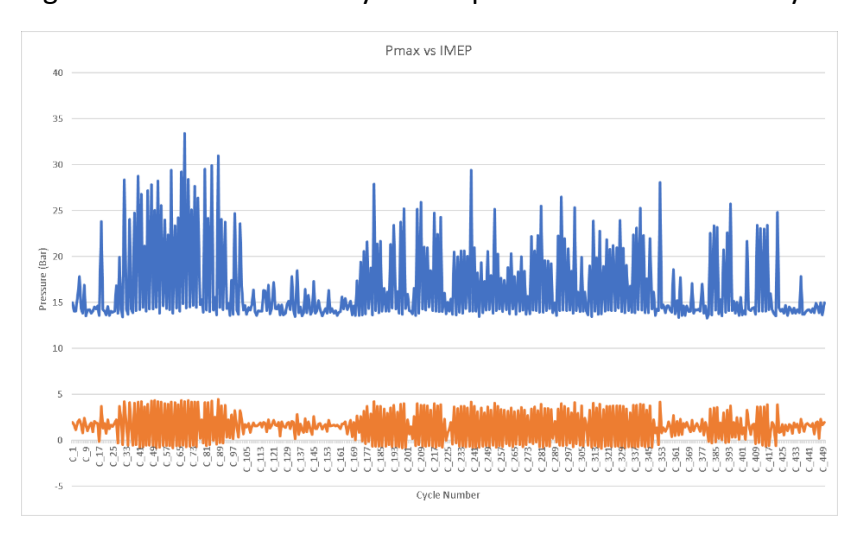


Figure 39 – Cycle-to-Cycle Peak Pressure Amplitude (blue) and Cycle-to-Cycle IMEP (orange)

Figure 39 shows the cycle-to-cycle peak pressure amplitudes plotted against cycle-to-cycle IMEP. This shows some distinctly different areas of operation. Figure 40 shows a clearer breakdown of the complete sample set into several different regions labelled A, B, C, D, E and F. Each of the regions will be analysed separately but as a general comment it can be seen that the 0% throttle sample set shows quite significant visual instabilities. Such instabilities have been discussed in reference [27] and are considered to be the result of the poor scavenging characteristics at this low load operating condition leading to varying amounts of residual gas trapped in the cylinder. The section-by-section analysis below will aim to develop a better understanding of this phenomenon.

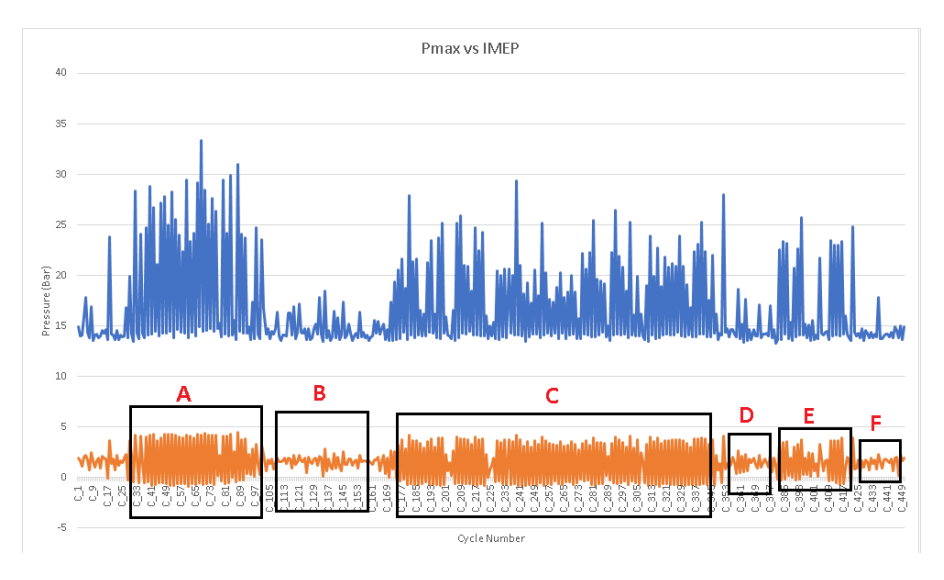


Figure 40 – Cycle-to-Cycle Peak Pressure Amplitude (blue) and Cycle-to-Cycle IMEP (orange)

6.2.1.1 - Region A

Figure 41 shows cycles 38 to 76 from this region and the calculated IMEP of each cycle.

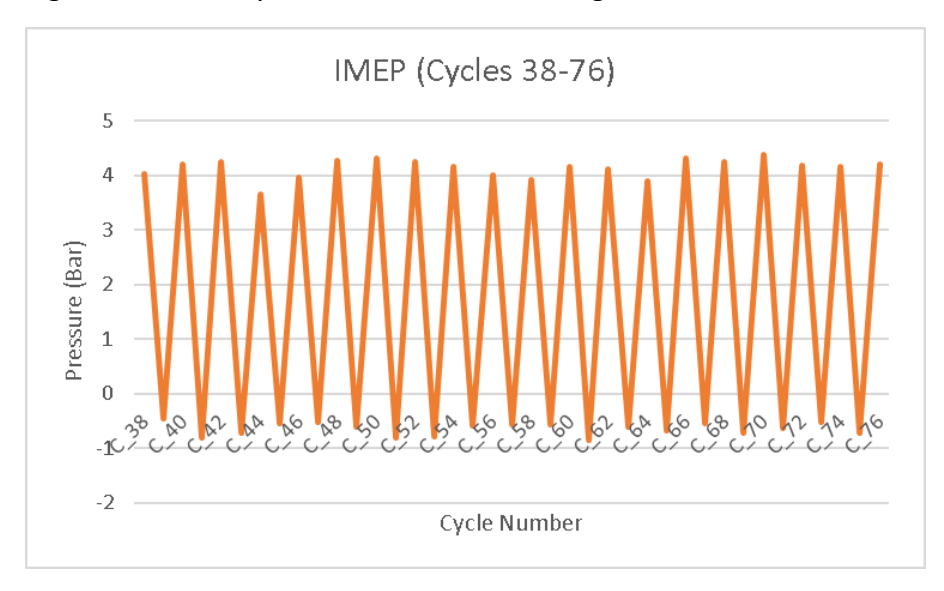


Figure 41 – Cycle-to-Cycle IMEP in Section A

It can be clearly seen that the IMEP is going negative every other cycle. This phenomenon of going from a positive negative IMEP cycle-to-cycle is known as 4-stroking [27]. The engine is clearly firing correctly only every other revolution. The fact that the IMEP goes negative reflects the situation that negative work is required during the non-firing cycle to overcome pumping and compression losses. Figure 41 shows very clearly that the engine is 4-stroking for some 40 cycles in a row. The consistency of the cycle in this region shows that it is a real engine phenomenon and not a data collection or noise issue.

Figure 42 shows the cycle-to-cycle pressure amplitude per degree for each of the cycles 38-76 overlayed on a single graph.

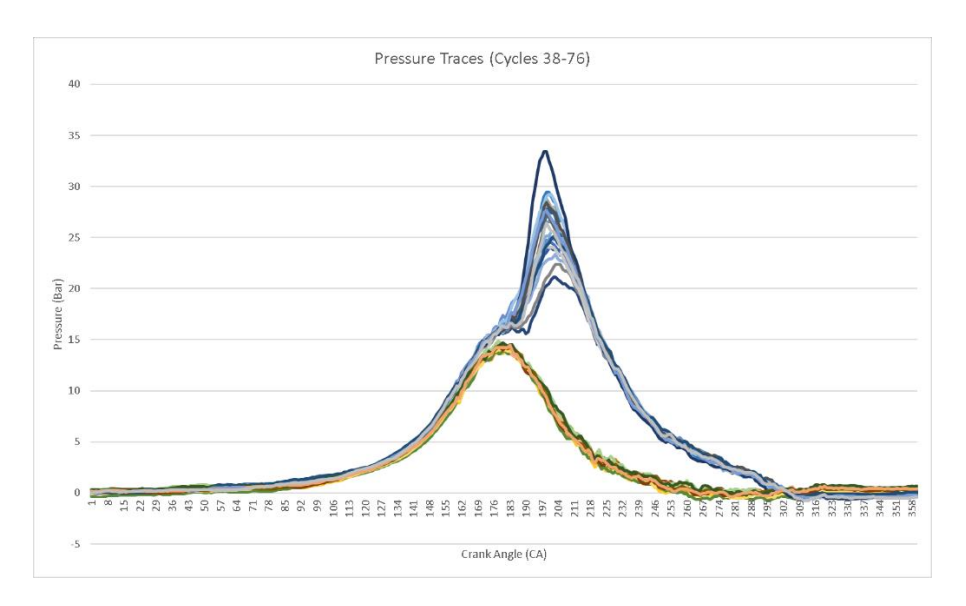


Figure 42 – Pressure Amplitude Per Degree for Cycles 38-76

This graph clearly shows the cycles are separated into two different camps and reinforces the understanding that the engine is operating as a 4-stroke, firing every other cycle. The two different camps show cycles that clearly have combustion activity and cycles that appear completely dead. It can be seen from figure 42 that even when firing the peak pressure amplitude is varying from around 21Bar to 34Bar even though the corresponding IMEP values in figure 41 appear to show more consistency. The variation in peak pressure amplitude indicates that even when firing the combustion is not totally stable. The fact that the IMEP appears to show a smaller variation during the firing cycles partly reflects that calculated work done is associated with the area of the pressure graph rather than just its peak value.

Of further interest it can be seen that for the firing cycles the pressure amplitude is clearly rising more significantly before TDC to achieve a TDC pressure some 3Bar or more than the non-firing cycles. The author postulates that this may well be because the cylinder is better filled during a firing cycle. During the firing cycles the start of combustion can be seen to be occurring approximately at or just after TDC rising to a higher peak pressure the earlier the start of combustion occurs.

Also, of real interest is to compare the pressure amplitudes of the firing and non-firing cycles at exhaust port opening (EPO). EPO occurs at a crank angle circa 300 degrees on this engine. It can be seen that there is a crossover point between the firing and non-firing cycles at EPO with the firing cycle pressure amplitudes falling below the non-firing cycle pressure amplitudes once the exhaust is starting to exit the cylinder. The author postulates that this phenomenon is being caused by and increased gas velocity and its suction activity in the exhaust port following a real combustion cycle.

To really understand these phenomena better the engine would need to be equipped with not only a cylinder pressure transducer but additionally with exhaust port, crankcase and transfer port pressure transducers.

The alternating cycle-to-cycle behaviour seen in section A is so consistent that it will be used as a reference point when analysing the other sections in the sample set.

6.2.1.2 - Region B

Figure 43 shows a 39-cycle sample set from region B.

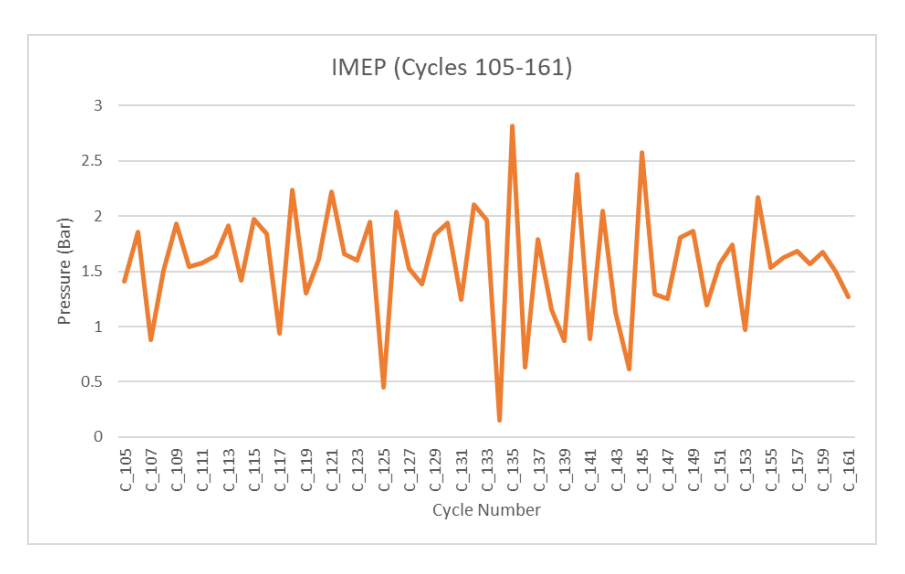


Figure 43 - IMEP (Cycles 105-161) Region B

This graph does not appear to show much – though it could be said at certain points the behaviour is tending towards that of region A. Cycles 134 & 135 have lowest and highest values respectively, though both still have positive values, whereas the lower values in the 4-stroke region of section A are always negative. Interestingly there does appear to be symmetry, in as much that if a flat average line was plotted through the data, then cycles 134 & 135 appear to be equidistant in amplitude from the flat line average.

Figure 44 shows the 39-cycle sample set from region B overlayed with that from region A. This further enforces the idea that cycles 134 & 135 from figure 43 (18 & 19 in figure 44) are tending towards conforming to the typical 4T behaviour of region A although this appraisal is not conclusive.

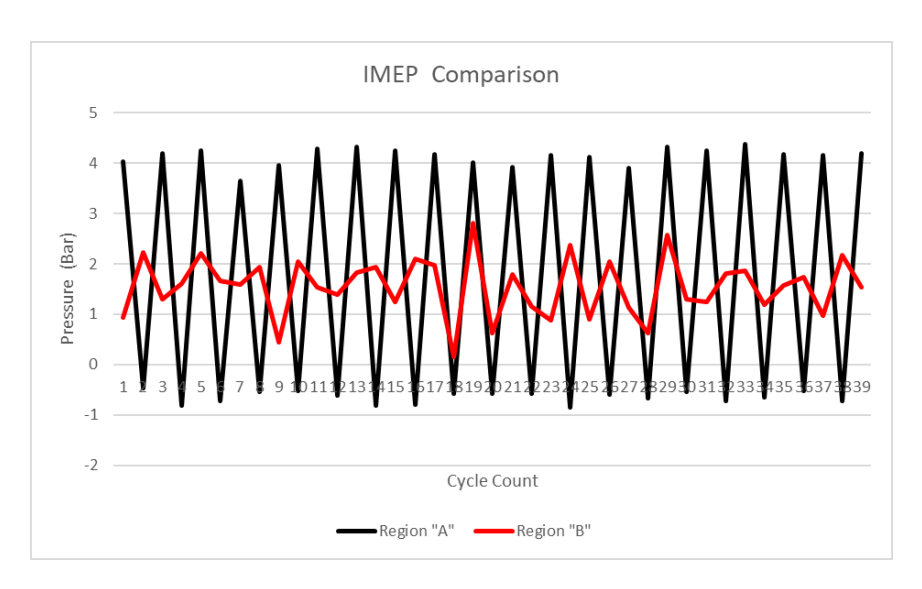


Figure 44 - IMEP Comparison Region A vs Region B (Equal Sample Size). Red -transitional. Black – region A reference.

Figure 45 shows the plotted pressure traces for the sample set from region B. It can be clearly observed that they have not separated into two different camps and are spread fairly evenly across a small range.

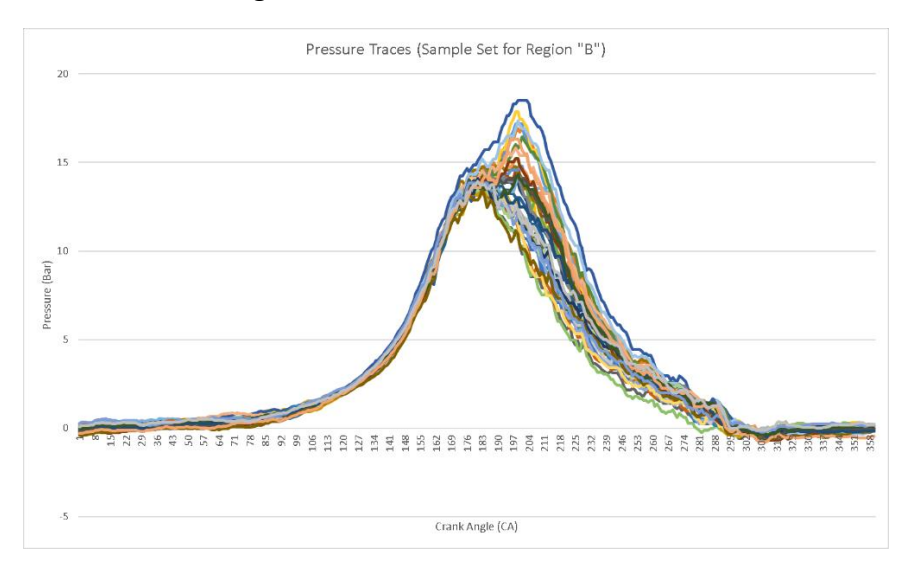


Figure 45 - Pressure Traces - Region B

Figure 46 shows a sample set taken from the transition of region A into region B. A breakdown/weakening in the consistency of the 4-stroke behaviour can be observed until eventually any kind of synchronicity is lost. In figure 46 the red cycles are showing the transition from region A to B whilst the black cycles are the reference cycles from region A used as the baseline for comparison. The red cycles 1-39 in figure 46 correspond to cycles 80-119 in figure 40.

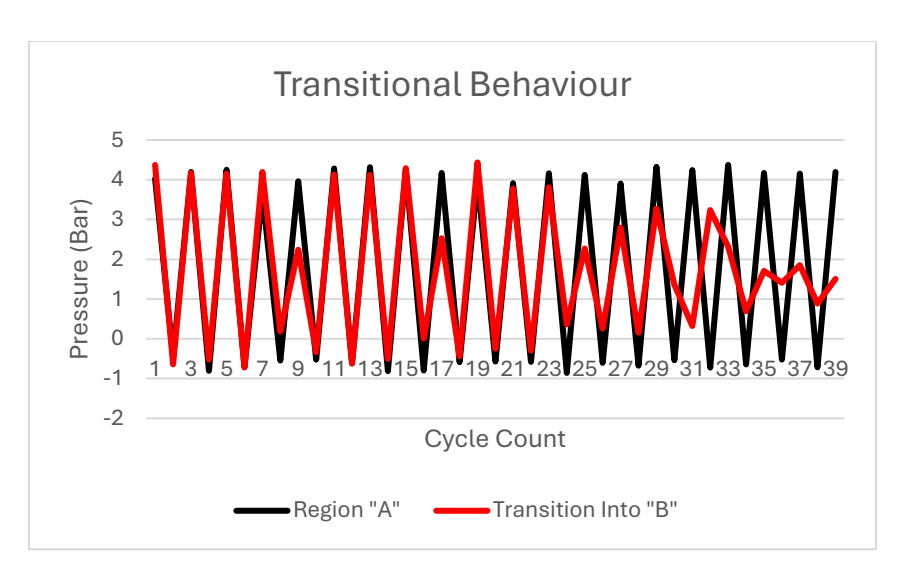


Figure 46 - Transitional Behaviour into Region B. Red -transitional. Black – region A reference.

Figure 47 shows the pressure traces for the transition into region B. There does appear to be two different camps. These two different camps are not as clearly defined as in region A and there are several cycles that lie in between and do not conform clearly to either camp.

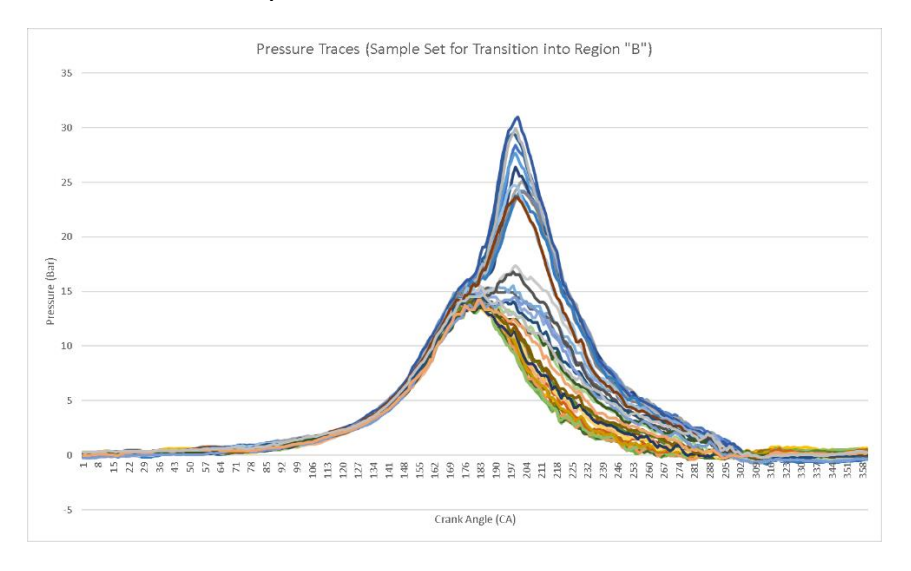


Figure 47 - Pressure Traces for Transition From Region A to Region B

6.2.1.3 - Region C

Figure 48 shows the transition from region B to region C. This graph shows an example of the very clear increasing oscillation behaviour as alternate cycles settle to show positive and negative IMEP values when fully transitioned into region C.

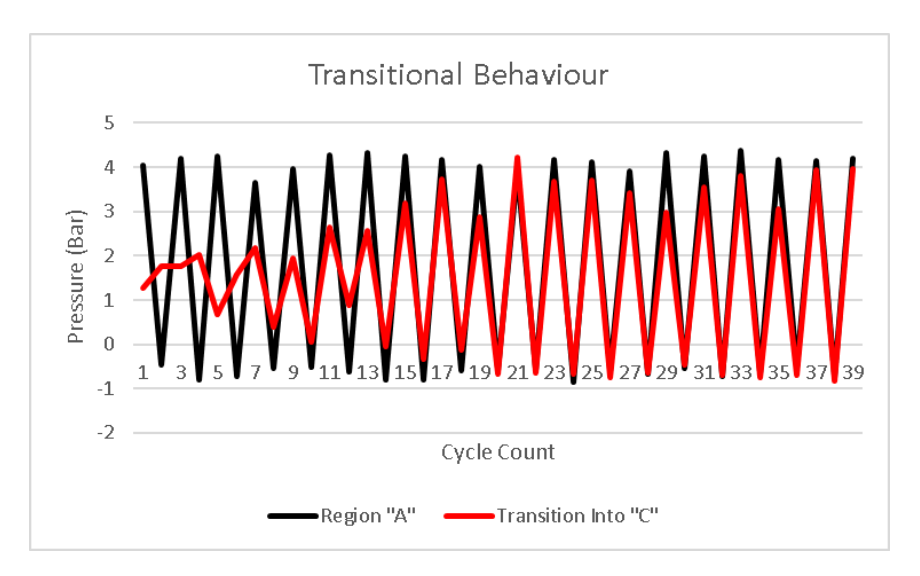


Figure 48 - Transitional Behaviour Into C. Red -transitional. Black – region A reference.

At the beginning of this transition the oscillation is small enough that the bad cycles still have a positive IMEP value. The transition then progresses to the point where all cycles show a consistent alternation between positive and negative IMEP values. An alternating behaviour (regardless of the engine exhibiting 4-stroke behaviour) is present almost completely throughout the transition into region C. The alternating behaviour of the IMEP is a very interesting phenomenon.

The plot of pressure traces shown in Figure 49 clearly shows a spread of values across the void between good and bad cycles. This again shows a transition between two different states of operation and modes of behaviour.

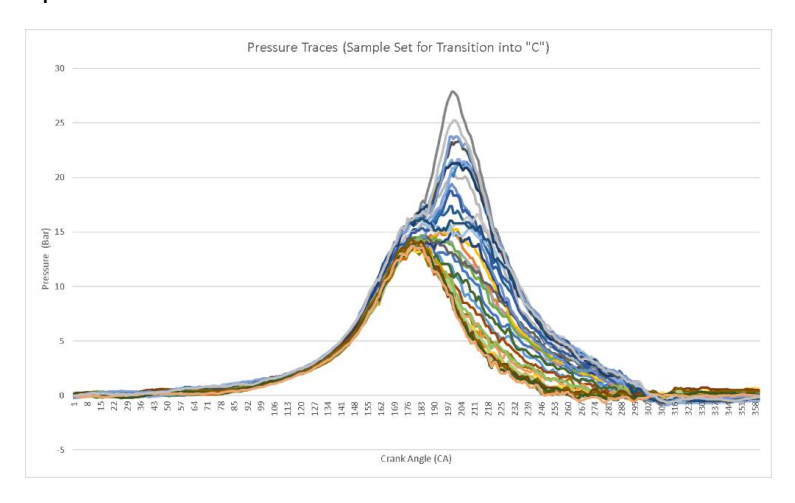


Figure 49 - Pressure Traces for Transition into Region C

6.2.1.4 - Region E

Figure 50 shows a comparison of region E against region A. The figure shows that the underlying characteristics of 4-stroke behaviour (as shown in region A) are present, albeit interrupted and not as strong in their oscillation. This further reinforces the idea that much of the engine behaviour exhibited is not random or anomalous but instead related to an inherent mechanism of the engine's operation and gas exchange process.

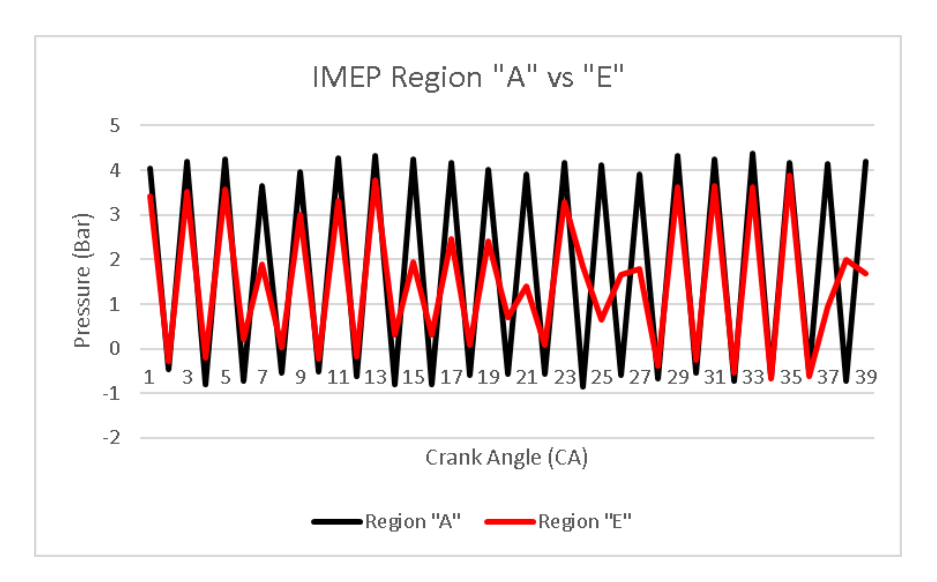


Figure 50 - IMEP Comparison (Region A vs E)

Figure 51 shows signs of 4-stroke behaviour, where two camps are forming - but the mediocre cycles are also shown in between.

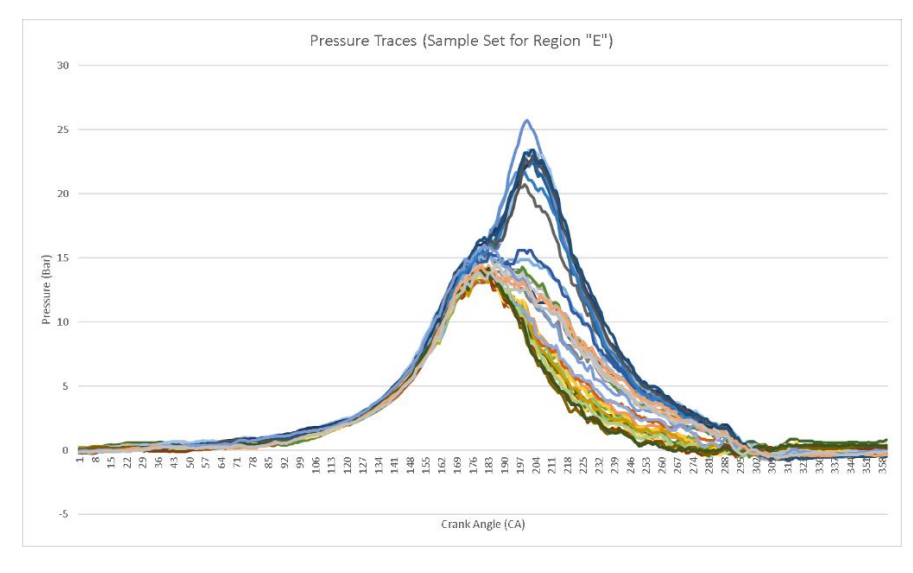


Figure 51 - Pressure Traces for Region E Sample Set

6.2.1.5 - Transition into Region A

Figure 52 shows IMEP plotted for the transition into region A again showing how the engine's behaviour tends naturally towards 4-stroke operation. A certain amount of breakdown in the synchronicity can be observed.

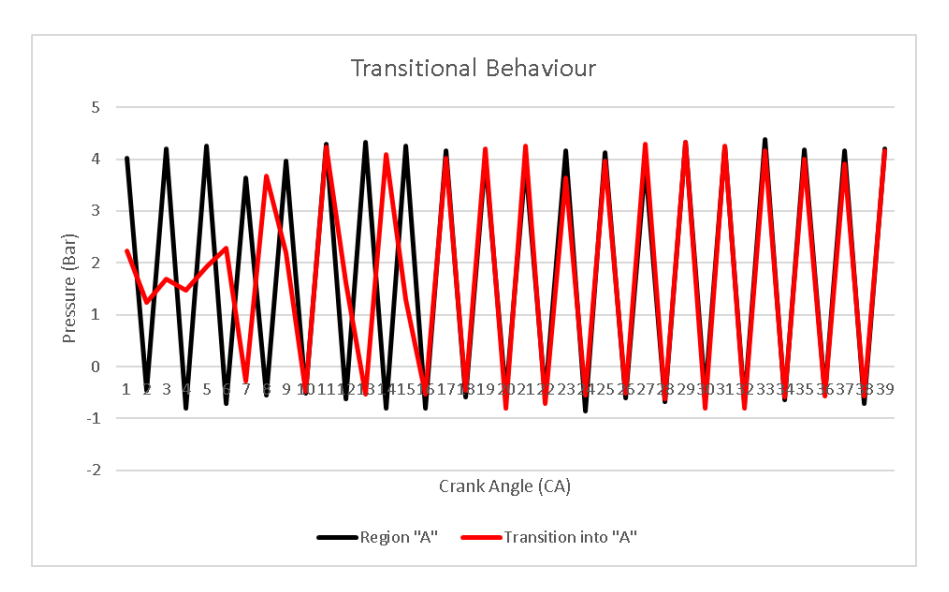


Figure 52 - Transition into Region A (IMEP)

Figure 53 shows the pressure traces for the transition into region A, showing the two opposing camps clearly, and also showing a number of cycles in between these two opposing camps.

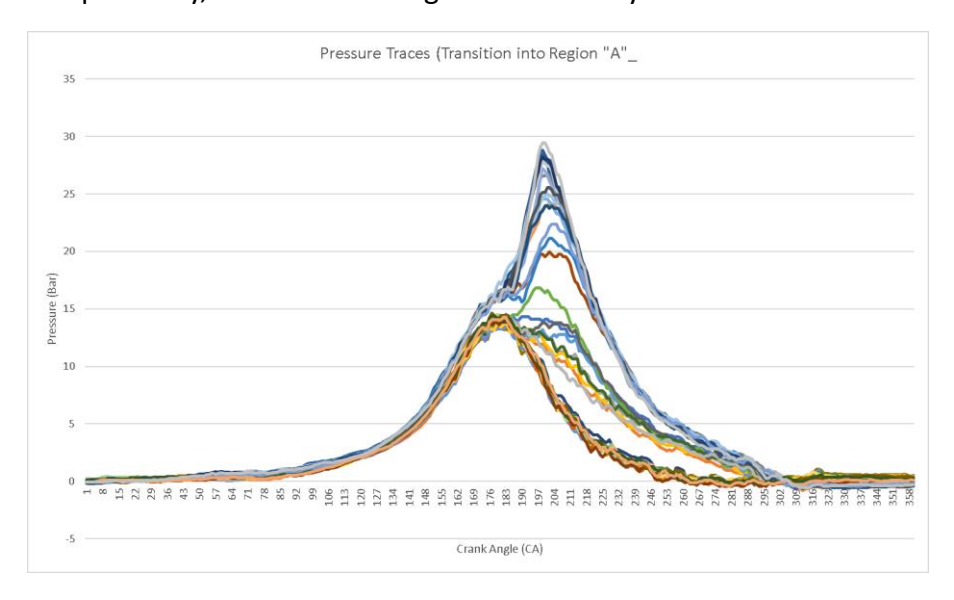


Figure 53 - Pressure Traces (Transition into Region A)

From this data set 4-stroke behaviour can clearly be observed, along with the engine system being a system that needs to be well balanced to operate optimally.

The author believes that this possibly shows the varying degrees of mixing cycle-to-cycle. The author postulates that a pocket of fresh (but isolated/surrounded by dead mixture) mixture may ignite and start to burn, but the in-cylinder combustion activities have limited scope to advance. The deterioration of this combustion event may coincide with further improved mixture of the charge, but by the time this improved mixture has occurred, the original pocket of ignited mixture may no longer hold sufficient energy (and be too late) to prompt or set off a good combustion cycle. Hence initial combustion is likely starting at a normal time, but the start of combustion (SOC) is hard to spot because it never really gets going. In addition, on a cycle-to-cycle basis SOC is harder to determine because of pressure noise in the data.

6.2.1.6 – Determining Start of Combustion (SOC)

Figure 54 is an example to show why a more scientific data driven approach would not be useful in this scenario. The calculating method to determine the start of combustion is based on the Rassweiler and Withrow method outlined in reference 155.

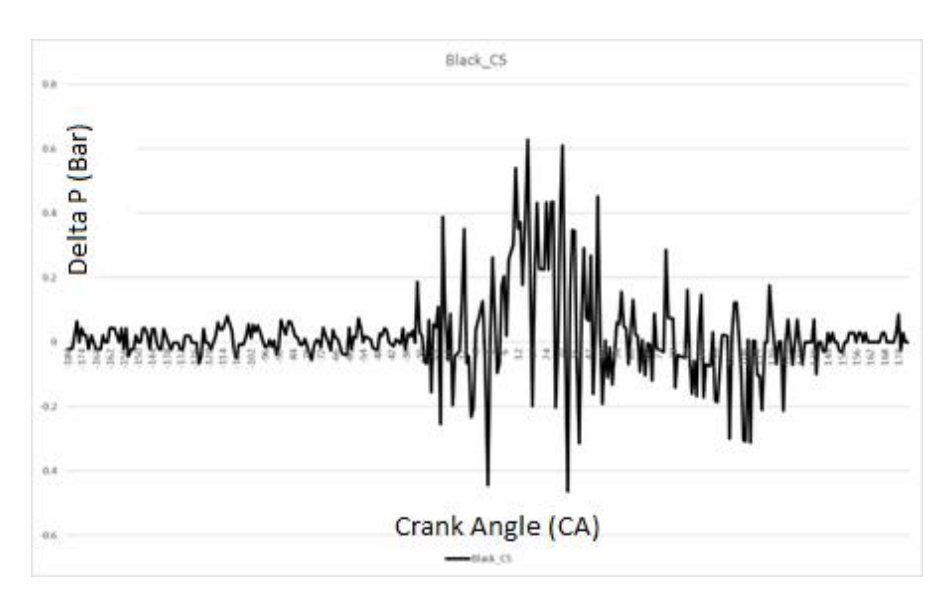


Figure 54 - Delta P Cycle 5 2500RPM

From the plot of delta P in Figure 54 it can be clearly observed that the SOC is not easily identifiable. The author would not have confidence in making a reasonable estimate. Figure 55 on the other hand shows this cycle plotted as a pressure trace, and although there is noise and some lack of clarity, the author would have confidence in determining a reasonable point for the start of combustion. Figure 55 exhibits less noise than figure 54 because the graph of figure 54 represents a differential of the pressure graph of figure 55.

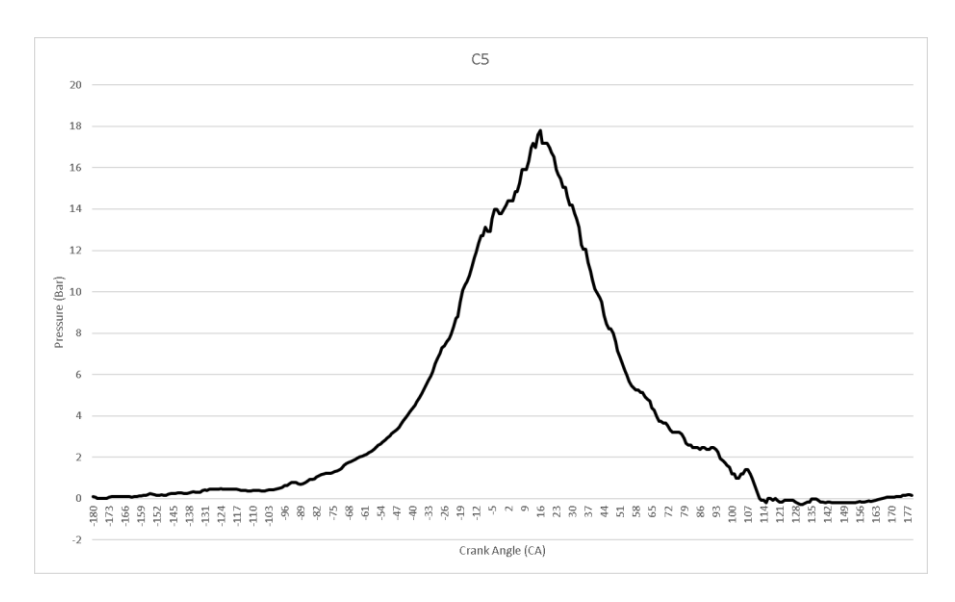


Figure 55 - Pressure Trace Cycle 5 2500rpm

6.2.1.7 - Regions D and F

Regions D and F have not been included in the detailed analysis mainly due to their limited duration (in terms of number of cycles). These regions however look visibly comparable to region B and the discussions of region B can also be applied to a large extent.

6.2.2 - 1600 RPM Analysis

Figure 56 shows the 300-cycle data selection sample set used for this analysis. The figure shows the raw data cycle-to-cycle peak pressure amplitude in PSI (purple) versus the RPM (white). The pink trace is the moving average of the peak pressure amplitude.

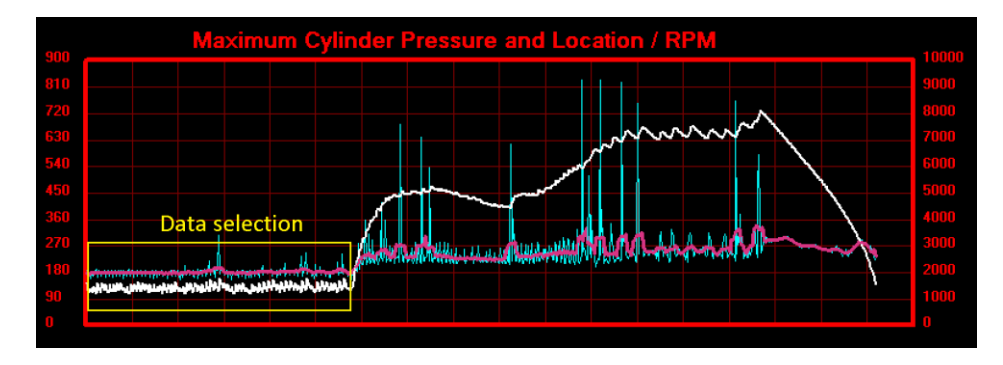


Figure 56 - Overview of Data Selection 1600rpm

Figures 57, 58 and 59 are plots of cycle-to-cycle peak pressure amplitude (Pmax) in 100 cycle steps for the data selection set shown in figure 56.

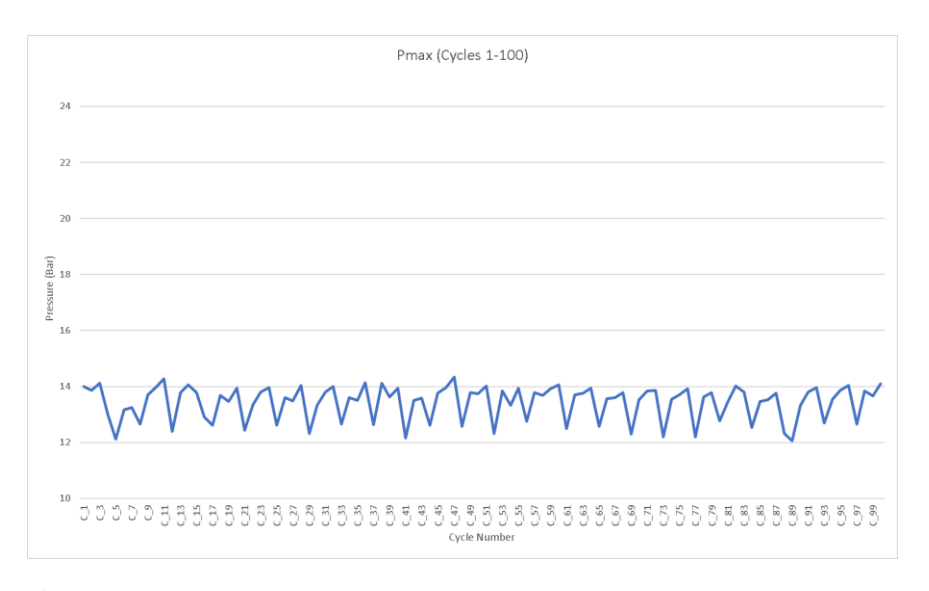


Figure 57 - Pmax (Cycles 1-100) 1600rpm

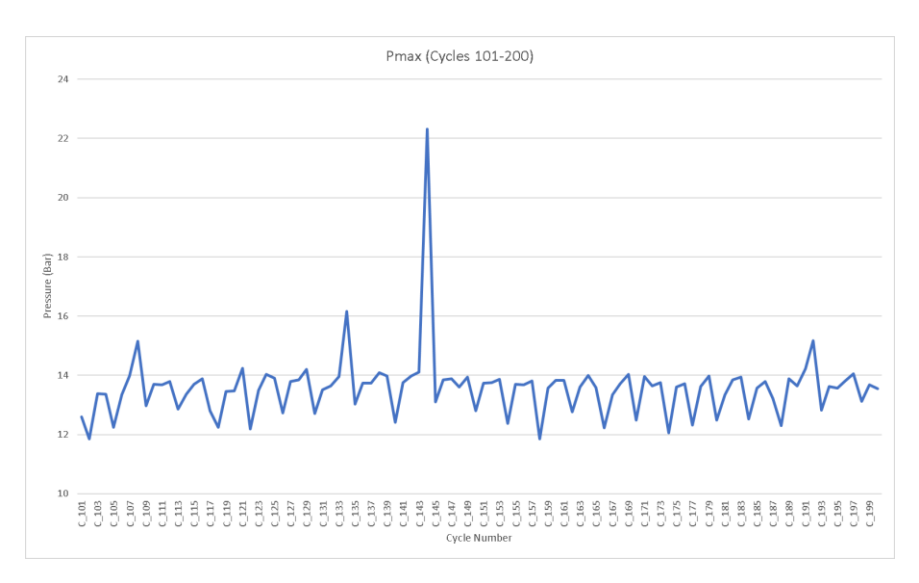


Figure 58 - Pmax (Cycles 101-200)

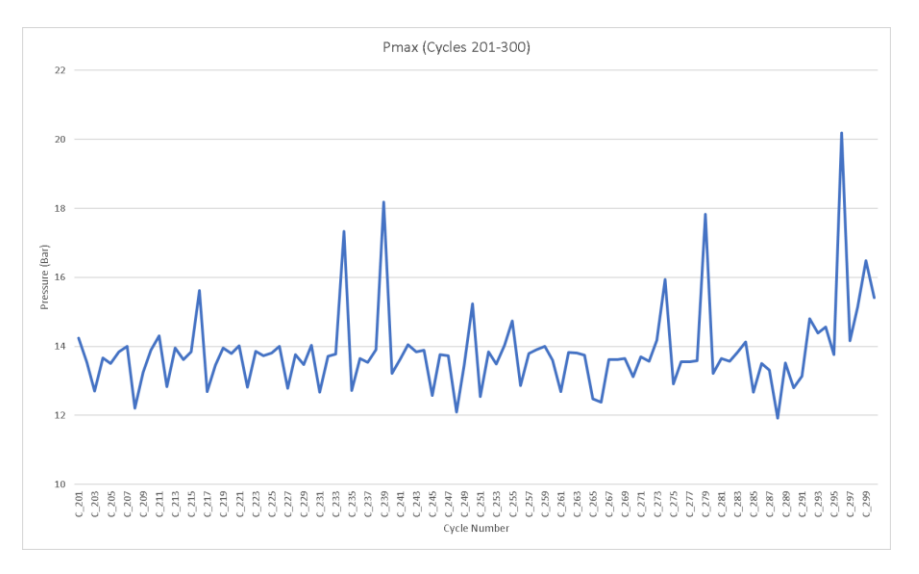


Figure 59 - Pmax (Cycles 201-300)

Plotting the data as three separate 100 cycle graphs allowed the author to identify some initial signs of repeated behaviour. However, the author felt that this gave a distorted and limited picture and that it was better to carry out the analysis for all 300 cycles together as shown in figure 60.

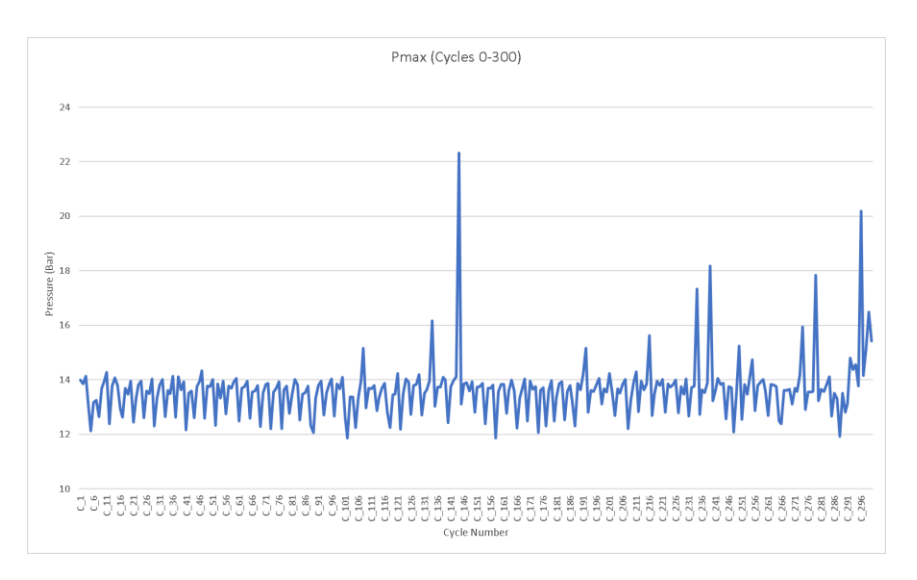


Figure 60 - Pmax (Cycles 0-300)

Figure 60 shows a graph of the peak pressure values for all 300 cycles. Appraising an overview of the peak cylinder pressures has proved to be a good starting point from which to conduct further analysis, giving the user a basic indication as to whether the engine is likely firing or not, the magnitude of each pressure cycle (live or dead), trends of transitional behaviour between the two states and the ability to spot anomalous cycles that lie outside the normal range (i.e., extreme low/high cycles). The purpose of viewing the data in this manner is that it is used a visual prompt, showing potential trends and patterns of behaviour, and in this respect, it has worked very well. Though, as will be discussed further on, the true appraisal of what is happening can be distorted, hidden or inverse of what these visual prompts initially suggest.

6.2.2.1 - Comparison with 2500RPM Data Set

The 2500RPM data analysed in section 6.2.1 showed a general trend of cycle-to-cycle alternating or on/off behaviour. In some areas this showed clear 4-stroke behaviour, easily seen by both peak cylinder pressure and by IMEP. Even when in not distinctly 4-stroke behaviour the engine showed a trend of almost never having more than one consecutive live cycle.

When analysing the 1600RPM data in figure 60 it initially looked considerably different from the 2500RPM data shown in figure 40 in that there appeared to be consecutive cycles with similar amplitudes of peak pressure.

Figure 60 suggested that from the cycle-to-cycle peak pressures there may be three or four live cycles in a row at 1600RPM. This seemed to be in initial contradiction to the 2500RPM findings. It was decided to plot both cycle-to-cycle peak pressure amplitudes and IMEP (as in section 6.2.1) together to further understand the 1600RPM phenomenon. Figure 61 shows the cycle-to-cycle peak pressure amplitude and IMEP for the 300-cycle 1600RPM data set.

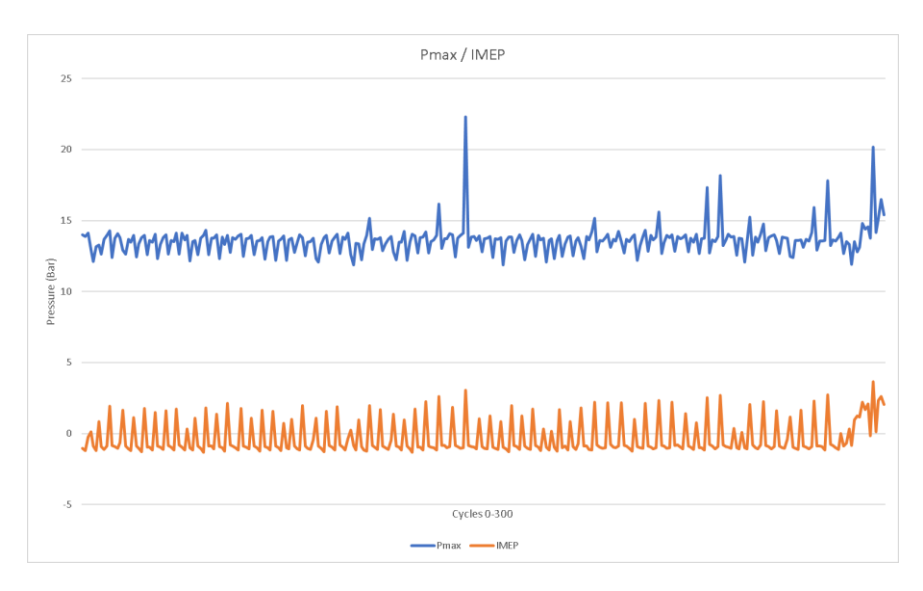


Figure 61 - Pmax & IMEP (Cycles 0-300) 1600RPM

This figure including IMEP shows that the 1600RPM data set is not as dissimilar from the 2500RPM data set as originally thought from a study of peak pressure amplitudes alone.

The IMEP in figure 61 clearly shows that there are no consecutive properly live combustion cycles at 1600RPM other than in the transition period at the end of the sample set.

A properly live cycle is defined as one with a positive IMEP when a nett positive amount of work is done by the engine in a cycle. Put more simply, a properly live cycle is defined as a cycle that whatever the combustion activity (little or large), there is sufficient combustion energy to overcome the energy losses of the rotating and pumping assembly (the engine).

In contrast, a negative IMEP cycle is a cycle when a nett negative amount of work is done by the engine in the cycle (i.e. the combustion energy is insufficient to overcome the energy losses of the engine).

This is an important definition of a properly live cycle which will be carried forward in the analysis.

The fact that there are no consecutive properly live cycles at 1600RPM (as is the case at 2500RPM) but that it was hard to pick up from the peak pressure amplitudes was a result of the low load situation creating a firing peak pressure not dissimilar from the motored peak pressure values. It needed the IMEP values to pick it up. In contrast, at 2500RPM there is a larger difference between the peak pressure amplitudes of the firing and motored cycles meaning that the alternating firing sequence could be more readily seen from the pressure amplitudes alone at this higher RPM.

6.2.2.2 - Detailed 1600RPM IMEP Cycle-to-Cycle Analysis

It can be seen in figure 61 that there is a visual "saw-tooth" pattern in the peak values of the negative IMEP cycles in between adjacent positive (properly firing) IMEP cycles.

This pattern highlighted in the boxed section in figure 62 and further highlighted in detail in figure 63.

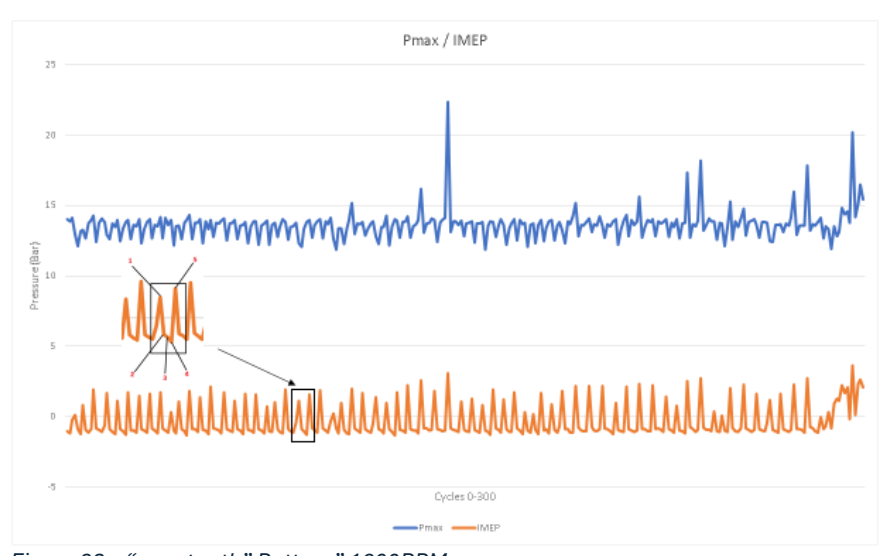


Figure 62 – "saw-tooth" Pattern" 1600RPM

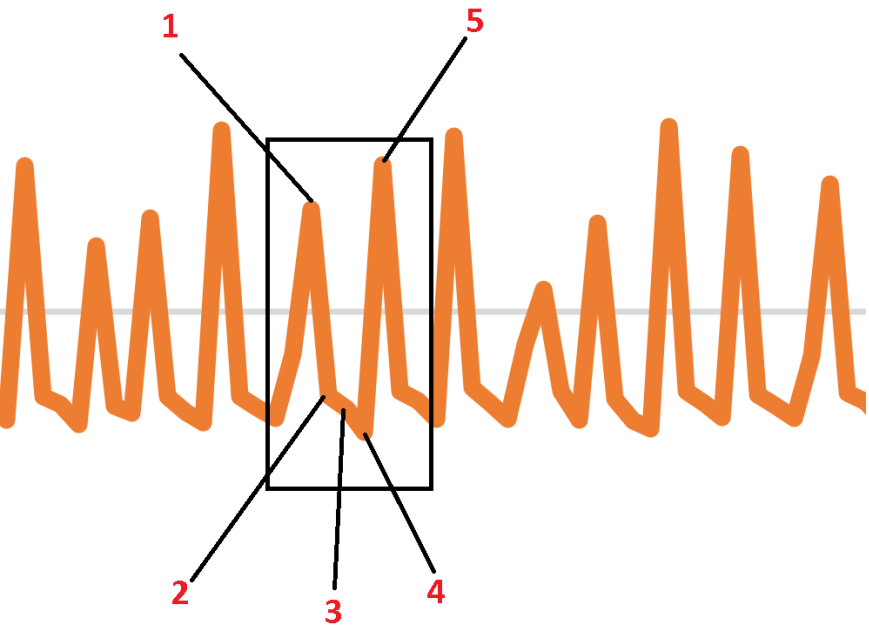


Figure 63 – "saw-tooth" Pattern 1600rpm

Figure 63 clearly shows the "saw-tooth" pattern in IMEP values going from cycle 1 to cycle 5. This "saw-tooth" pattern is named by the author because the IMEP amplitude data appears as if it is the blade of a saw, it repeats itself along all the cycles in figure 63.

At this stage comparison can be made with reference 143, the only paper the author was able to discover with some consecutive cycle data, albeit at a higher engine speed of 3000RPM.

There is some initial similarity in the IMEP trace of figure 63 to that in reference 143 but on closer examination it can be seen that the "saw-tooth" behaviour measured by the author is the inverse of that shown in the paper. Whether that is because of the different engine speed condition or the fact that it is a different engine the author is unable to say. Undoubtedly, at a different engine speed of 3000RPM the balance of the engine would inherently be different, which may account for the discrepancy in the "saw-tooth" pattern. However, the author's data comprised of some 300 cycles, longer than the 100 cycles shown in the paper and apart from anomalies discussed in section 6.2.2.4, all the author's cycles follow the same "saw-tooth" IMEP patterns shown in figure 63 giving confidence in the author's data.

Further analytical comparison with the paper will be made looking at individual cycle pressure data in section 6.2.2.3.

Returning to the analysis of the author's work, figure 63 shows the general trend of the measured repeating 5-cycle IMEP pattern; cycle 1 is a positive IMEP cycle, cycle 2 is a negative IMEP cycle, cycle 3 further negative, cycle 4 even more negative with finally cycle 5 has a positive IMEP cycle again.

The trend in going from a live cycle through a few dead cycles until the next live cycle can be described as a "recovery" phase. Recovery can take the form of a number of mechanisms, from mixture composition to the timing and harmonic balance of the engine (where a modern

high performance 2-stroke engine can be viewed simply as a series of resonance chambers). [27]

If cycles 2, 3 and 4 of figure 63 are to be considered a recovery phase then the author would have initially thought it fair to assume that their perceived transition would be one that goes from having less potential for combustion to one of having more potential for combustion.

However, looking at the isolated "saw-tooth" pattern in figure 63, this seems to have been contradicted as the interim cycles 2, 3 and 4 get progressively worse in terms of IMEP.

To break early or easy assumptions and to better understand the phenomenon across these cycles, a graph (figure 64) was initially plotted of work done per crank angle degree for interim cycles 2, 3 and 4.

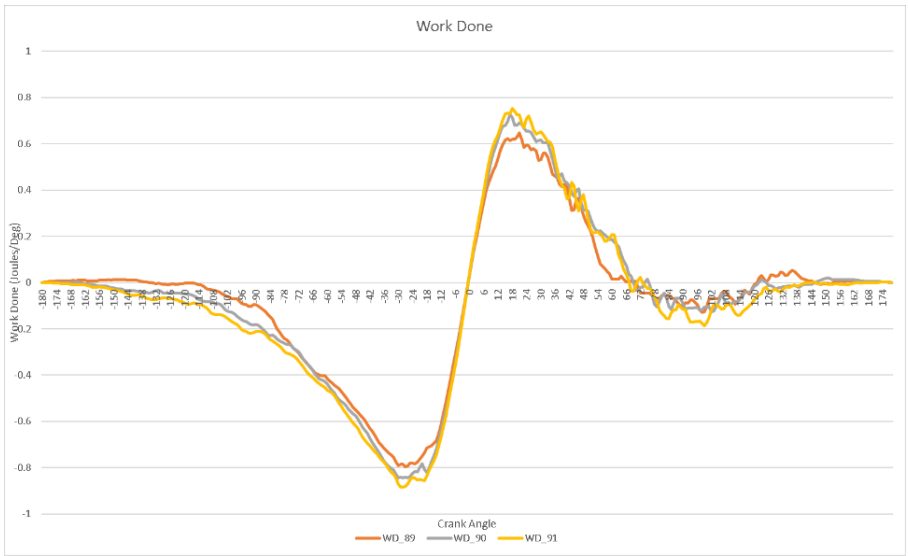


Figure 64 - Work Done (Cycles 89-91) 1600RPM

From observation of the plots of figure 64 there are differences between the cycles. Cycle 89 (cycle 2) has the lowest peak value of positive work done per degree during the combustion phase but this is compensated by also having the least negative work per degree value during the compression phase.

There are also differences between the cycles during the intake and exhaust regions. The author believes that the exhaust port pressure activity reflects the degree of partial combustion in that a higher peak work done per degree in the combustion phase leads to a lower in-cylinder pressure at and around exhaust port opening. The variation in cylinder pressure at intake port opening would be a subject of further study but undoubtedly reflects the previous exhaust port pressure. These variations reflect the unbalanced nature of the engine when running at sub optimal conditions

Although the work done graph in figure 64 was not directly conclusive, the author believes that the decline in IMEP across the recovery phase should not be seen as being contradictory to the term "Recovery". Rather what is being displayed is possibly a sign the engine is settling and recovering its balance, albeit in a compromised and sub optimal way.

At such low load operation where the combustion activity is inherently weak in the live firing cycles the author postulates that this weak live combustion activity is insufficient to maintain stability and continually knocks the engine out of balance. Knocked out of balance by a combustion cycle the engine takes several cycles to regain this balance and fire again, when the "Recovery" phase of dead cycles repeats itself.

Whilst subtle, this data set shows how sensitive the 2-stroke engine is when operating at sub optimal conditions.

Further detailed analysis will be carried out in the following sections to try to improve the understanding of these conditions.

6.2.2.3 - Cycle-to-Cycle Pressure Per Degree Analysis

To understand better the "Recovery" pattern identified in figure 63 the full pressure traces for all of the five cycles highlighted have been plotted in figure 65.

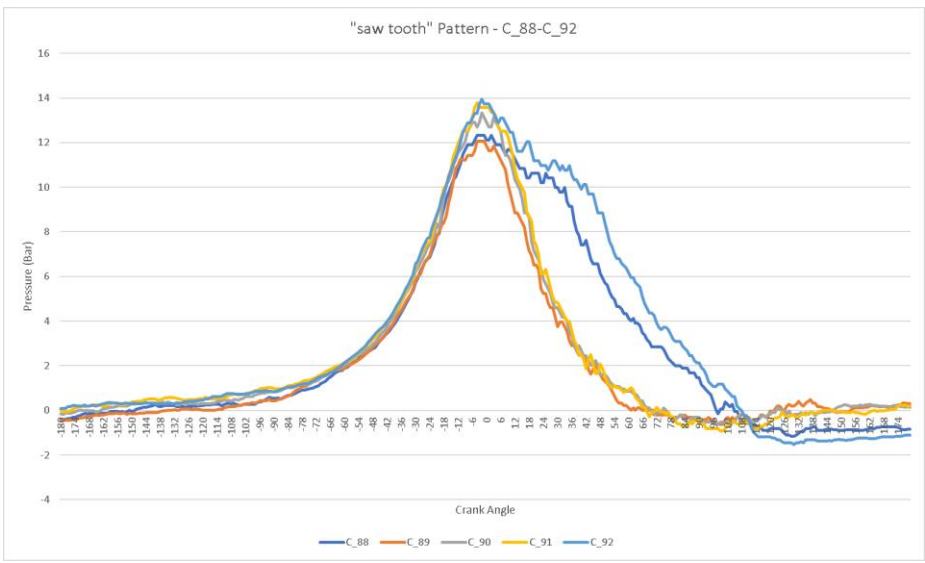


Figure 65 - Pressure Traces (cycles 88-92)

In this figure cycles 88 to 92 represent cycles 1 to 5 respectively shown in figure 63.

At this stage further comparison can be made to reference 143, the only paper the author was able to locate with a similar analysis of five consecutive cycles.

At first glance there appears again to be similarities in the work although the understanding of the filling mechanism cycle-to-cycle is different and importantly the reference paper does not show any separation in the pressures for any of the cycles at exhaust port opening.

In fact, the reference paper traces appear to show some anomalous behaviour at EPO and the author is not sure whether this truly reflects the cylinder pressure at EPO or is the result of some editing to the pressure results.

The author describes the reference trace behaviour at EPO as anomalous because it seems to defy physical sense and because through all the author's hundreds of cycles there is always a deterministic change in cylinder pressure at EPO reflecting the degree of combustion in the cycle.

The author is very confident in the accuracy of his data collection and the quality of the depth of analysis and believes that his findings at EPO hold a key to understanding the irregular cycle behaviour and its recovery mechanism over 5 cycles.

Returning to the author's analysis of his measured data, the consecutive cycles shown in figure 65 can be described as follows; cycle 1 (dark blue trace) can be seen to be a properly live cycle with visible combustion, albeit post TDC and with a low peak pressure amplitude. In

fact, the peak pressure did not occur due to combustion and can be observed to be not dissimilar from the motored pumping pressure at TDC.

The following cycle (cycle 2 – dark orange) followed a more intuitive path and had a marginally lower peak pressure at TDC, the lowest of all the cycles within the section.

Cycle 3 (grey) showed a significant jump in peak pressure around TDC and cycle 4 (light orange) further increased the peak pressure around TDC.

Cycle 5 (light blue) had a similarly high peak pressure around TDC compared with cycle 4 but showed a strong amount of combustion after TDC.

Analysis of this pattern illustrated a more traditional idea of recovery if recovery focused on cylinder pressure conditions around TDC.

The fact that cycles 3 and 4 also showed a progressive worsening of IMEP as described in section 6.2.2 can be explained in figure 65 as the cylinder pressure can be visibly seen to be rising before TDC thereby increasing the magnitude of the negative work in those cycles. The author postulates that the declining IMEP simply indicates that the cylinder is filling better as it recovers, thereby increasing the pumping and compression losses.

Figure 64 also highlighted the behaviour around exhaust port opening (EPO), this behaviour being interrelated to the current cycle.

Figure 66 zooms in around EPO and shows that pressure conditions at this point are likely to have a significant effect on the following cycle in-cylinder conditions.

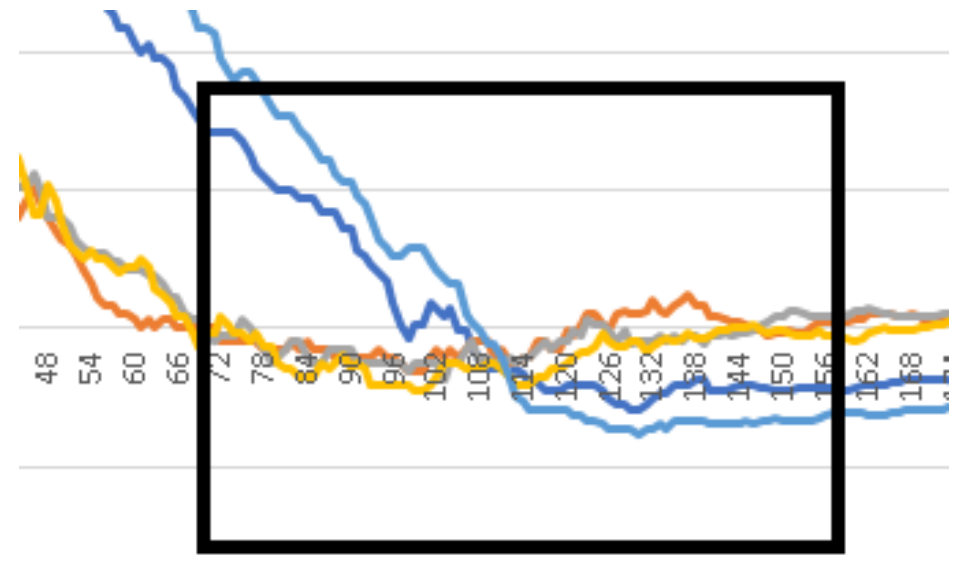


Figure 66 - EPO Activity (cycles 88-92)

To explore these thoughts, repetitions of the pattern were plotted in a similar manner and cycle-to-cycle behaviour was observed. The first repetition of the pattern looked at the cycles immediately after cycles 88-92. Cycles 92-96 are shown in figure 67.

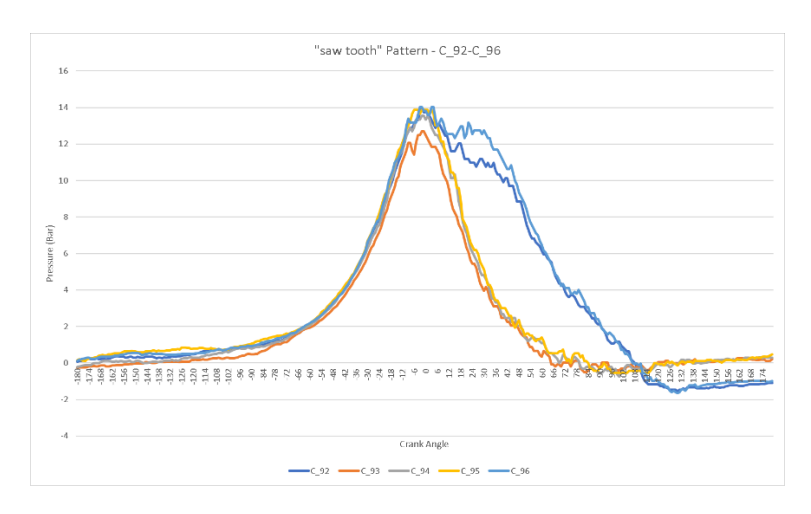


Figure 67 - Pressure Traces (cycles 92-96)

The repetition of the pattern in figure 67 for cycles 92 to 96 proved to be remarkably similar to that shown in figure 65 for cycles 88-92.

Following the pattern again, cycle 1 is live with significant post TDC combustion and low peak pressure during combustion, cycle 2 is motored and with the lowest peak pressure, cycle 3 is motored shows a higher peak pressure around TDC, cycle 4 is motored with a peak pressure higher still around TDC followed by properly live cycle 5 with significant post TDC combustion and a low peak pressure during its combustion.

Activity around the exhaust port for these cycles is shown in Figure 68.

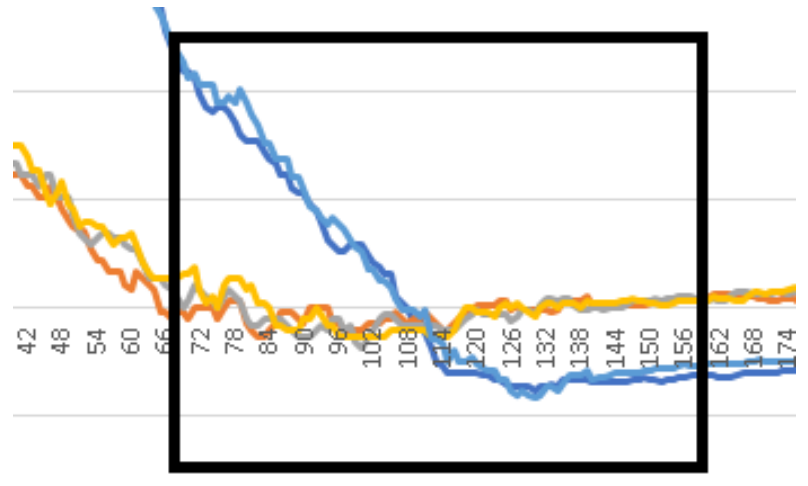


Figure 68 - EPO Activity (cycles 92-96)

The figure shows clear separation properly live cycles with significant combustion and cycles without, the cycles with clear combustion having a significant negative pressure around this area. The author postulates that the negative pressure is due to the suction effect of the exhaust resonance chamber, this suction effect being enhanced when combined with the pressure and temperature of the hot gases from a true combustion event.

Figure 68 shows that the properly live cycles are clearly separated from the interim dead cycles. It can be observed that the behaviour of the pressure trace prior to EPO very much relates to what happens after EPO.

The pressure traces for the live cycles 92 and 96 are very similar prior to and after EPO whereas, in figures 65 and 66, the pressure traces for the live cycles 88 and 92 were not as similar before EPO and their subsequent behaviour after EPO reflected this difference.

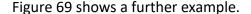
In both cases the activity leading up to EPO has a clear and measurable effect on the suction created by the exhaust. This in theory should influence the cylinder conditions of the following cycle.

This is demonstrated in figures 65 and 67 for cycles 88, 89 and 92, 93 respectively. Cycles 89 and 92 are properly live cycles and their subsequent cycles 89 and 93 respectively both show the lowest peak pressures at TDC following the measurable suction effect of the previous live cycles. The peak pressure of the following motored cycles then recovers over the following cycles of the pattern.

This is clearly a display of how a finely tuned component of the system (the exhaust resonance chamber) is out of synchronisation or balance when the engine (a high performance modern 2-stroke) is operating to sub optimal conditions. This imbalance is considered to be fundamentally the cause of the repeating five cycle recovery pattern.

The relationship between the pressure prior to EPO and the subsequent suction effect afterwards rings true for any selection of cycles or pattern sample in this steady RPM data set.

Whilst the general trend of recovery was ever present the graduation and the magnitude of the pressure change between cycles did vary to some extent.



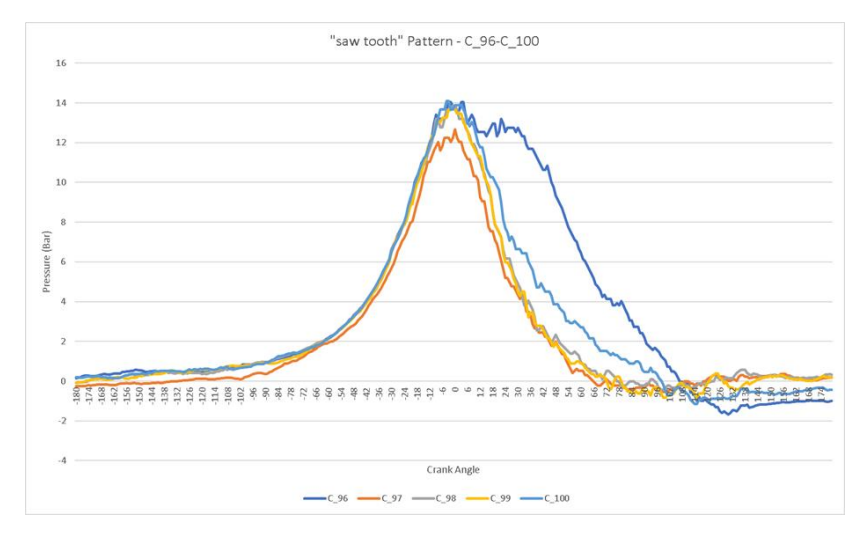


Figure 69 - Pressure Traces (cycles 96-100)

It can be said that the examples present in figures 67 and 69 are indicative of most of the pattern samples.

6.2.2.4 - Anomalous Behaviour In the 5-Cycle Pattern

6.2.2.4.1 – First Anomaly Type (IMEP Trace Anomaly)

Figure 70 shows IMEP plotted for the full 300 sample set at 1600 RPM. It shows a low focus pattern trend.

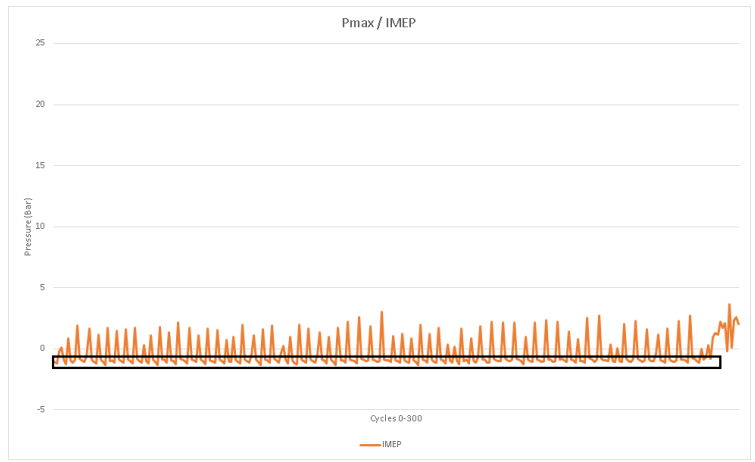


Figure 70 - 300 Cycle Sample Set (1600RPM)

Figure 71 shows a zoomed in view highlighting the typical 5-cycle "saw-tooth" IMEP pattern.

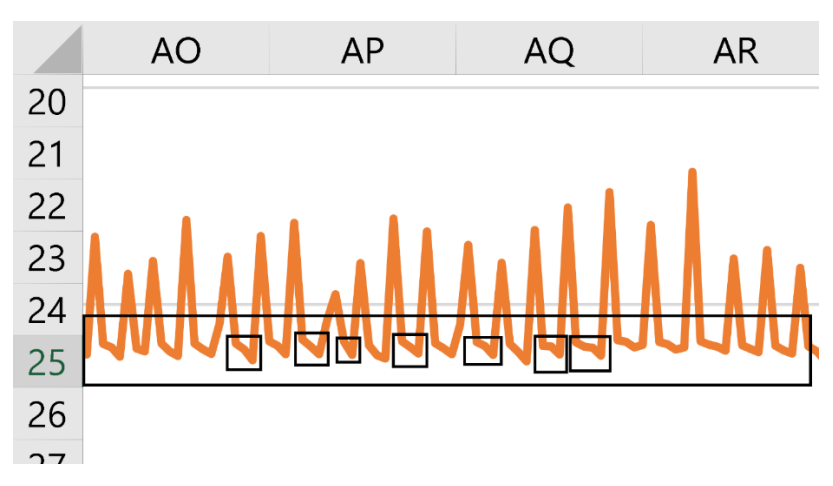


Figure 71 – "saw-tooth" Pattern (1600RPM)

Figure 72, however, shows the 300-cycle sample in which the author has identified 4 regions (A,B,C and D) in which the normal 5-cycle pattern seems to deviate somewhat from the typical behaviour across the sample set.

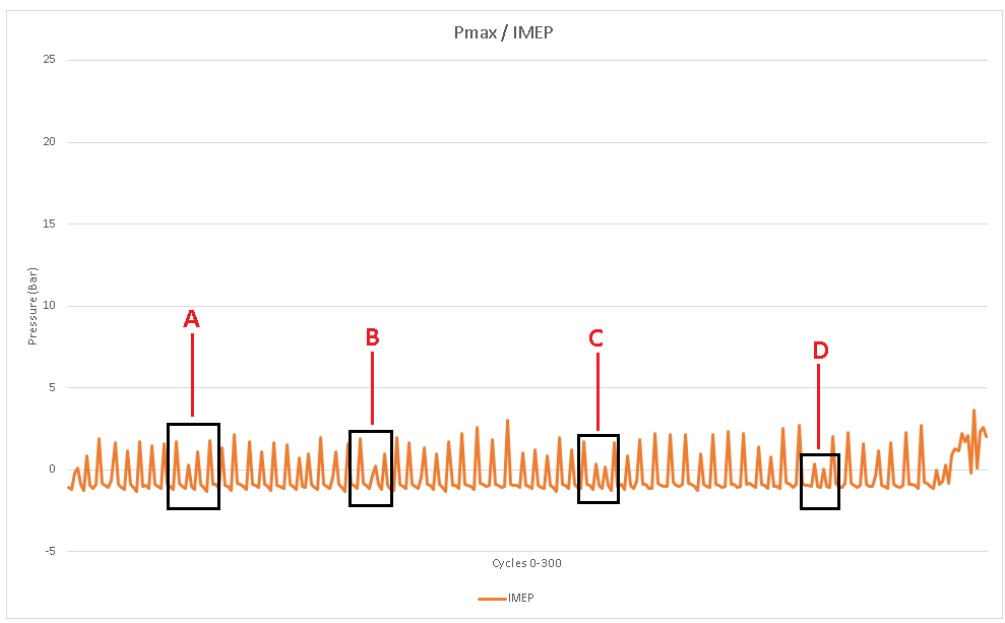


Figure 72 - "saw-tooth" Pattern Deviations (1600RPM)

This anomalous IMEP behaviour can now be studied.

Whilst figure 69 shows an example of the 5-cycle pattern that follows the rule of "live, weak, less weak, further less weak and live" in terms of peak cylinder pressure and follows the general trend, the pattern sample nevertheless shows an interesting anomaly.

Figure 73 highlights the plot of IMEP for the same cycles 96 to 100 and clearly shows a deviation from the general IMEP "saw-tooth" pattern.

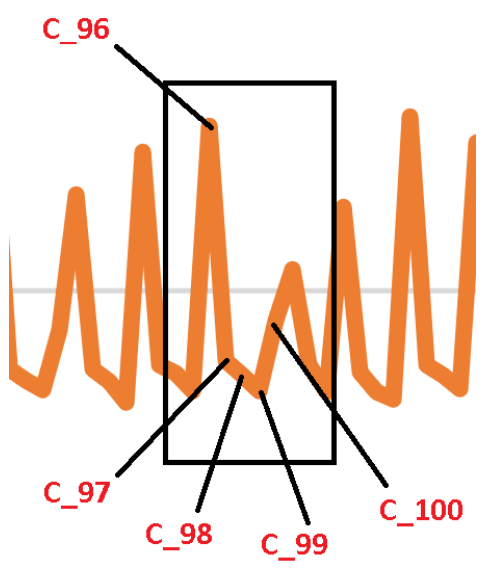


Figure 73 - IMEP "saw-tooth" Pattern (cycles 96-100)

When previously it had been discussed about identifying a properly live cycle as one with a positive value of IMEP, figure 73 questions the validity of this approach as cycle 5 (C_100) clearly shows post TDC combustion in the pressure graph of figure 69 but still has a negative

IMEP value. Clearly the released energy from combustion is insufficient to overcome the energy losses in the cycle.

This anomaly highlights how multiple approaches and viewpoints are needed to uncover what is really going on when appraising pressure and IMEP data rather than simply identifying a live cycle as one with a positive IMEP value.

Although one approach by itself may be questionable, confidence can be had in the general approach of looking for visual patterns and then observing how anomalies can deviate. This general approach in studying visual patterns in cylinder pressure and IMEP can achieve a large amount of insight without the need for complicated computation.

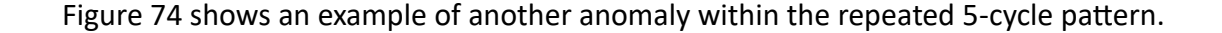
Appraising as a group of cycles proves useful. For instance, looking at cycle 100 in figure 69 on its own it might be difficult to identify the presence of combustion or the point of start of combustion. The motored cycles present provide a guide making it easy to then identify the small amount of post TDC combustion present in cycle 100.

Looking for the start of combustion (SOC) is harder as the combustion is fairly weak but comparing with the motored cycles and cycle 96 in figure 69 it can be reasonably identified as being around 15 degrees ATDC.

Another clear marker of combustion is the activity around exhaust opening (EPO) in figure 68. Cycle 100 shows negative pressure (albeit small in magnitude) and differentiates itself clearly from the motored cycles with their positive pressure after EPO.

Looking at the data from multiple angles such as these gives the approach a dexterity that could be fitting of a more advanced approach of possible automated pattern recognition.

6.2.2.4.2 – Second Anomaly Type (Pressure Trace Anomaly)



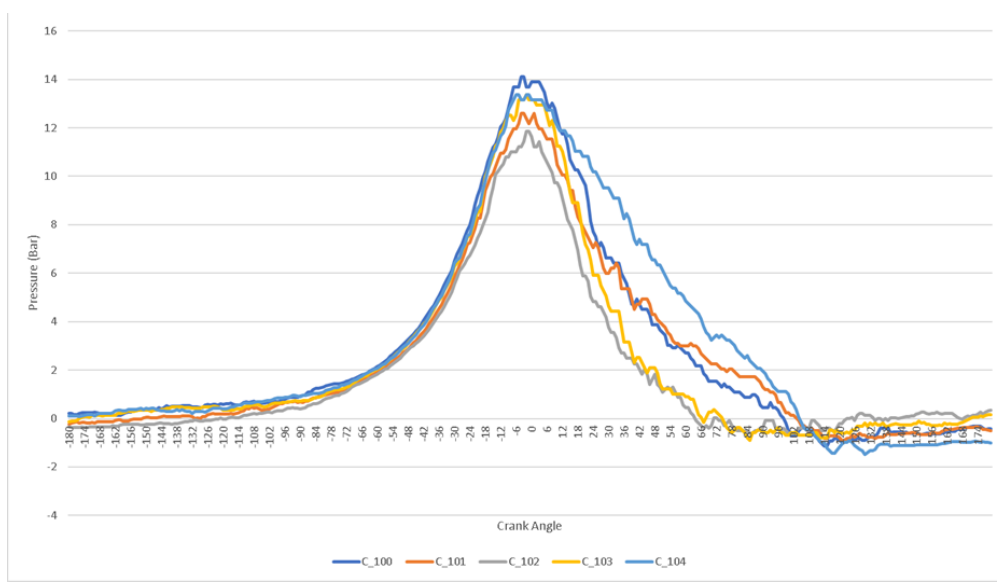


Figure 74 - Pressure Traces Second Anomaly (cycles 100-104)

Whereas the pressure traces in figure 69 for cycles 96 to 100 held true to the general rule, the pressure traces of cycles 100 to 104 in figure 74 do not.

Cycle 1 (C_100) is live, cycle 2 is live, cycles 3 is motored with weakest pressure around TDC, cycle 4 is motored with a measurable jump in peak pressure circa TDC and cycle 5 is live and strongest out of all five in terms of combustion pressure and IMEP (as reflected by the area under the graph).

Figure 74 shows that cycle 2 exhibits post TDC combustion. It is interesting to note in figure 74 that cycle 104 has the strongest combustion post TDC but does not have the highest peak pressure at TDC (albeit it is close).

Cycle 100 has the strongest peak pressure around TDC but has late and very poor combustion which appears to create a much-reduced suction effect around exhaust port opening with the fact that the next cycle (cycle 101) becomes a live combustion cycle whereas usually it would be a non-combustion motored cycle in the generally observed pattern in the 300-cycle sample set.

This indicates that the presence of combustion cannot be simply related to the pressure condition at TDC but that there is a clear relationship here to the pressure activity at exhaust port opening (EPO) of the previous cycle. Figure 75 shows a zoomed in focus on EPO activity for these cycles.

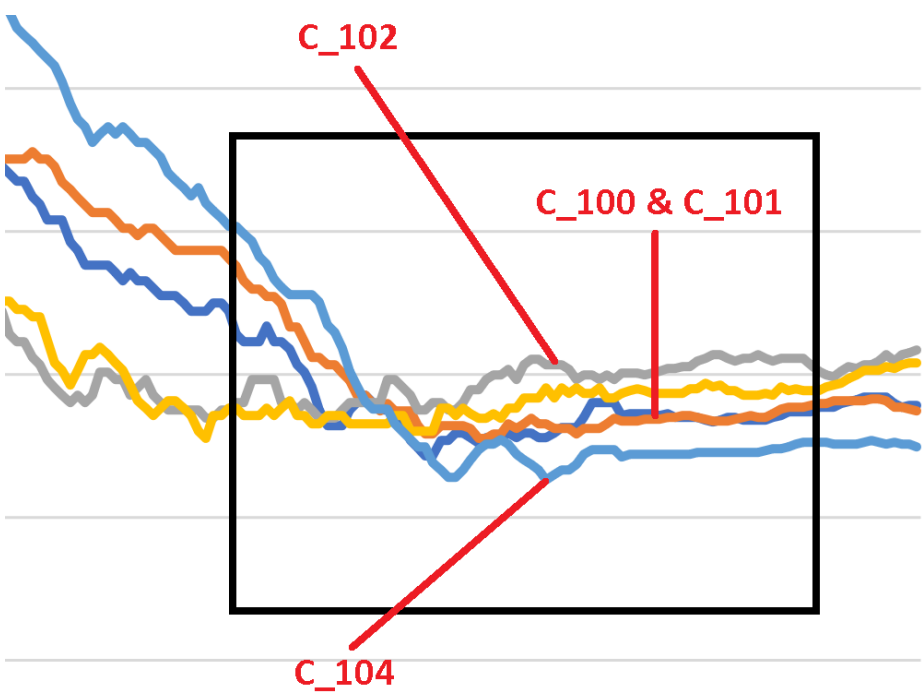


Figure 75 - Second Anomaly EPO Activity Pressure Traces

Cycle 100 can be seen to produce a mediocre suction effect around EPO, visibly sitting in the middle of the normal range.

Interestingly, the peak pressure of the following cycle 101 shown in figure 74 sits in the middle of the normal range for values around TDC. Figure 76 shows this clearly in a zoomed in diagram around TDC

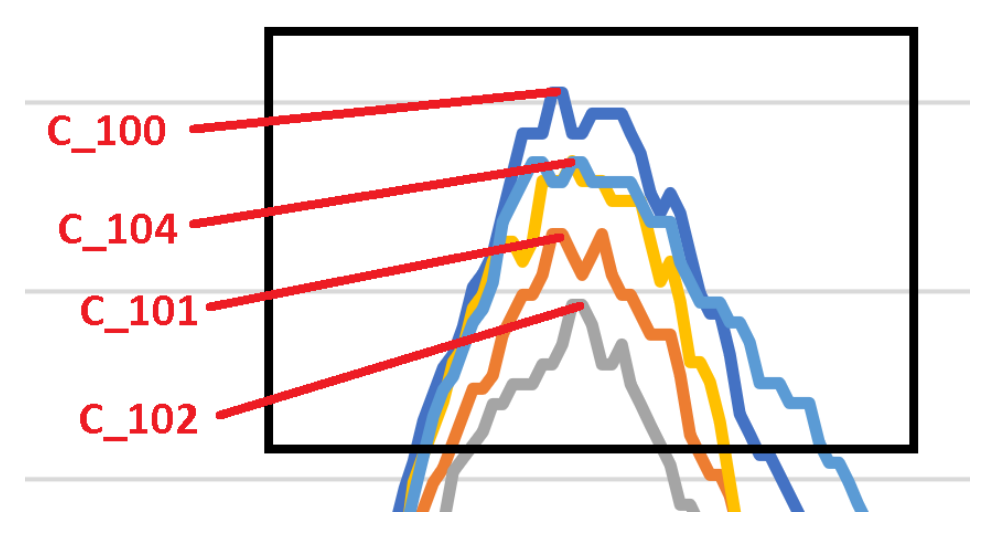


Figure 76 - Second Anomaly (Pressure Traces Around TDC)

This points to the system being harder to explain by just concentrating on one observed relationship. It backs up the idea of the system being out of balance and that the magnitude

of the suction effect around EPO appears to correlate to the magnitude of the peak pressure at TDC of the next cycle.

In a most simple explanation, cycle 100 is a particularly weak combustion cycle and does not create a suction effect at EPO.

A comparison of the pressure traces for cycles 100 and 101 are shown in figure 77.

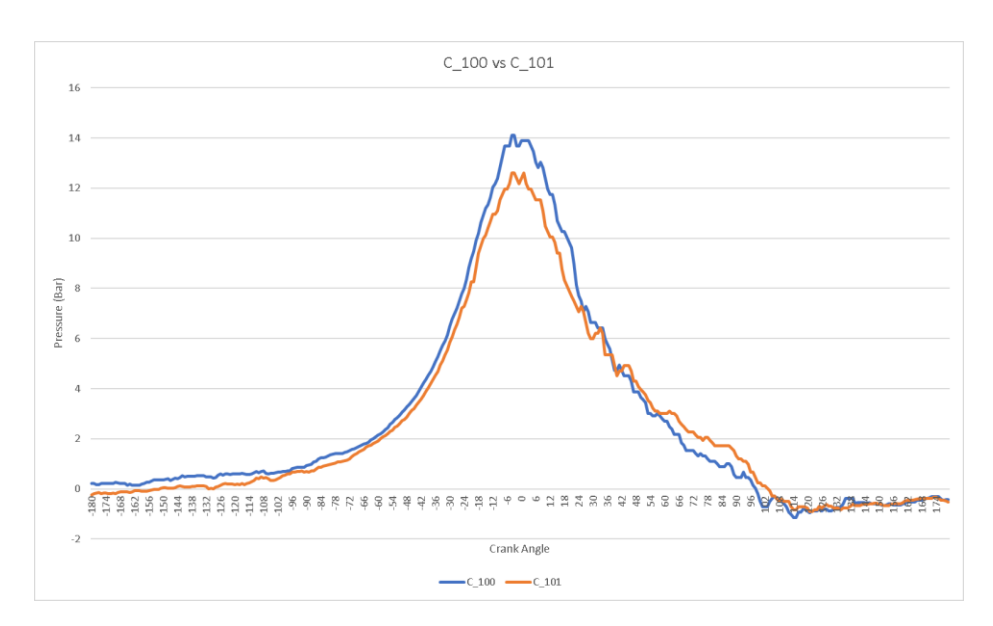


Figure 77 - Pressure Traces (cycles 100 and 101)

Figure 78 shows the traces of work done per degree for cycles 100 and 101 to aid understanding. It clearly shows the effect of late combustion in cycle 101.

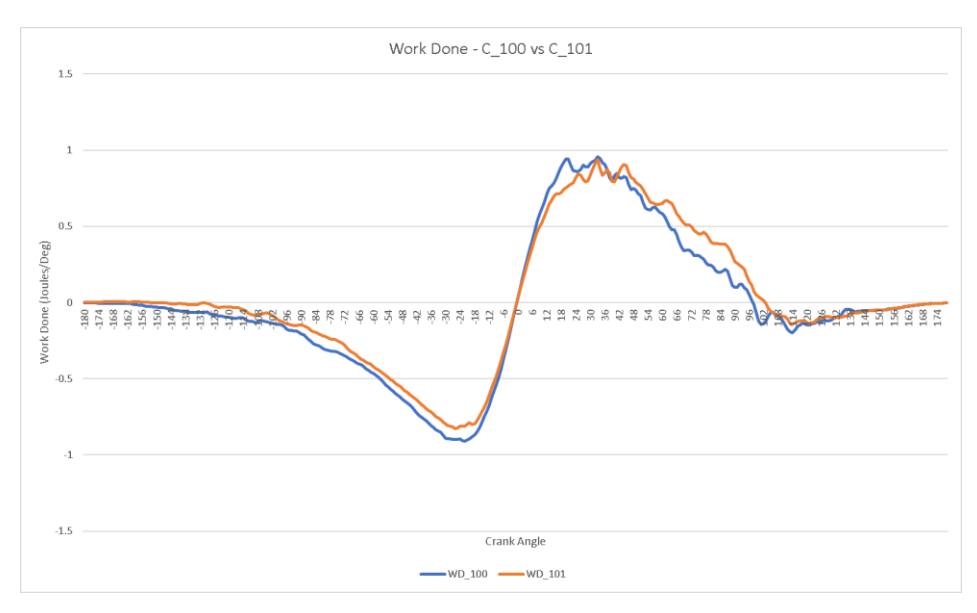
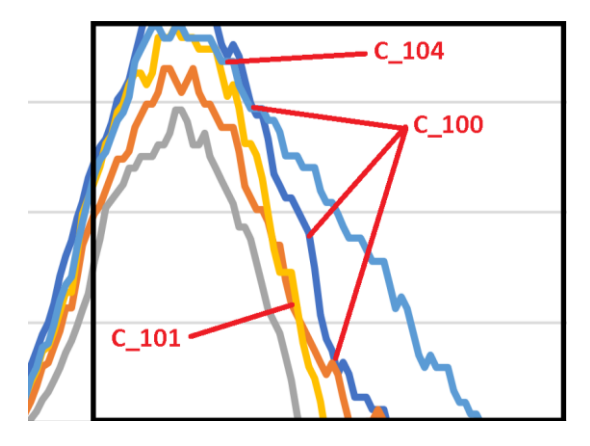


Figure 78 - Work Done Per Degree (cycles 100 and 101)

Figure 79 and 80 are zoomed in plots specifically looking at combustion and its likely start point.



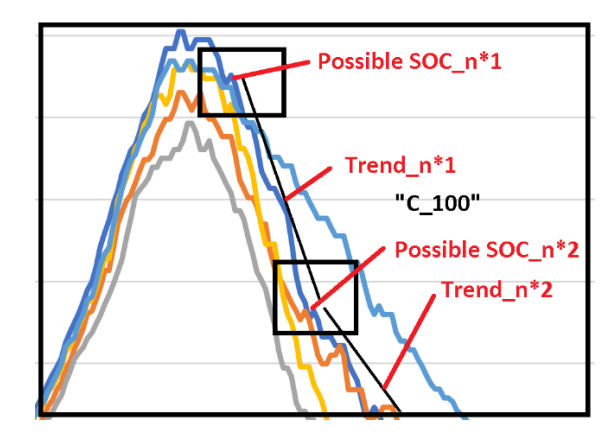


Figure 79 - SOC Points/Behaviour Anomaly 2

Figure 80 - SOC Points/Behaviour Anomaly 2

Both figures show the difficulty in assessing combustion activity in isolation from the motored cycles.

In figure 79, cycle 100 clearly has some combustion but its start of combustion point is difficult to assess. Similarly, cycle 104 demonstrates stronger combustion but again lacks a clearly discernible start of combustion point.

Figure 80 homes in on cycle 100 looking to identify the start of combustion point from geometric trends but again illustrates the difficulty when assessing a single cycle containing normal pressure noise (as opposed to the more easily determined start of combustion points from data averaged over 300 cycles say).

Of the final note to the anomalous sample set 100 to 104, figure 81 shows their pressure traces leading up to TDC

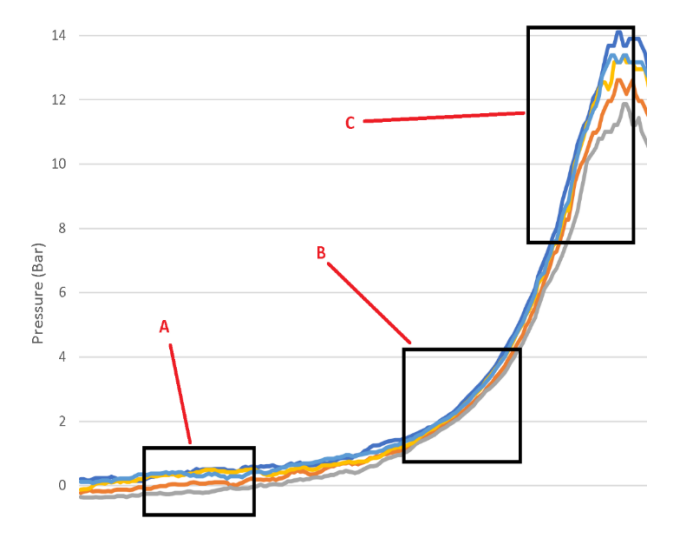


Figure 81 - Pressure Traces Pre-TDC Anomaly 2

The order in terms of pressure values leading up to and at TDC is seen to be maintained consistently throughout. In simpler terms a cycle starting with a lower pressure rises to a lower peak pressure at TDC.

The higher pressure traces are believed to potentially indicate cycles containing more mass in the cylinder. The cylinder pressure during the compression phase is directly linked to the previous cycle pressure at exhaust port opening.

The author believes that this behaviour is heavily related to the 2-stroke combustion system gas dynamics and timing but to speculate further would not be possible without an increased level of data.

6.2.2.5 – Importance of Exhaust Port Opening (EPO) Activity and Correlation with Data Set at 2500 RPM

EPO pressure activity has been shown to have a very deterministic effect on the cycle-to-cycle behaviour at 1600RPM.

The author was interested to revisit how EPO activity played a role in the 2500RPM data set.

Figure 82 shows cycles 248 and 249 at 2500 RPM.

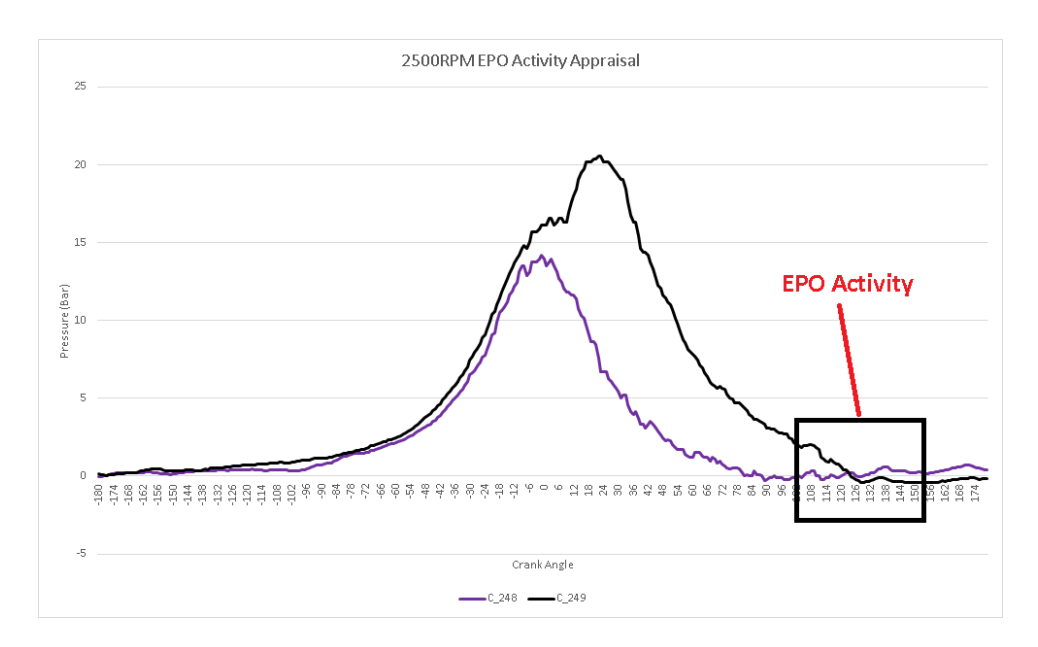


Figure 82 - Pressure Traces and EPO Activity Cycles 248 and 249 (2500RPM)

These are consecutive cycles from the alternating 4-stroke region C in figure 40. The figure clearly shows the non-combustion cycle 248 having a higher exhaust port pressure than the firing cycle 249.

Figure 83 shows non-consecutive non firing and firing cycles from the alternating 4-stroke region A in figure 40 showing the same trend in that the firing cycle (C_76) has a significantly lower pressure around exhaust port opening.

The figures 82 and 83 above represent typical cycles in the alternating 4-stroke region at 2500RPM and clearly show that the exhaust port pressure activity and its influence on following cycles is equally present at the higher 2500RPM case as is at 1600RPM.

The author had suspected that this would be the case but that the higher RPM the spread in pressure at EPO between firing and motored cycles would be less. This indeed proved to be the case as shown by the number of samples at 2500RPM shown in figure 84.

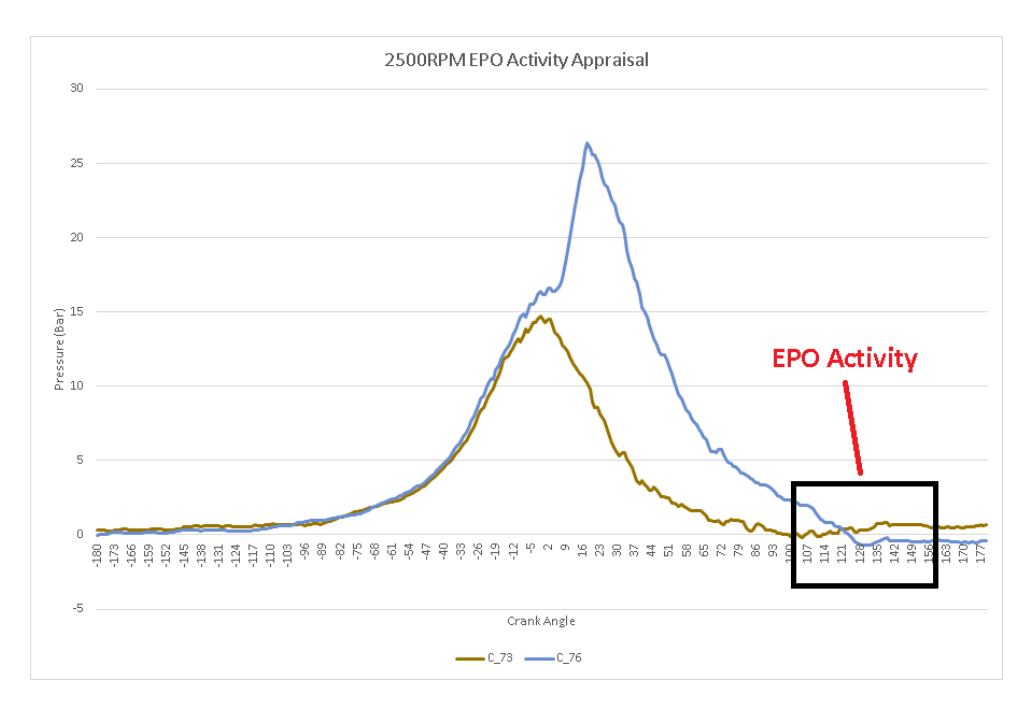


Figure 83 - Cycles 73 and 76 (2500RPM)

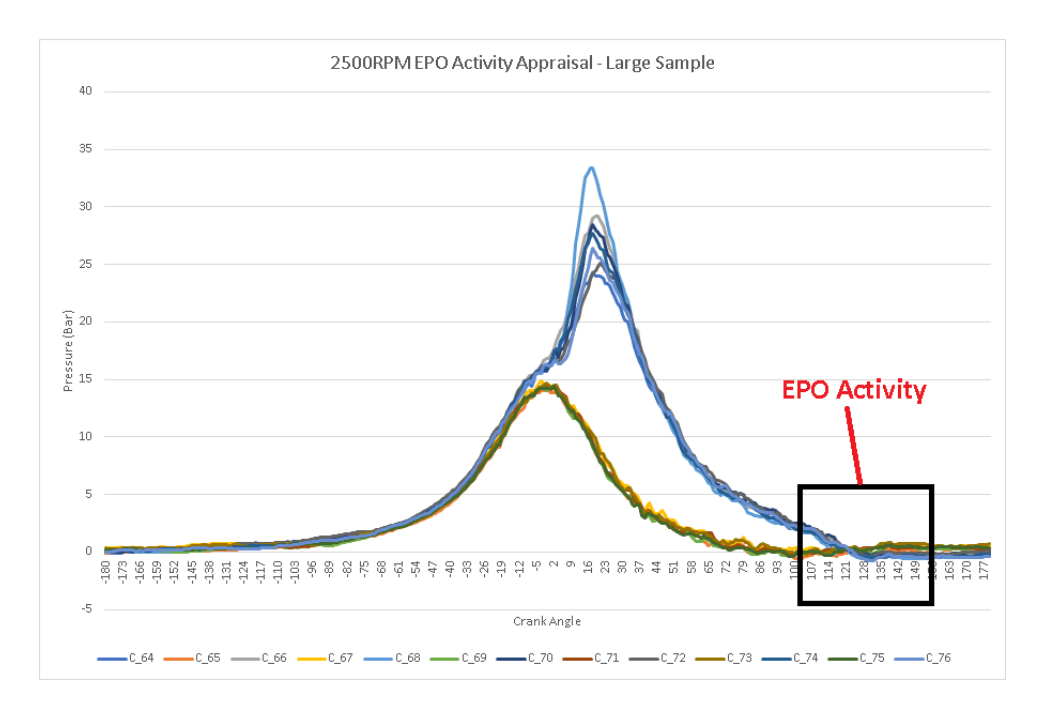


Figure 84 - Pressure Traces Large Sample Set (2500RPM)

The author postulates that at the higher RPM the transition period between gas exchange states happens over a shorter period of time; that there is a smaller time window in which transitory and unstable behaviour is possible leading to a smaller variation or spread in the magnitude of the pressure around EPO.

6.2.2.6 – Identifying Cycles with Combustion

The author has identified through this work that firing cycles can have varying degrees of combustion.

The author sought a method to determine when a cycle exhibits combustion.

Figure 85 shows a plot of the crank angle of peak pressure on a cycle-to-cycle basis.

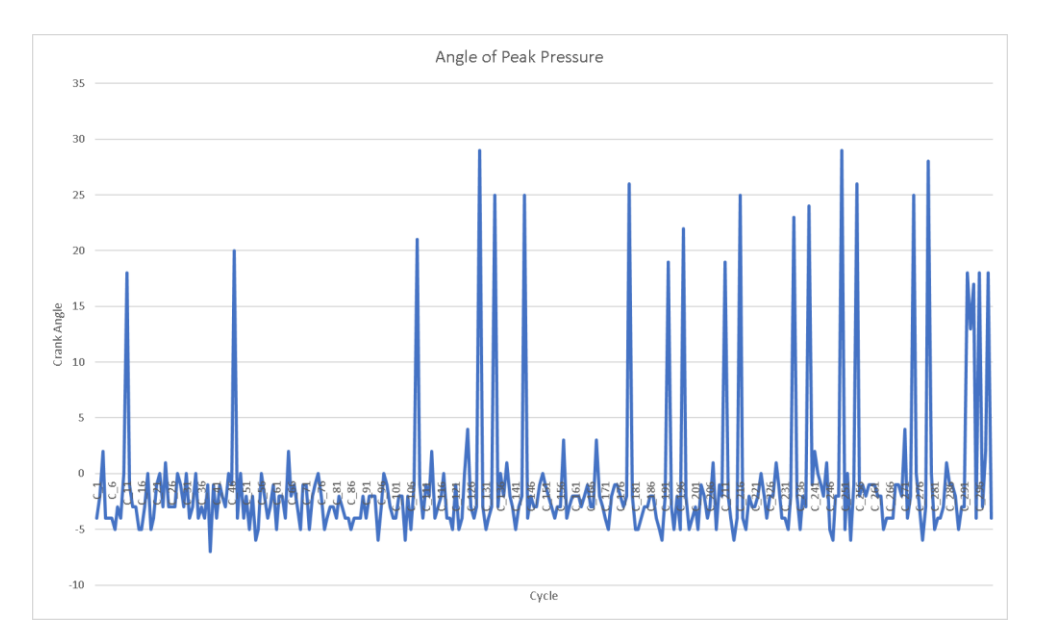


Figure 85 - Angle of Peak Pressure (1600RPM)

Most of the time the figure shows the angle to be around TDC. However, some cycles obviously deviate from this and have significantly later angles of peak pressure. A reader could clearly say that these cycles with later angles of peak pressure contain combustion, but these cycles are in the minority and conversely you cannot say that all cycles with angles of peak pressure around TDC are without combustion.

Figure 86 shows a plot of a large sample of pressure traces plotted on a single graph at 1600RPM.

Figure 85 has been annotated to show that many of the cycles have what appears to be combustion activity after TDC but whose peak pressure magnitude is lower than the motored magnitude around TDC. Clearly magnitude of the pressure trace cannot be used by itself as an absolute indication or guide towards the presence of combustion.

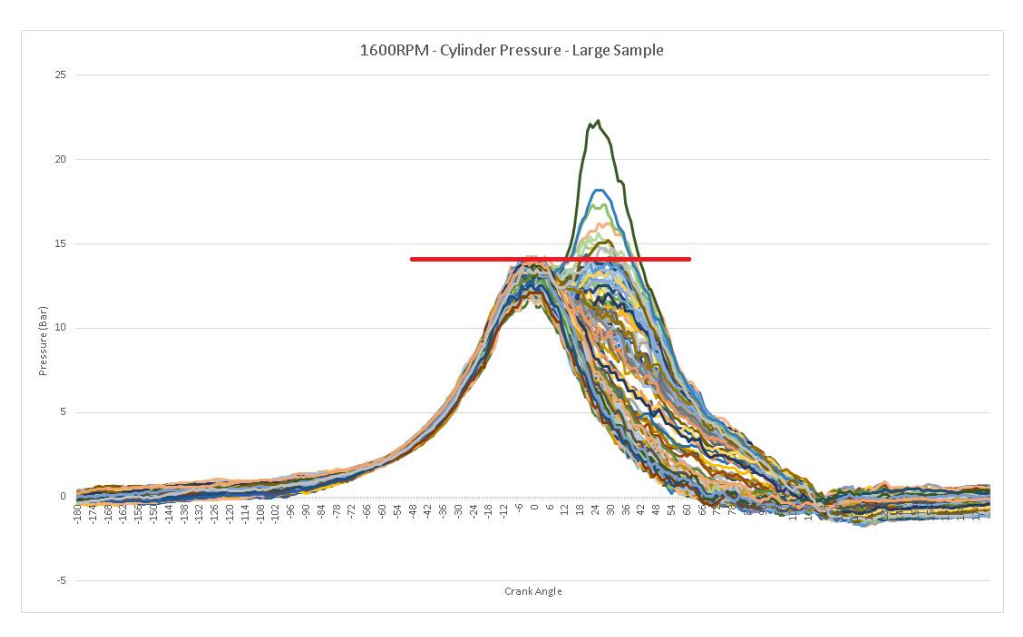


Figure 86 - Pressure Traces (1600RPM)

6.2.2.7 - Understanding of The Effect of Pressure at EPO

The author postulates that the suction effect at EPO following a properly live cycle as seen in the general 1600RPM behaviour (and also in the 4-stroke behaviour at 2500RPM) creates a negative pressure at EPO which significantly affects the filling of the next cycle whose motored peak pressure at TDC will then be low. This non firing cycle creates a positive pressure at EPO helping the filling of the next recovery cycle to create a significant increase in pressure at TDC. The recovery cycles are gaining pressure at TDC, very likely a reflection of the increasing mass trapped in the cylinder, until a cycle is capable of firing properly again.

This has repeatedly been observed to be a five-cycle pattern throughout the 1600RPM data set with the anomalies explained in the above analysis.

The author proposes an analogy to this recovery sequence in that one cannot simply take something out of balance and then expect it to return precisely to a nominal position or state. It's analogous to bouncing a rubber ball against something and watching the subsequent actions of the ball rapidly decrease.

To give a pictorial explanation of the engine during this 5-cycle recovery pattern, the author imagines that the exhaust is sucking through a straw and cannot suck in sufficient fresh mixture (although it is trying). When it doesn't get sufficient fresh mixture from the transfer ports eventually the suction effect subsides, and mixture is drawn back from the exhaust resulting in poor filling of the cylinder both in terms of quantity and the quality of the air and fuel mixture.

This is acting against how the engine wants to perform (the engine is a system of inter-tuned resonance chambers) and because it is acting against how the engine wants to perform it is creating an imbalance (for example, pulses being out of synchronisation and destructively interfering with each other).

6.2.2.8 - The "saw-tooth" IMEP Pattern and Cylinder Pressure Recovery at 1600RPM

The general 5-cycle IMEP "saw-tooth" pattern at 1600RPM discussed in section 6.2.2 and shown in figure 63 shows a steadily declining IMEP during recovery cycles 2, 3 and 4. However simultaneously the pressures of the motored cycles at TDC are increasing from cycle 2, through cycle 3 to cycle 4. The author can explain that this is not in contradiction but that the rising pressure at TDC is likely a reflection of the increasing amount of trapped mass in the cylinder. However, the increasing amounts of trapped gas also increase the pumping and compression work carried out in the cycle thereby worsening the IMEP.

6.2.2.9 - Pattern Recognition

The author proposes that a simple method for appraising the likelihood of the pattern repetition would be a combination of basic visual and statistical appraisal.

For example, if the 5-cycle pattern contains 2 firing cycles and 3 non-firing cycles, then and ideal sample of 50 cycles (or 10 pattern samples) would contain 20 firing cycles and 30 non-firing cycles. There is an obvious margin for error depending on when the sampling is started but this would be reduced with an increased sample size.

This method would use a basic automated calculation to determine the presence of combustion (although the analysis has shown that this is not trivial). Whilst not advanced, using such a method would enable rapid appraisal of the likelihood of pattern presence when looking at a large quantity of data. It could also be a good indicator of the frequency of occurrence of anomalies.

6.3 – Summary of Analysis at 2500RPM and 1600RPM

6.3.1 - 2500RPM

The KTM 2-stroke engine shows clear alternating behaviour at low load, 2500RPM. Large regions of the sample set exhibit 4-stroke behaviour, alternating between firing and non-firing cycles.

The alternating cycles show clear differences between peak cylinder pressure with IMEP values per cycle going from positive to negative.

6.3.2 - 1600RPM

At low load, 1600RPM clear evidence can be seen of a firing cycle followed by recovery cycles until a properly firing cycle occurs again.

A typical 5-cycle pattern emerges across the sample set.

Analysis shows that the cylinder pressure around exhaust port opening has a very significant effect on the following cycle.

A truly properly firing cycle creates a negative pressure at exhaust port opening which has been demonstrated to decrease the filling of the cylinder on the next cycle to the detriment of its combustion.

It takes 3 recovery cycles until the next properly firing cycle can occur.

In the data set there are only a few anomalies as discussed but these still display the importance of the pressure at exhaust port opening on the next cycle.

Of interest, comparison with the only paper the author was able to find containing any similar analysis [143] shows distinct differences in cylinder pressure and IMEP behaviour, the paper showing no change in pressure at EPO regardless of the cycle combustion activity. The author believes that the results show a clarity and understanding not seen in the reference.

6.3.3 – Overall

The data collected at 2500RPM and 1600RPM at low load has provided a new insight into the sub optimal running of a 2-stroke engine not previously seen in the literature by the author.

7 - Conclusion

7.1 – General

The aim of the project was to develop an understanding of cycle-to-cycle variation in a modern 2-stroke engine, an understanding not currently available in academic literature. 2-stroke engines are known to suffer from very poor cyclic variation under low load and low RPM conditions which have rendered them unsuitable in meeting the demanding automotive emissions standards currently mandated and also in meeting acceptable fuel consumption and carbon dioxide targets.

The ultimate goal of the project was to determine a method to practically implement the concept of Controlled Auto Ignition (CAI) from the enhanced understanding of cycle-to-cycle behaviour at the low load and low RPM operating conditions. Controlled Auto Ignition has been shown in the literature [60-67] to provide large benefits in reducing the unwanted cycle-to-cycle variation damaging to the control of emissions.

To these ends the author can state that the project has been very successful in producing high quality data clearly showing the cycle-to-cycle behaviour under a large sample set of cycles at low load under the engine speed conditions of 1600RPM and 2500RPM. Despite a large literature survey the author had been unable to obtain this information from the literature.

The data has provided a new insight into the cycle-to-cycle behaviour when a 2-stroke engine is running under sub-optimal operating conditions and has allowed the author to gain a much better understanding of the practical requirements needed to implement Controlled Auto Ignition.

7.2 - Background

As a background and before discussing the way forward to implement Controlled Auto Ignition, the author would like to summarise the depths and successes within the project which has led to the capture of data and its analysis. Also summarised is the design and manufacture work already completed to allow the next steps in obtaining practical implementation.

The author can state that the core aim of obtaining high quality data was achieved. The data showed good cycle-to-cycle resolution and proved totally sufficient for the analysis of 2-stroke behaviour under part load. Up to circa 6000 cycles of continuous operation had been successfully recorded to a resolution of one crank-shaft degree.

The data demonstrated accuracy in both pressure amplitude and crank angle position. Cylinder pressure values, both in terms of amplitude and crank angle, related closely to

averaged data for this engine previously obtained by the author from KTM giving further confidence in the accuracy of the calibration.

There were further practical achievements within the project. The author successfully designed, developed and produced several physical parts within the project timescale. These included exhaust restrictors, a modified standard cylinder head incorporating a measuring cylinder pressure transducer and ten cast prototype cylinder heads incorporating sufficient rough stock to allow machining to carry out a comprehensive sweep of the combustion controlling variables of compression ratio, squish and combustion chamber profile. The designs were informed by research and in particular the work carried out by Honda (60-67).

The process involved to develop these parts incorporated the use of 3D data capture using CT scan equipment, tactile CMM measurement and digital processing with subsequent reverse engineering of the data.

This was successfully followed by the author's use of parametric modelling, experience of design for manufacture (DFM) techniques and rapid plastic prototyping to create solid 3D parts to allow confirmation of fit to the standard engine and to ensure quality and finish of the components before final manufacture.

The author successfully researched and purchased a reliable cylinder pressure data logging system which undoubtedly helped achieve very satisfactory data collection within the timeframe of the project.

The subject of this project has been a long-held interest of the author. Whilst on an industrial placement during the author's undergraduate studies the author spent a year at the casting foundry Grainger and Worrall whose help producing the prototype cylinder head castings added a new dimension to this project. During the placement year the author developed contact with KTM whose help in providing components and engine data led to a final year undergraduate project understanding the KTM engine and developing a full combustion model for the engine.

This Master's project was inspired by the undergraduate project in which the author was motivated to obtain cycle-to-cycle data and an understanding not provided by KTM.

The Master's project required significant independent facilitation, with the author creating both the academic direction and having to largely specify and resource the equipment required, including the measuring equipment. Adding further to the learning experience and challenge, the author was one of the first people to use the University's newly commissioned chassis dynamometer facility. Throughout the project an essential driving factor was the author's continuity of interest and passion for the subject area making it possible to convince external stakeholders to provide necessary support. This ability to convince external stakeholders to invest continued throughout the project and the author is very grateful that GTPE in Plymouth provided help to machine modified cylinder heads and that Grainger and Worrall provided very significant assistance in bringing the prototype cylinder head design into the real world by casting.

7.3 - Technical Conclusion

The project has uncovered and documented several nuances regarding the operation and behaviour of the 2-stroke engine which the author was unable to find in the academic literature.

The data collected showed extensively how the 2-stroke engine was unstable at low load, low RPM, highlighting a Coefficient of Variance (COV) of IMEP as high as 24.2%, far greater than the current automotive industry standard of less than 3%. (116)

At low load, 1600RPM, the analysis in section 5 has shown the engine to be struggling cycle-to-cycle over the duration of the test run. Cycle-to-cycle the engine showed in general a clearly repeatable 5-cycle pattern where the engine was struggling for stability and balance. This followed the rule of "1 - firing, 2 - a motored or dead cycle with negative IMEP and low peak pressure at TDC, 3 – a motored or dead cycle with further reduced IMEP but noticeably higher peak pressure at TDC, 4 – a motored or dead cycle with even further reduced IMEP but higher still peak pressure at TDC and finally 5 – a properly firing live cycle".

This 5-cycle pattern, with a few anomalies as previously discussed in depth, repeated itself across hundreds of cycles.

For completeness figures 86 and 87 show the IMEP and cylinder pressure values during a typical 5-cycle pattern.

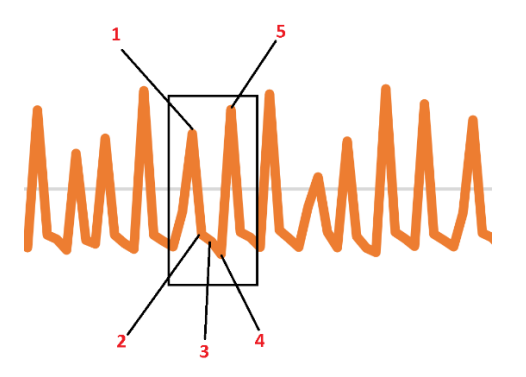


Figure 87 - IMEP 5-Cycle Pattern 1600RPM

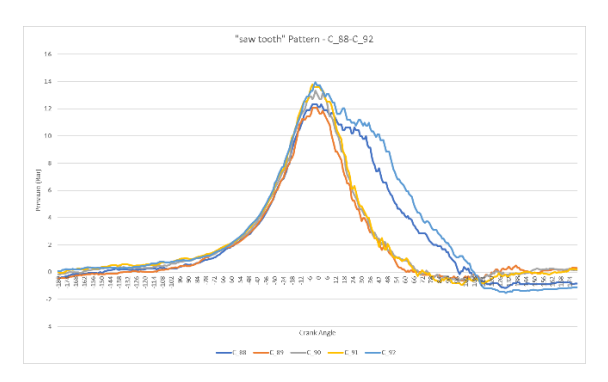


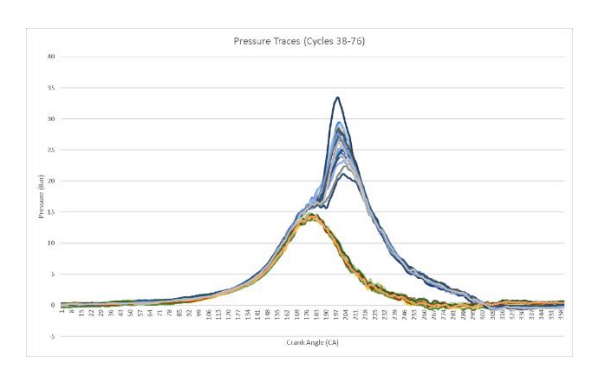
Figure 88 - Pressure Traces 5-Cycle Pattern 1600RPM

Of real significance is the importance of the pressure at exhaust port opening (EPO) shown in figure 88 and its effect on the following cycle. This will have a real meaning for the following steps of introducing Controlled Auto Ignition.

The second region of technical analysis was at low load, 2500RPM. At 2500RPM the analysis showed clear evidence of so-called 4-stroke operation during the regular part of the running.

The 1600RPM analysis does not show 4-stroke operation but rather a repetitive 5-cycle pattern. The author can state that both regions of technical analysis show a clear imbalance.

Of particular interest again at 2500RPM and shown clearly in figures 89 and 90 is that the pressure at exhaust port opening is again very important at 2500RPM in the effect it has on the following cycle.



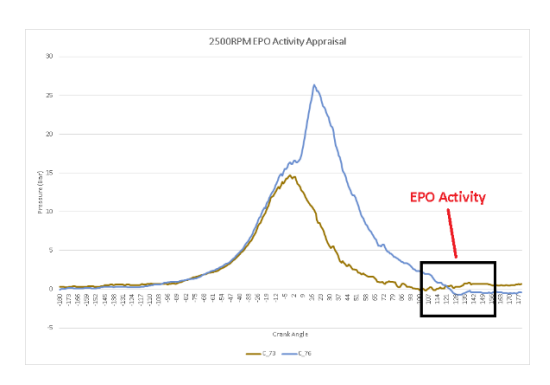


Figure 89 - Pressure Traces for Cycles 38-76 2500RPM

Figure 90 - EPO Activity Cycles 73 & 76 2500RPM

Figure 89 shows that the pressure traces fall into two camps over 39 consecutive cycles, the firing cycles leading to a distinctly lower pressure at exhaust port opening. Figure 89 demonstrates clearly the separation between the firing and non-firing cycles at exhaust port opening.

7.4 – Implementation of Controlled Auto Ignition and the Next Research Steps

The author's work has highlighted cycle-to-cycle behaviour at low load, low RPM not previously seen in detail in the academic literature.

At 1600RPM, a regular 5-cycle pattern has been identified whilst at 2500RPM the tendency is to go into 4-stroke operation whereby cycles alternate from live to motored.

However, in both cases the project has identified the importance of the pressure at exhaust port opening on the following cycle.

Despite the author's best efforts to design the rough stock prototype cylinder heads and exhaust restrictors early in the project, timescale limitations prevented any subsequent testing following the cycle-to-cycle analysis discussed in depth in the dissertation.

However, the analysis has indicated a potential path forward. The importance of the pressure at exhaust port opening on the following cycle is clearly very important at both 1600RPM and 2500RPM. A live cycle is shown to result in a negative pressure at exhaust port opening which seems to have a detrimental effect on the filling of the cylinder for the next cycle. The work carried out by Honda Motor Corporation in particular [60-67] shows the importance of using an exhaust restrictor. The author now understands the mechanism by which such a restrictor can work.

It is believed that the exhaust restrictor would prevent the pressure at exhaust port opening going as negative following a live cycle. With a suitably sized exhaust restrictor, the sizing of which may well depend on load and RPM, the pressure at exhaust port opening could

probably be stabilised to be very similar in magnitude for all cycles in this sub-optimal operating range.

In this way, the filling of the cylinder in the following cycles could also be made much more similar. Undoubtedly much of the cylinder contents would be composed of residual exhaust gas rendering it very difficult to ignite with a conventional spark plug. This is when the concept of Controlled Auto Ignition comes into effect allowing the combustion of a very diluted airfuel mixture to take place through the mechanism of a raised compression ratio and modified combustion chamber shape to achieve a suitably high cylinder gas temperature with a suitable inhomogeneity of combustion gas hot spots [32] to allow spontaneous ignition at these hot spots.

As such, combustion could be achieved every cycle with a dramatic improvement in stability and Coefficient of Variance of IMEP, thereby allowing for better mapping ability to meet regulatory emissions requirements.

If time had permitted, the author would have undertaken a series of practical experiments, firstly introducing exhaust restrictors and carrying out a full sweep of restrictor sizes whilst monitoring their effect on the cylinder pressure at exhaust port opening. Initially this would target the low load, 1600RPM operating condition already studied.

The next step would be the introduction of the cast prototype cylinder head designed by the author. The main design feature of the head was to incorporate the concepts developed by Honda Motor Corporation for the application of controlled auto-ignition. The concept includes a spherical combustion chamber and a pronounced squish band amongst other things making it quite different to the KTM design.

The first head to be tested would be machined to be as similar as possible to the KTM head in terms of squish clearance and compression ratio.

Testing would be an iterative experimental process studying the cylinder pressure activity looking for signs of auto ignition and analysing cycle-to-cycle behaviour. The iterative steps would always reflect the analysis and require ongoing interpretation as an optimum design is developed.

In overall summary, the project has provided an enhanced insight into the cycle-to-cycle behaviour of a modern 2-stroke engine running under sub-optimal low load, low RPM conditions and has identified the importance of the pressure at exhaust port opening on the success of the following cycle.

It has provided a very good understanding of what the next steps need to be to successfully implement Controlled Auto Ignition in order to improve the cycle-to-cycle stability and Coefficient of Variance of IMEP to acceptable automotive wide standards.

Reference List

- 1. (2019, March). Retrieved from Kistler: www.kistler.com
- 2. (2019, March 12). Retrieved from GTPE: www.performance-engineering.co.uk
- 3. A. Wyczalek, F. (1991 International Congress and Exposition). *Two-Stroke Engine Technology in the 1990's*. Detroit: SAE.
- 4. A.Blank, D. (2007 World Congress). Radical Ignition Combustion Studies with Hydrogen in a Two-Stroke DI-HCRI Diesel Engine. Detroit: SAE.
- 5. A.Boretti, A. (2002 SAE Motorsports Engineering Conference and Exhibition). Parametric Design of FIM WGP Engines. Indianopolis: SAE.
- 6. A.Randolph. (1990). *Cylinder-Pressure-Transducer Mounting Techniques to Maximize Data Accuracy.* Detroit: SAE 900171.
- 7. Ambler, M., & Zocchi, A. (2001 Small Engine Technology Conference and Exhibition). Development of the Aprilia DITECH 50 Engine. Pisa: SAE.
- 8. Anschuetz, D. (2018, January 12).
- 9. Antonelli, E., Nuccio, P., Dongiovanni, C., & R.Marzano, M. (2004 Small Engine Technology Conference). A New GDI 2-Stroke Engine to Meet Future Emission Limits: The Design and Prototype Architecture. Graz: SAE.
- 10. Antonio Mariani, F. F. (2013). The Effects of a Radio Frequency Ignition System on the Efficiency and the Exhaust Emissions of a Spark-Ignition Engine. *SAE*.
- 11. Araki, M., Kishimoto, H., Nakajima, K., Maehara, M., Shiga, S., Nakamura, H., & Obokata, T. (2008). *A CNG Two Stroke Cycle S.I. Engine Using Intermittent Low Pressure Fuel Injection from Scavenging Ports.* Gunma: Dept of Mechanical Engineering, Gunma University.
- 12. Asai, M., & Ishibashi, Y. (1996 International Congress & Exposition). *Improving the Exhaust Emissions of Two-Stroke Engines by Applying the Activated Radical Combustion*. Detroit: SAE.
- 13. Asai, M., Ishibashi, Y., Isomura, S., & Kudo, O. (1993). *Japan Patent No. EP 0606095 A1*.
- 14. Asai, M., Ishibashi, Y., Isomura, S., Kudo, O., & Nishida, K. (1993). *Japan Patent No. US* 5697332 A.
- 15. Asai, M., Ishibashi, Y., Isomura, S., Nishida, K., Noritake, H., & Takubo, M. (1996). *Japan Patent No. EP 0831214 B1*.
- 16. Asai, M., Kurosaki, T., & Okada, K. (1995). *Analysis on Fuel Economy Improvement and Exhaust Emission Reduction in a Two-Stroke Engine by Using an exhaust Valve.* Saitama: Honda R&D Co., Ltd.

- 17. Asgari, O., Kazemzadeh Hannani, S., & Ebrahimi, R. (2012). Improvement and experimental validation of a multi-zone model for combustion and NO emissions in CNG fueled spark ignition engine. *Journal of Mechanical Science and Technology*, 4(26), 1205-1212.
- 18. B.Heywood, J. (1988). *Internal Combustion Engine Fundamentals*. New York: McGraw-Hill.
- 19. B.Millet, J., Maroteaux, F., & Ravet, F. (2007 8th International Conference on Engines for Automobiles). Modeling of HCCI Combustion by One Step Reaction Function: in View of Assisting the Optimization of Engine Management System. Capri: SAE.
- 20. B.Poola, R., Nagalingam, B., & V.Gopalakrishnan, K. (1994 Fuels & Lubricants Meeting & Exposition). Performance of Thin-Ceramic-Coated Combustion Chamber with Gasoline and Methanol as Fuels in a Two-Stroke SI Engine. Baltimore: SAE.
- 21. Badami, M., Nuccio, P., & Andriano, M. (1999). The Influence of Crankcase Clearance Volume on Two-Stroke S.I. Engine Performance. Politecnico di Torino: 1999 SAE Small Engine Technology Conference.
- 22. Bartolini, C. M., Caresana, F., & Pelagalli, L. (2004 Small Engine Technology Conference). Development of a Two-Cylinders-Two-Stroke Gasoline-Direct-Injected Engine. Graz: SAE.
- 23. Benajes, J., Novella, R., De Lima, D., Dugue, V., & Quechon, N. (2012). *The Potential of Highly Premixed Combustion for Pollutant Control in an Automotive Two-Stroke HSDI Diesel Engine*. Valencia: CMT-Universitat Politècnica de València.
- 24. Bergman, M., Enander, N., & Lawenius, M. (2013). *CFD Scavenging Simulation and Verification of a Sequentially Stratified Charged Two-Stroke Engine*. Huskvarna: Husqvarna AB.
- 25. Bermudez, V., Payri, R., Javier Lopez, J., Campos, D., Coma, G., & Justet, F. (2016). Comparative Analysis of Particle Emission with Two Different Injectors in a CAI 2-Stroke Gasoline Engine. Valencia: CMT Motores Termicos Universidad.
- 26. Blair, G. (1991 SAW1 Mech E EXCHANGE LECTURE). The Two-Stroke Cycle Engine, Proscribe or Prosper? Portland: Queen's University Belfast.
- 27. Blair, G. P. (1994). *Design and Simulation of Two-Stroke Engines* (1 ed.). Warrendale: SAE International.
- 28. Boretti, A., & Jiang, S. (2015). *Two Stroke Direct Injection Jet Ignition Engines for Unmanned Aerial Vehicles.* West Virginia: West Virginia University.
- 29. Brynych, P., Macek, J., Tribotte, P., De Paola, G., & Ternel, C. (2014). System Optimization for a 2-Stroke Diesel Engine with a Turbo Super Configuration Supporting Fuel Economy Improvement of Next Generation Engines. Prague: Czech Technical Univ.

- 30. Chen, R., Milovanovic, N., Turner, J., & Blundell, D. (2003 SAE World Congress). The Thermal Effect of Internal Exhaust Gas Recirculation on Controlled Auto Ignition. Detroit: SAE.
- 31. Ciju, P., Pradeep, V., & Ramesh, A. (2013). *Air Assisted Direct Cylinder Barrel Injection of Gasoline in a Two-Stroke S.I. Engine.* Madras: Indian Institute of Technology Madras Chenai.
- 32. Duret, P. (2001). A New Generation Of Combustion Processes For The Future? (1 ed.). Rueil-Malmaison: Editions TECHNIP.
- 33. Duret, P., & Venturi, S. (1996 International Congress & Exposition). *Automotive Calibration of the IAPAC Fluid Dynamically Controlled Two-Stroke Combustion Process.*Detroit: SAE.
- 34. Duret, P., Dabadie, J., & Colliou, T. (1995 Small Engine Technology Conference). Application of IAPAC Fuel Injection for Low Emissions Small Two-Stroke Engines. Milwaukee: SAE.
- 35. Fasolo, B., Doisy, A.-M., Dupont, A., & Lavoisier, F. (2005 SAE World Congress). Combustion System Optimization of a New 2 Liter Diesel Engine For EURO IV. Detroit: SAE.
- 36. Ferrara, G., Balduzzi, F., & Vichi, G. (2012). *An Innovative Solution for Two-Stroke Engines to Reduce the Short-Circuit Effects.* Firenze: Universita degli Studi di Firenze.
- 37. Fujikawa, T., & Ohtsu, M. (1990). *Development of Automatic Exhaust Valve Control Device of 2 Stroke Engines*. Kobe: Kawasaki Heavy Industries, Ltd. Japan.
- 38. Fujita, K., & Takewaki, I. (2011). An efficient methodology for robustness evaluation by advanced interval analysis using updated second-order Taylor series expansion. *Engineering Structures*, *33*(12), 3299-3310.
- 39. G.Groff, E. (2016). *Automotive Two-Stroke-Cycle Engine Development in the 1980-1990's*. Milwaukee: SAE.
- 40. Gambino, M., & Iannaccone, S. (2001 Small Engine Technology Conference and Exhibition). Two Stroke Direct Injection Spark Ignition Engine for Two Wheelers. Pisa: SAE.
- 41. *Gausian Distribution Function*. (2018). Retrieved January 1, 2018, from http://hyperphysics.phy-astr.gsu.edu/hbase/Math/gaufcn.html
- 42. Gentili, R., Frigo, S., & Tognotti, L. (1994 International Congress & Exposition).

 Development of a Pumpless Air Assisted Injection System for Two-Cycle, S.I. Engines.

 Detroit: SAE.
- 43. Gentili, R., Frigo, S., Cozzolino, F., & Zanforlin, S. (2001 Small Engine Technology Conference and Exhibition). Influence of Engine Parameters on ATAC Behaviour in a G.D.I. Two-Stroke Engine. Pisa: SAE.

- 44. Gimelli, A., Boza, F., Fontanesi, S., & Saveri, E. (2011). 1D and 3D CFD Investigation of Burning Process and Knock Occurrence in a Gasoline or CNG fuelled Two-Stroke SI Engine . Modena: University of Modena and Reggio Emilia.
- 45. Grainger & Worrall. (2019, March 12). Retrieved from www.gwcast.co.uk
- 46. H.Gadallah, A., A.Elshenawy, E., M.Elzahaby, A., A.ElSalmawy, H., & H.Bawady, A. (2009). Effect of In Cylinder Water Injection Strategies on Performance and Emissions of a Hydrogen Fuelled Direct Injection Engine. Tanta: SAE.
- 47. H.-J. Kress, J. M. (1995). *Integrated Silicon Pressure Sensor for Automotive Application with Electronic Trimming*. Detroit: SAE 950533.
- 48. Hanabusa, H., Kondo, T., Hashimoto, K., Sono, H., & Furutani, M. (2013). *Study on Homogeneous Lean Charge Spark Ignition Combustion*. Nagoya: Nagoya Institute of Technology.
- 49. Hancock, D., Fraser, M., Jeremy, M., Sykes, R., & Blaxill, H. (2008 World Congress). A New 3 Cylinder 1.2l Advanced Downsizing Technology Demonstrator Engine. Detroit: SAE.
- 50. Harker, N., R.Denbraven, K., Johnson, J., & Findlay, A. (2008 Small Engine Technology Conference). University of Idaho's Clean Snowmobile Design Using a Direct-Injection Two-Stroke Engine. Milwaukee: SAE.
- 51. Heywood, J., & Chun, K. (1987). Estimating Heat-Release and Mass-of-Mixture Burned from Spark-Ignition Engine Pressure Data. *Combustion Science and Technology, 54*(1), 133-143.
- 52. Honda. (1997). *Press Information FACT BOOK*. Retrieved 02 04, 2018, from http://www.honda.co.jp/factbook/motor/CRM250AR/199701/crm97-005.html
- 53. Hong Jo, S., Do Jo, P., Gomi, T., & Ohnishi, S. (1973). *Development of a Low-Emission and High-Performance 2-Stroke Gasoline Engine (NiCE)*. Milwaukee: SAE.
- 54. Hooper, P., Al-Shemmeri, T., & J.Goodwin, M. (2011). Advanced modern low-emission two-stroke cycle engines. *Proceedings of the Institution of Mechanical Engineers*, 1(1), 1531-1543.
- 55. Huei-Huay Huang, P.-H. H.-J.-H.-C.-F. (1992). Improvement of Irregular Combustion of Two-Stroke Engine by Skip Injection Control. SAE 922310.
- 56. Ichihashi, S. (2016). *Applying Combustion Chamber Surface Temperature to Combustion Control of Motorcycle Engines.* Tochigi: Keihin Corp.
- 57. IFP. (n.d.). Paris.
- 58. lijima, A., Watanabe, T., Yoshida, K., & Shoji, H. (2006 Small Engine Technology Conference and Exhibition). A Study of HCCI Combustion Using a Two-Stroke Gasoline Engine with a High Compression Ratio. San Antonio: SAE.

- 59. liJima, A., Yoshida, K., & Shoji, H. (2005 Powertrain & Fluid Systems Conference and Exhibition). A Comparative Study of HCCI and ATAC Combustion Characteristics Based on Experimentation and Simulations Influence of the Fuel Octane Number and Internal EGR on Combustion. San Antonio: SAE.
- 60. Ishibashi, Y. (2000). Basic Understanding of Activated Radical Combustion and Its Two-Stroke Engine Application and Benefits. *International Spring Fuels & Lubricants Meeting & Exposition Paris, France*, 1-13.
- 61. Ishibashi, Y., & Asai, M. (1998). A Low Pressure Pneumatic Direct Injection Two-Stroke Engine by Activated Radical Combustion Concept. Detroit: SAE.
- 62. Ishibashi, Y., & Morikawa, H. (2010). *A Macroscopic Understanding of the Controlled Auto-Ignition for Vehicle Engines*. Saitama: Honda R&D Co Ltd.
- 63. Ishibashi, Y., & Nakano, Y. (1993). Japan Patent No. US 5701851 A.
- 64. Ishibashi, Y., & Sakuyama, H. (2004 Fuels & Lubricants Meeting & Exhibition). An Application Study of the Pneumatic Direct Injection Activated Radical Combustion Two-Stroke Engine to Scooter. Toulouse: SAE.
- 65. Ishibashi, Y., Asai, M., & Nishida, K. (1997). *An Experimental Study of Stratified Scavenging Activated Radical Combustion Engine*. Saitama: Honda R&D Co., Ltd.
- 66. Ishibashi, Y., Isomura, S., Kudo, O., & Tsushima, Y. (1994). A Trial for Stabilizing Combustion in Two-Stroke Engines at Part Throttle Operation. *HONDA R & D Technical Review*, *6*, 80-88.
- 67. Ishibashi, Y., Nishida, K., & Asai, M. (2001). Activated Radical Combustion in a High-Speed High Power Pneumatic Direct Injection Two-Stroke Engine. In P. Duret (Ed.), *A New Generation of Engine Combustion Processes For The Future?* (pp. 141-152). Rueil-Malmaison: Editions TECHNIP.
- 68. Ishibe, N., & Ohira, T. (1995). *Combustion Analysis and Its Optimization in Two-Stroke Engines*. Hokkaido: Suzuki Motor Corp.
- 69. Ivansson, N. (2003). *Esimation of the Residual Gas Fraction in an HCCI-engine using Cylinder Pressure*. Linköping: Linköping University.
- 70. J.Callahan, B., J.Kee, R., D.McCartan, C., Fleck, R., G.Kenny, R., & O.Mackey, D. (2002 Small Engine Technology Conference). Simulation of Dynamic Operation of a Single-Cylinder Two-Stroke Engine. Kyoto: JSAE.
- 71. J.D.Powell. (1993). Engine Control Using Cylinder Pressure: Past, Present, and Future. *ASME J. of Dynamic Systems, Measurement, and Control*, 343-350.
- 72. J.Fleck, B., Fleck, R., J.Kee, R., F.Chatfield, G., & O.Mackey, D. (2004 SAE Motorsports Engineering Conference and Exhibition). Validation of a Computer Simulation of a High Performance Two-Stroke Motorcycle Racing Engine. Dearborn: SAE.

- 73. J.Shayler, P., W.Wiseman, M., & Ma, T. (1990 International Congress and Exposition). Improving the Determination of Mass Fraction Burnt. Michigan: SAE.
- 74. James, K., Chen, R., & Turner, J. (2010). *Ionisation and Ionisation Rate of a Two-Stroke HCCI Engine Fuelled with E85 for Control Feedback*. Loughborough: Loughborough University.
- 75. Javier Lopez, J., Novella, R., Valero-Marco, J., Coma, G., & Justet, F. (2015). *Evaluation of the Potential Benefits of an Automotive, Gasoline, 2-Stroke Engine.* Valencia: Universitat Politècnica de València.
- 76. Kelly, K., Kennedy, S., & Spagnoli, J. (2000). Performance of an Advanced Synthetic Diesel Engine Oil. Paris, France: International Spring Fuels & Lubricants Meeting & Exposition.
- 77. Klein, M., & Erikson, L. (2005). Utilizing Cylinder Pressure Data for Compression Ratio Estimation. Laxenberg: IFAC.
- 78. Kong, S.-C., D.Marriott, C., D.Reitz, R., & Christensen, M. (2001). Modeling and Experiments of HCCI Engine Combustion Using Detailed Chemical Kinetics with Multidimensional CFD. Detroit World Congress: SAE.
- 79. KTM. (2017). Data. Mattighofen.
- 80. Kumar, S., W.Stanton, D., Fang, H., J.Gustafson, R., R.Frazier, T., G.Bunting, B., . . . R.Wolf, L. (2009). *The Effect of Diesel Fuel Properties on Engine-out Emissions and Fuel Efficiency at Mid-Load Conditions*. Oak Ridge: Cummins Technical Centre.
- 81. Kusano, K., & Hitoshi, K. (1990). *Development of Programmed-Fuel Injection for Two-Stroke Cycle Racer Engine*. Saitama: Honda R&D Co Ltd,.
- 82. L.Duret, P., Girard, A., & Elmaleh, A. (1997). World Overview of New Generation Two-Stroke Engine Activities from Patent Analysis. Paris: IFP.
- 83. Laget, O., Ternel, C., Thiriot, J., Charmasson, S., Tribotte, P., & Vidal, F. (2013). *Preliminary Design of a Two-Stroke Uniflow Diesel Engine for Passenger Car.* Paris: IFP Energies nouvelles.
- 84. Lavy, J., Angelberger, C., Guibert, P., & Mokhtari, S. (2001). Towards a Better Understanding of Controlled Auto-Ignition (CAITM) Combustion Process from 2-Stroke Engine Results Analyses. Pisa: SAE.
- 85. Lavy, J., Raux, S., Esterlingot, E., & Guibert, P. (1994). *Thermodynamical AND Optical Analyses Of Controlled Auto-Ignition Combustion In Two-Stroke Engines*. Paris: IFP.
- 86. M.Bartolini, C., Caresana, F., & Vincenzi, G. (2001 Small Engine Technology Conference and Exhibition). Experimental Analysis of a Two-Stroke Direct Injection Engine Prototype. Pisa: SAE.
- 87. Manente, V., Tunestal, P., & Johansson, B. (2008 Small Engine Technology Conference). A Novel Model for Computing the Trapping Efficiency and Residual Gas Fraction Validated with an Innovative Technique for Measuring the Trapping Efficiency. Milwaukee: SAE.

- 88. Marotin, A. (2018). Equation. Swansea: UWTSD.
- 89. Mattarelli, E., Rinaldini, C. A., Cantore, G., & Agostinelli, E. (2015 SAE Int. J. Alt. Power). Comparison between 2 and 4-Stroke Engines for a 30 kW Range Extender. Detroit: SAE.
- 90. Milovanovic, N., & Chen, R. (2001 International Spring Fuels & Lubricants Meeting & Exhibition). *A Review of Experimental and Simulation Studies on Controlled Auto-Ignition Combustion*. Orlando: SAE.
- 91. Milovanovic, N., Blundell, D., Pearson, R., Turner, J., & Chen, R. (2005 SAE World Congress). *Enlarging the Operational Range of a Gasoline HCCI Engine By Controlling the Coolant Temperature*. Detroit: SAE.
- 92. Mitianiec, W. (2003 SAE/JSAE Small Engine Technology Conference & Exhibition). Reduction of Exhaust Gas Emission in a SI Two Stroke Engine with Direct Fuel Mixture Injection. Madison: SAE/JSAE.
- 93. Mitianiec, W. (2008 Small Engine Technology Conference). Pneumatic Fuel Injection in a Coupled Two-Stroke Engine. Milwaukee: SAE.
- 94. Morikawa, H. (2010). A Further Approach to Controlled Auto- Ignition Using a Sequence of Low-Temperature Combustion-States. Saitama: Honda R&D Co Ltd.
- 95. Morikawa, H. (2011). Studies of self-ignition combustion using a series of low-temperature combustion cycle. *Honda R & D Technical Review, 23*(1), 70-76.
- 96. Morikawa, H., & Ishibashi, Y. (2007 World Congress). An Experimental Approach to the Controlled Auto-Ignition. Detroit: SAE.
- 97. Motorcity. (2010). *Motorcity*. Retrieved 01 15, 2018, from http://www.geocities.co.jp/MotorCity/5167/f-honda.htm
- 98. Nierkerk. (2018). Engmod2T. SA.
- 99. Nino, E., F.Gajdeczko, B., & G.Felton, P. (1992 International Fuels and Lubricants Meeting and Exposition). Two-Color Particle Image Velocimetry Applied to a Single Cylinder Two-Stroke Engine. San Francisco: SAE.
- 100. Nishida, K., Kimijima, T., Sakuyama, H., & Murakami, Y. (2007). Enlargement of Auto-Ignition Regions by Applying a Stratified Charge Concept. Nigata: JSAE.
- 101. Nishida, K., Sakuyama, H., & Kimijima, T. (2005). *Japan Patent No. US 7685989 B2*.
- 102. Nishida, K., Sakuyama, H., & Kimijima, T. (2009). *Improvement of Fuel Economy Using a New Concept of Two-Stroke Gasoline Engine Applying Stratified-Charge Auto-Ignition*. Saitama: Honda R&D Co.,Ltd.
- 103. Nuti, M. (1986 International Congress and Exposition). *Direct Fuel Injection: An Opportunity for Two-Stroke SI Engines in Road Vehicle Use.* Detroit: Piaggio Group.
- 104. Nuti, M., Pardini, R., & Caponi, D. (1997 Internation Congress & Exposition). *FAST Injection System: PIAGGIO Solution for ULEV 2T SI Engines.* Detroit: SAE.

- 105. O Zur Loye, A., C Akinyemi, O., P Durrett, R., F. Flyn, P., L Hunter, G., A Moore, G., . . . F Wright, J. (1996). *USA Patent No. US 6915776 B2.*
- 106. Ognik, R. (2005). Approximation of Detailed-Chemistry Modeling by a Simplified HCCI Combustion Model. Capri: SAE.
- 107. Oguma, H., Ichikura, T., & Iida, N. (1997). *A study on Adaptability of Alternative Fuels for Lean Burn Two-Stroke ATAC Engine*. Keio: Keio University.
- 108. Oike, I., & Hiasa, T. (1996). *Japan Patent No. US 5829394 A.*
- 109. Okada, K., Koike, I., Maeda, H., Takizawa, K., & Arai, K. (1995). Driveability Evaluation of Two-stroke Engine at Part Throttle Operation Using Torque Map. *HONDA R & D Technical Review, 7*, 24-29.
- 110. Onishi, S., Hong Jo, S., Shoda, K., Do Jo, P., & Kato, S. (1979). *Active Thermo-Atmosphere Combustion A New Combustion Process for Internal Combustion Engines*. Detroit: Nippon Clean Engine Reasearch Institute Co., Ltd.
- 111. Oswald, R., Ebner, A., & Kirchberger, R. (2010). *High Efficient 125- 250 cm3 LPDI Two-Stroke Engines, a Cheap and Robust Alternative to Four-Stroke Solutions?* Graz: Graz University of Technology.
- 112. Perkins, C. (2017, SEPT 21). *Mercedes-AMG's F1 Can Make More Power Than Waste Energy*. Retrieved from roadandtrack: https://www.roadandtrack.com/motorsports/a12443313/mercedes-amgs-f1-engine-is-amazingly-efficient/
- 113. Pohorelsky, L., Brynych, P., Macek, J., Vallaude, P.-Y., Ricaud, J.-C., Obernesser, P., & Tribotte, P. (2012). *Air System Conception for a Downsized Two-Stroke Diesel Engine*. Prague: Czech Technical Univ in Prague.
- 114. R.Hansen, K., S.Nielsen, C., C.Sorenson, S., & Schramm, J. (2008 SAE International Powertrains, Fuels and Lubricants Congress). A 50cc Two-Stroke DI Compression Ignition Engine Fuelled by DME. Shanghai: SAE.
- 115. R.Svarcas, L., & S.Brenner, M. (2005). New Powervalve Additive Technology Suitable for Two-Stroke Engines Containing Powervalves or Exhaust Port Modifiers. Wickliffe: JSAE.
- 116. Rami Y. Dahham, H. W. (2022). Improving Thermal Efficiency of Internal Combustion Engines: Recent Progress and Remaining Challenges. *MDPI*.
- 117. Rassweiler, G., & Withrow, L. (1938). *Motion Pictures of Engine Flames Correlated with Pressure Cards*. USA: SAE.
- 118. Richard Samson, A.-G. M. (2023). Effects of the Combustion Enhancer Containing Alkyl Nitrate (CEN) to Methanol in a Direct-Injection Compression Ignition (DICI) Engine. *SAE*.

- 119. Romani, L., Vichi, G., Ferrara, G., Balduzzi, F., Trassi, P., Fiaschi, J., & Tozzi, F. (2015). Development of a Low Pressure Direct Injection System for a Small 2S Engine. Part II - Experimental Analysis of the Engine Performance and Pollutant Emissions. Florence: University of Florence.
- 120. Schmidt, S., Eichlseder, H., Kirchberger, R., Nimmervoll, P., Ohrnberger, G., & Wagner, M. (2004 Small Engine Technology Conference). GDI with High-Performance 2-Stroke Application: Concepts, Experiences and Potential for the Future. Graz: SAE.
- 121. T. Poorman, L. X. (1997). *Ignition System-Embedded Fiber-Optic Combustion Pressure Sensor for Automotive Engine Control and Monitoring,.* SAE 970853.
- 122. Takashi. (2003). *crm250ar_geocities*. Retrieved 03 10, 2016, from http://www.geocities.jp/crm250ar_website/
- 123. TCDIRECT. (2019, March 12). Retrieved from www.tcdirect.co.uk
- 124. Trassi, P., Fiaschi, J., Tozzi, F., Ferrara, G., Romani, L., Vichi, G., & Balduzzi, F. (2015 SAE Int. J. Engines 8(4)). *Development of a Low Pressure Direct Injection System for a Small 2S Engine.Part I CFD Analysis of the Injection Process.* Detroit: University of Florence.
- 125. Tsushima, Y., Akamatsu, S., & Takada, Y. (1999 Symposium on International Automotive Technology). Fuel Economy Improvement and CO2 Reduction of Motorcycle Gasoline SI Engine and Its Simulation. Asaka: JSAE.
- 126. Turner, J., Blundell, D., Pearson, R., Patel, R., Larkman, D., Burke, P., . . . Kee, R. (2010). Project Omnivore: A Variable Compression Ratio ATAC 2-Stroke Engine for Ultra-Wide-Range HCCI Operation on a Variety of Fuels. Hethel: Lotus Enginnering.
- 127. UWTSD. (2019, March 12). Retrieved from www.uwtsd.ac.uk
- 128. Vacas, J. (Author's Own). Authors Own. Author's Own: Authors Own.
- 129. van Niekerk, C. G. (2000). *Effect of the Tailpipe Geometry on a Two-Stroke Engine's Performance Prediction.* Pretoria: University of Pretoria.
- 130. W.Blundell, D., & H.Sandford, M. (1992 International Congress & Exposition). Two Stroke Engines The Lotus Approach. Detroit: SAE.
- 131. Wakabayashi, S., Masuda, S., Abe, M., Uchida, Y., & Ishibashi, Y. (1994). *Japan Patent No. US 5495836 A.*
- 132. Wijesinghe, J., & Hong, G. (2008 SAE International Powertrains, Fuels and Lubricants Congress). Experimental Investigation of Spark Assisted Auto-Ignition Combustion in a Small Two-Stroke Engine. Shanghai: 2008.
- 133. Winkler, F., Oswald, R., Schoegl, O., & Foxhall, N. (2016). *Characterization of Different Injection Technologies for High Performance Two-Stroke Engines*. Graz: Graz University of Technology.

- 134. Winkler, F., Oswald, R., Schogl, O., Abis, A., Krimplstatter, S., & Kirchberger, R. (2015). Layout and Development of a 300 cm³ High Performance 2S-LPDI Engine. Graz: Graz University of Technology.
- 135. Yamazaki, K., Kurosaki, T., Ouchi, K., Abe, M., & Morita, H. (1996). Introduction of the Motorcycle "EXP-2" for Granada-Dakar Rally. *HONDA R & D Technical Review, 8*, 56-63.
- 136. Yamazaki, R., Kurosaki, T., Tsushima, Y., Noda, K., & Ishibashi, Y. (1993). *Japan Patent No. US 5507263 A.*
- 137. Yui, S., & Ohnishi, S. (1969 Mid Year Meeting). A New Concept of Stratified Charge Two Stroke Engine Yui and Ohnishi Combustion (YOCP). Chicago: SAE.
- 138. Zhao, F., W.Asmus, T., N.Assanis, D., E.Dec, J., A.Eng, J., & M.Najt, P. (2003). Homogeneous Charge Compression Ignition (HCCI) Engines: Key Research and Development Issues (1 ed.). Warrendale: SAE International.
- 139. Zhao, H. (2007). *Hcci and Cai Engines for the Automotive Industry* (1 ed.). London: Woodhead.
- 140. In-Cylinder Fiber-Optic Pressure Sensors for Monitoring and Control of Diesel Engines 981913
- 141. Combustion Analysis with Residual Gas as a Design Parameter for Two-Stroke Engines 2018-32-0045
- 142. Studies on the Cyclic Variations of Single Cylinder Two-Stroke Engines Cycle Analysis. Lu, J., Wang, C. SAE 950225
- 143. A Study of Irregular Combustion in 2-Stroke Cycle Gasoline Engines. Tsuchiya, K., Nagai, Y., Gotoh, T. SAE 830091
- 144. Experimental Investigations of Two-Stroke SI Combustion with Simultaneous Cycle-Based Fuel Consumption Measurements. Beck, K., Sarikoc, F., Spicher, U. SAE 2010-32-0061.
- 145. Intermittent Injection for a Two-Stroke Direct Injection Engine. Balduzzi, F., Romani, L., Bosi, L. SAE 2019-32-0524
- 146. Technologies to Achieve Future Emission Legislations with Two Stroke Motorcycles. Oswald, R., Kirchberger, R., Krimplstatter, S. SAE 2018-32-0042.
- 147. Concept and Implementation of a Robust HCCI Engine Controller. Kang, J., Chen, J., Chang, M. SAE 2009-01-1131
- 148. Gasoline HCCI/CAI on a Four-Cylinder Test Bench and Vehicle Engine Results and Conclusions for the Next Investigation Steps. Gottschalk, W., Magnor, O., Jakobs, J. SAE 2010-01-1488.
- 149. Design of a 4-Cylinder GTDI Engine with Part-Load HCCI Capability. Wheeler, J., Polvina, D., SAE 2013-01-0287

- 150. A Review of Pre-Chamber Initiated Jet Ignition Combustion Systems. Toulson, E., P. Attard, W. SAE 2010-01-2263
- 151. Engine Testing: The Design, Building, Modification and Use of Powertrain Test Facilities Hardcover 4 Dec. 2012 A. J. Martyr, M.A. Plint
- 152. The Design of Experiments 1 April 1972 Ronald A. Fisher
- 153. Taguchi Methods: Design of Experiments (TAGUCHI METHODS SERIES) 1 Nov. 1993 Genichi Taguchi, Yoshiko Yokoyama
- 154 . TFX Engine Technology Canada.
- 155. The Design and Simulation of 4-Stroke Engines (Gordon P Blair)

Appendix A - Measured Raw Data

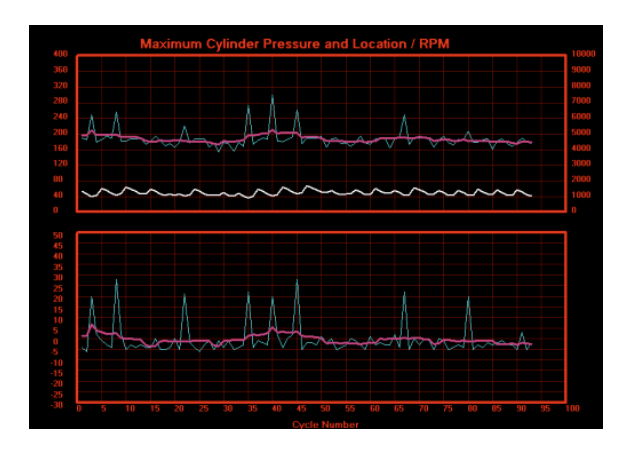
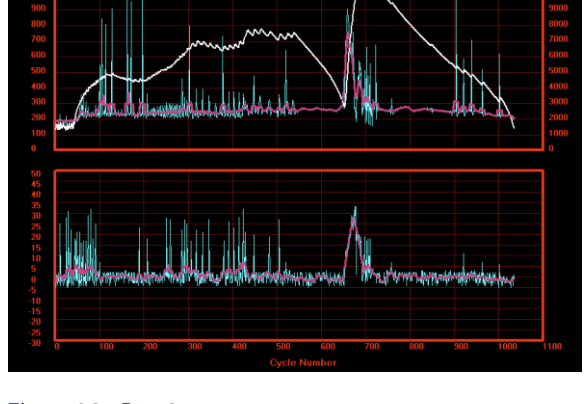


Figure 91 - Run 1 Figure 92 - Run 2



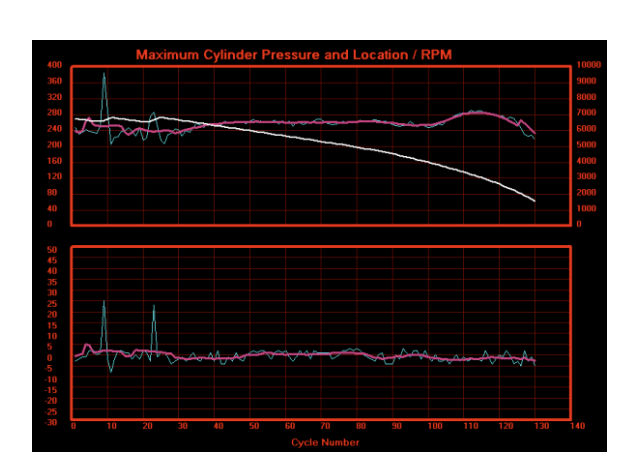
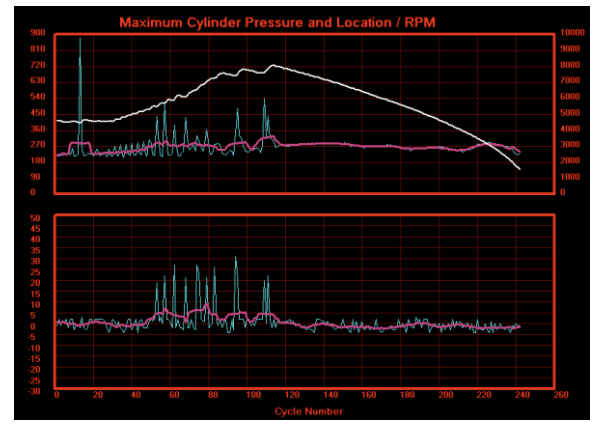
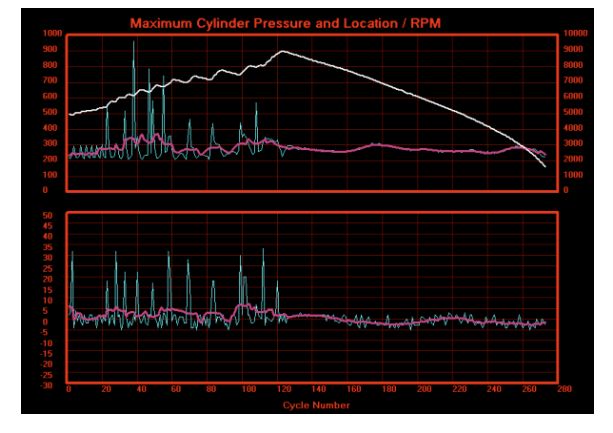
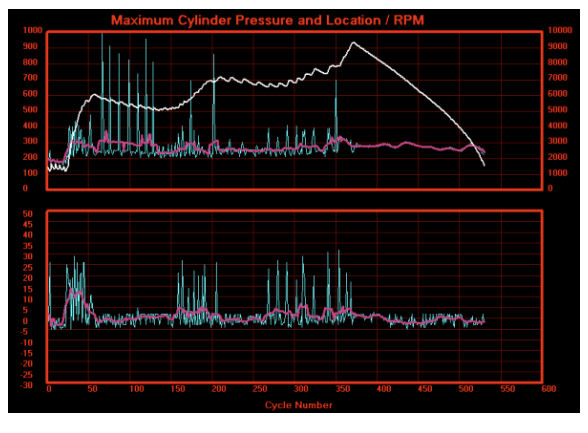


Figure 93 - Run 3 Figure 95 - Run 4









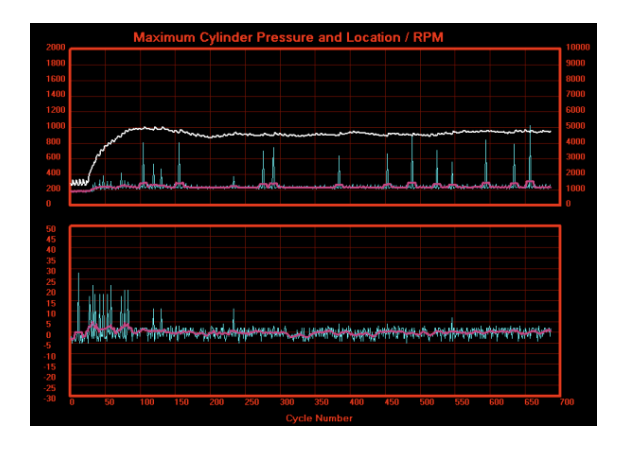


Figure 98 - Run 7

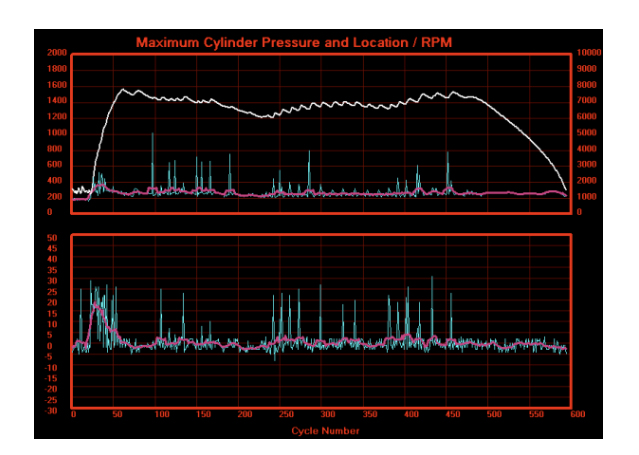


Figure 100 - Run 9

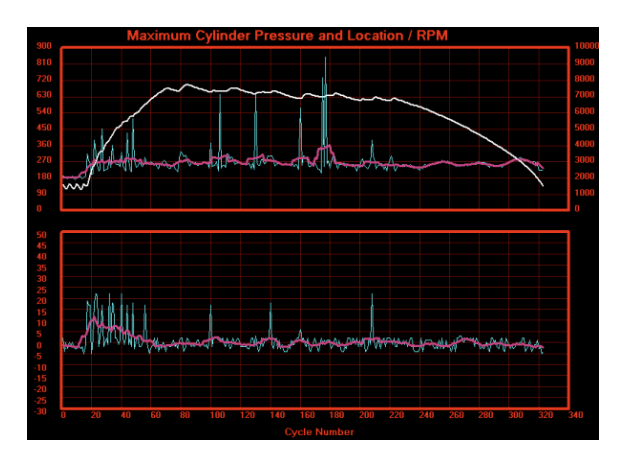


Figure 102 – Run 11

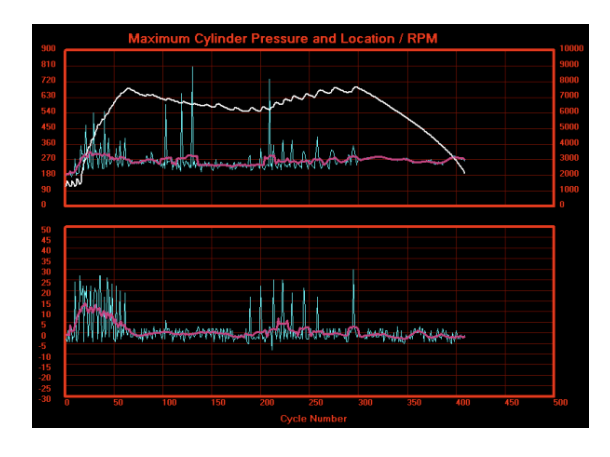


Figure 99 - Run 8

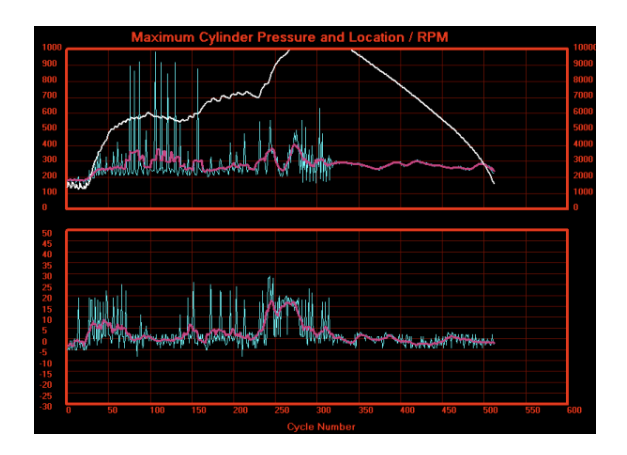


Figure 101 - Run 10

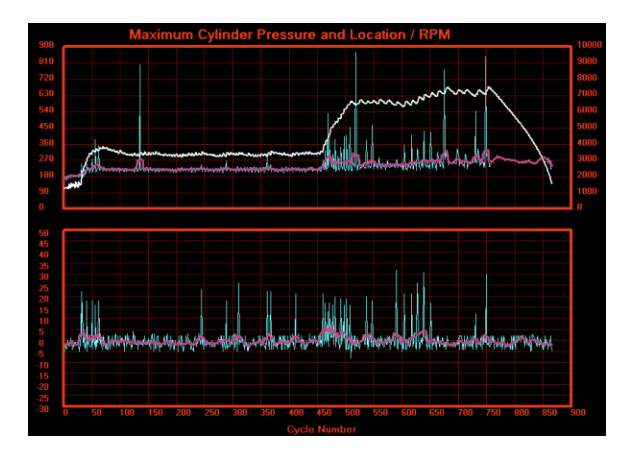


Figure 103 – Run 12

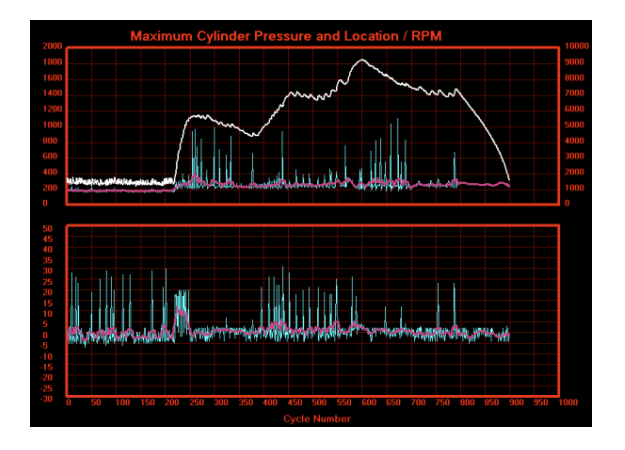


Figure 104 – Run 13

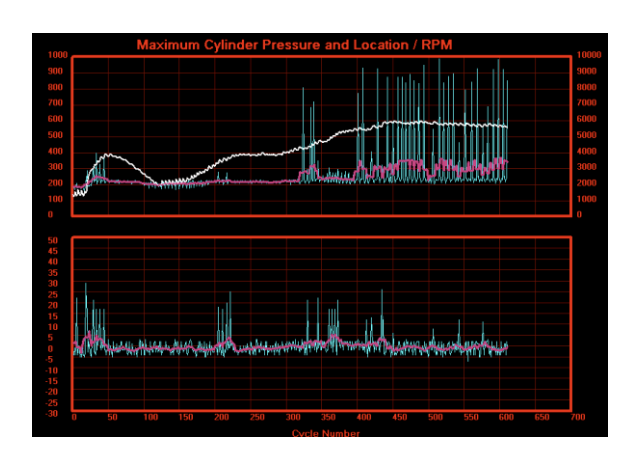


Figure 105 – Run 14

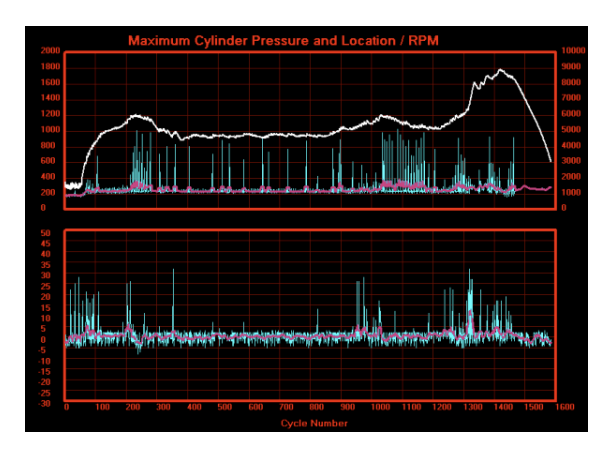


Figure 106 – Run 15

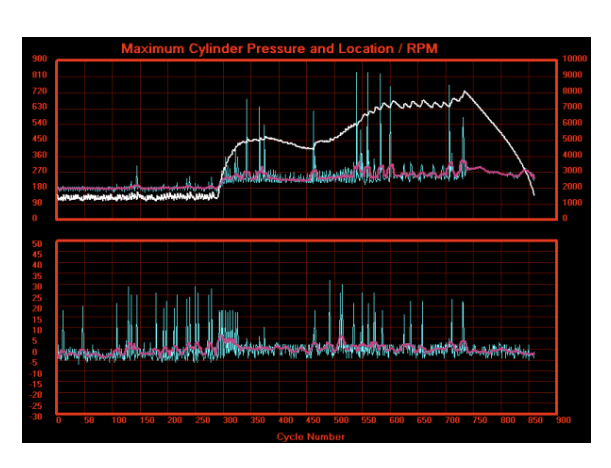


Figure 107 – Run 16

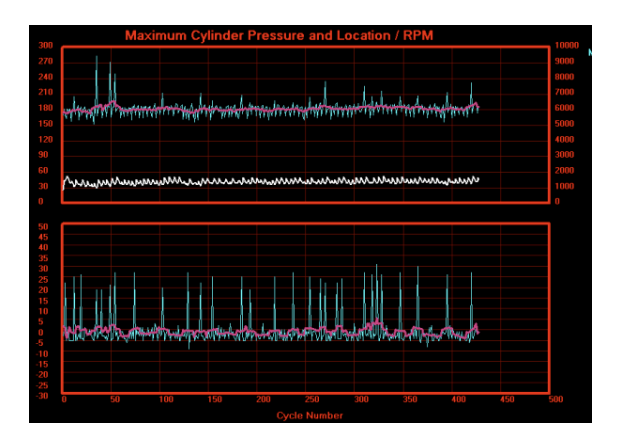


Figure 108 – Run 17

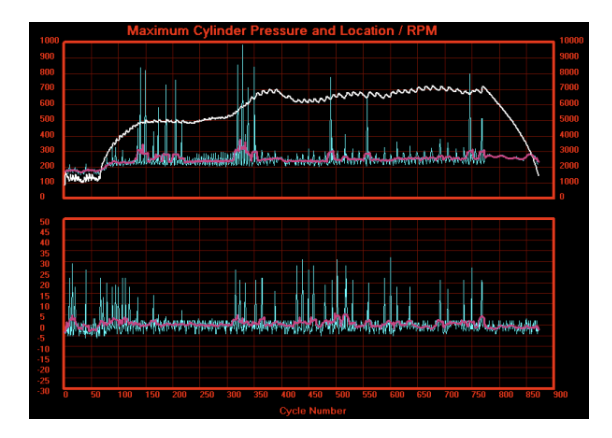


Figure 109 – Run 18

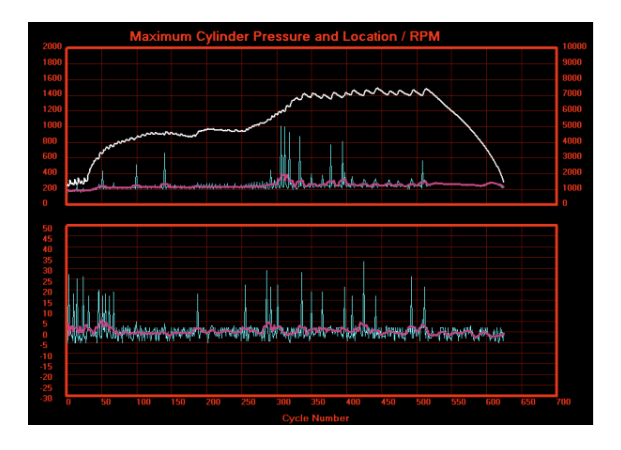


Figure 110 - Run 19

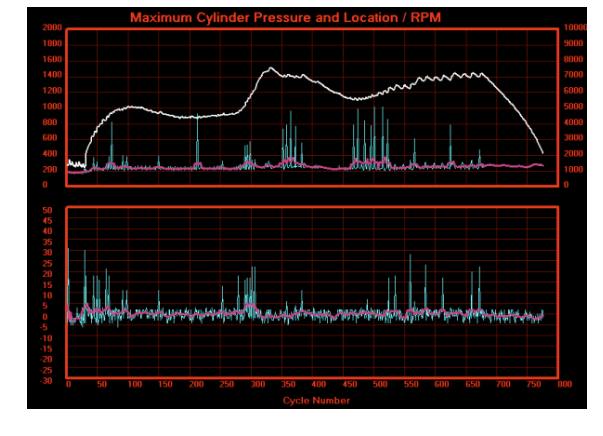


Figure 111 – Run 20

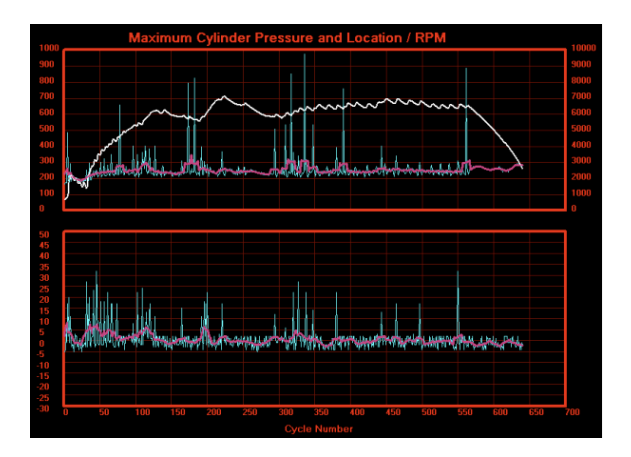


Figure 112 – Run 21

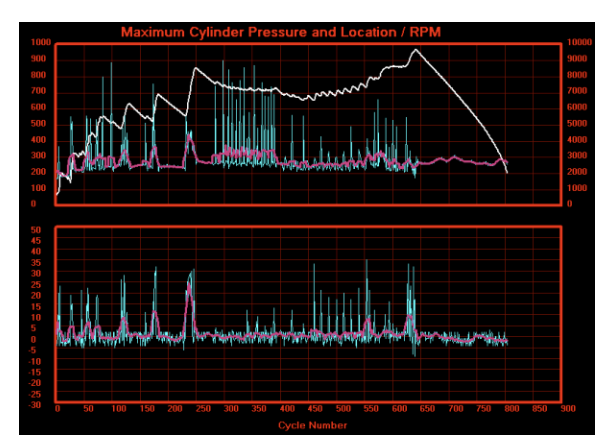


Figure 113 – Run 22

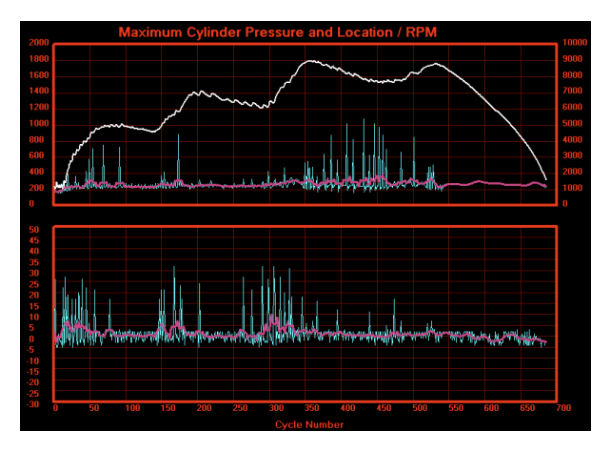


Figure 114 – Run 23

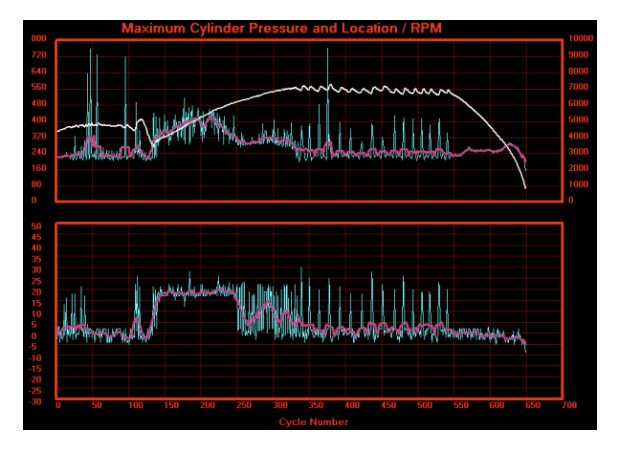


Figure 115 – Run 24

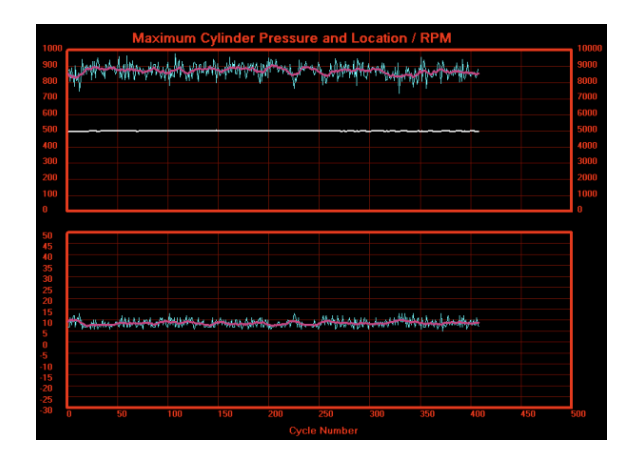


Figure 116 – Run 25

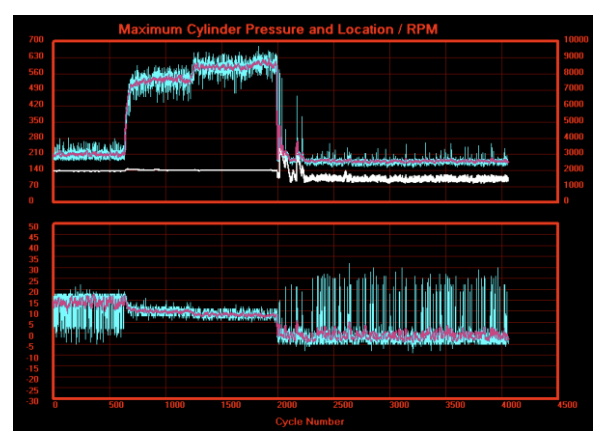


Figure 117 – Run 26

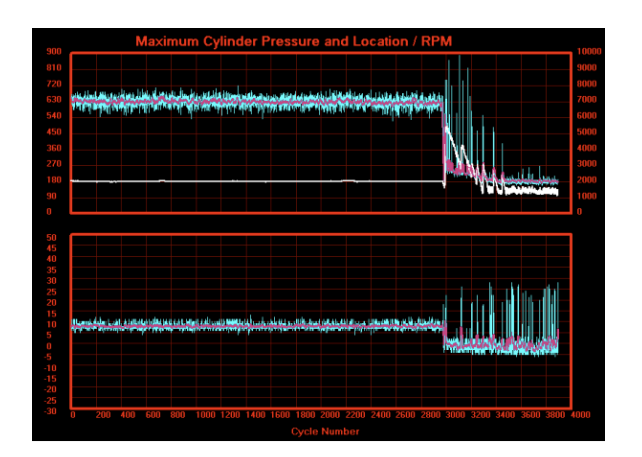


Figure 118 – Run 27

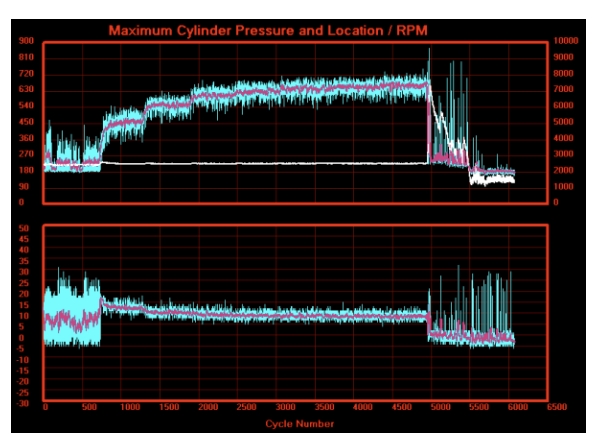


Figure 119 – Run 28

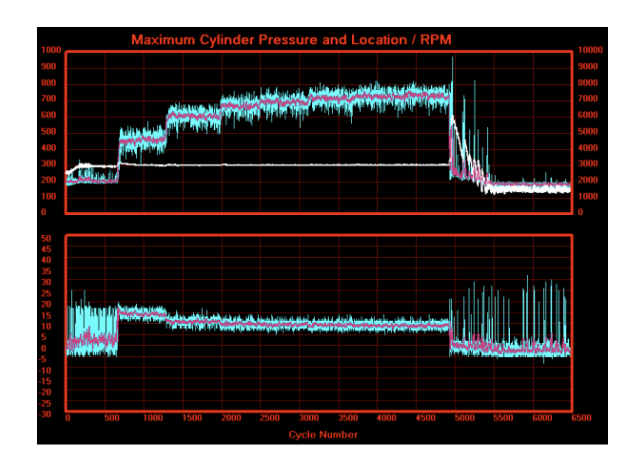


Figure 120 – Run 29

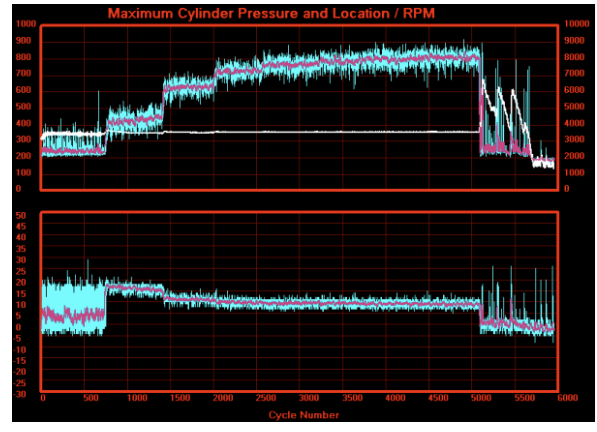


Figure 121 – Run 30